



ALASKA GEOBOTANY
CENTER DATA REPORT

2016 ARCSEES DATA REPORT

SNOW, THAW, TEMPERATURE, AND PERMAFROST BOREHOLE DATA
FROM THE COLLEEN & AIRPORT SITES, PRUDHOE BAY, AND PHOTOS OF
QUINTILLION FIBER OPTIC CABLE IMPACTS, NORTH SLOPE, ALASKA

DONALD A. WALKER, MIKHAIL KANEVSKIY, YURI L. SHUR, MARTHA K. RAYNOLDS,
JANA L. PEIRCE, MARCEL BUCHHORN, KSUSHA ERMOKHINA, LISA A. DRUCKENMILLER

AGC 18-01

EDITED BY D.A. WALKER, M. KANEVSKIY, M.K. RAYNOLDS, AND J.L. PEIRCE



JULY 2018

Funding:

National Science Foundation (NSF) ArcSEES Program, Award No. 1263854, and National Aeronautics and Space Administration (NASA) Land-Cover and Land-Use Change (LCLUC) Program Award No. NNX14AD906.

Cite this volume as:

Walker, D. A., M. Kanevskiy, Y. L. Shur, M. K. Raynolds, J. L. Peirce, M. Buchhorn, K. Ermokhina, and L. A. Druckenmiller. 2018. 2016 ArcSEES Data Report: Snow, thaw, temperature, and permafrost borehole data from the Colleen and Airport sites, Prudhoe Bay, and photos of Quintillion fiber optic cable impacts, North Slope, Alaska. Alaska Geobotany Center Data Report AGC18-01, Institute of Arctic Biology, University of Alaska Fairbanks, Fairbanks, Alaska, USA.

On the cover:

Martha Raynolds and Misha Kanevskiy at borehole in thermokarst pond, Airport site, Transect 5 (DSC 8706.jpg). Inset photos, left: Misha Kanevskiy and Ksenia Ermokhina measuring thaw depths at Airport site, Transect 3, 17 August 2016 (DSC 9328.jpg); center: Misha Kanevskiy and Martha Raynolds measuring snow depths at Airport site, Transect 3, 27 March 2016 (DSC 8677.jpg); right: Thermokarst along Quintillion Fiber Optic trench, 16 August 2016 (DSC 9279.jpg). Photos by D. A. Walker.





2016 ARCSEES DATA REPORT: SNOW, THAW, TEMPERATURE, AND PERMAFROST BOREHOLE DATA FROM THE COLLEEN & AIRPORT SITES, PRUDHOE BAY, AND PHOTOS OF QUINTILLION FIBER OPTIC CABLE IMPACTS, NORTH SLOPE, ALASKA

ALASKA GEOBOTANY CENTER DATA REPORT, AGC 18-01 :: JULY 2018

Edited by

DONALD A. WALKER, MIKHAIL KANEVSKIY, MARTHA K. RAYNOLDS, AND JANA L. PEIRCE

Table of Contents

<i>List of figures.....</i>	<i>ii</i>
<i>List of tables.....</i>	<i>iii</i>
<i>Contributors.....</i>	<i>iv</i>
1 Introduction	
1.1 Overview of the 2016 field season.....	1
2 Methods	
2.1 Snow, water, and thaw-depth studies.....	4
2.2 Thermokarst boreholes	5
2.3 Air, snow, and soil temperatures.....	6
2.4 Quintillion fiber optic cable disturbance observations	8
3 Results & Discussion	
3.1 Snow, water, and thaw-depths.....	9
3.2 Thermokarst-pond boreholes	15
3.3 Soil, snow, and air temperatures	19
3.4 Quintillion fiber optic cable disturbance observations	22
5 Conclusions	
4.1 Summary of major conclusions	24
4.2 Future directions.....	25
6 References.....	26
Appendix A: Data Tables.....	28
Appendix B: Photos and Descriptions of Snow Pits at Plots.....	48
Appendix C: Photos of Quintillion Fiber Optic Cable Impacts, 17 July 2016.....	61

INDEX OF FIGURES

Figure 1.1:	<i>Alaska Geobotany Center data reports AGC15-01 and AGC 16-01</i>	1
Figure 1.2:	<i>Location of Colleen Site A and the Airport site</i>	1
Figure 1.3:	<i>Locations of transects, permanent plots, and boreholes</i>	2
Figure 2.1:	<i>Measuring snow depths, snow density, and describing snow pits</i>	4
Figure 2.2:	<i>Transect 4 on 31 March after night of strong winds</i>	4
Figure 2.3:	<i>Measuring thaw and water depth on Transects 3 and 4</i>	5
Figure 2.4:	<i>Core removed from Pond Marcel, Colleen Site A, T1</i>	6
Figure 2.5:	<i>Borehole in thermokarst pond, Airport site, T5</i>	6
Figure 2.6:	<i>Placement of iButtons on PVC poles</i>	6
Figure 2.7:	<i>Tube wax, rubber gloves and contact lens cases</i>	8
Figure 3.1:	<i>Snow, water, and thaw depths by distance from road, T1–T5</i>	10-11
Figure 3.2:	<i>Trends in snow, water, and thaw depth, all points, T1–T4</i>	12-13
Figure 3.3:	<i>Snow, water, and thaw depth by vegetation moisture groups, T1–T4</i>	13
Figure 3.4:	<i>Trends in thaw vs. snow and water depths, all points, T1–T4</i>	14
Figure 3.5:	<i>Snow, water, and thaw depths and SWE for all plots grouped by centers and troughs, T1–T5</i>	15
Figure 3.6:	<i>Snow pit at plot T2-005-T</i>	16
Figure 3.7:	<i>Snow pit at plot T2-200-C</i>	16
Figure 3.8:	<i>Dust coated snow on downwind side of the road near Toolik Lake</i>	16
Figure 3.9:	<i>Photographs of frozen cores from Boreholes T1-74.0, T5-94.5, and T5-96.8</i>	17
Figure 3.10:	<i>Cryostratigraphic cross-sections across and along ice-wedge troughs, Airport site</i>	18
Figure 3.11:	<i>Mean annual surface temperatures in centers and troughs, flooded vs. non-flooded transects</i>	19
Figure 3.12:	<i>Depth and mean annual surface temperatures of polygon troughs, T1–T4</i>	19
Figure 3.13:	<i>Daily mean surface temperature in polygon troughs and centers, compared with snow depth</i>	20
Figure 3.14:	<i>Daily mean air and soil-surface temperatures in wet and dry polygons during freeze up</i>	20
Figure 3.15:	<i>Mean annual temperature by soil depth at polygon centers and troughs, T1–T4</i>	21
Figure 3.16:	<i>Mean annual air temperature by iButton height, all distances from road, T1–T4</i>	21
Figure 3.17:	<i>Mean annual air temperature by iButton height and distance from road, T1–T4</i>	21
Figure 3.18:	<i>Daily mean air temperature at road berm by iButton height</i>	21
Figure 3.19:	<i>Heat map, mean annual temperatures by iButton height and distance from the road, T1–T4</i>	22
Figure 3.20:	<i>Severe tundra disturbance caused by placement of the Quintillion fiber optic cable</i>	23
Figure 3.21:	<i>Thermokarst in the trench of the Quintillion fiber optic cable, Sagwon Upland</i>	23
Figure 3.22:	<i>Washed out section of the Dalton Highway near the Deadhorse Airport</i>	23
Appendix B:	<i>Snow pit photos and profiles by transect</i>	48
Appendix C:	<i>Photos of Quintillion fiber optic cable impacts, 17 July 2016</i>	61

INDEX OF TABLES

Table 2.1:	<i>Placement of Maxim iButton® temperature loggers, 2014-16</i>	7
Table 2.2:	<i>Microrelief at flag transect points where iButtons were placed</i>	7
Table A.1:	<i>Methods and results of protecting iButtons from water damage</i>	28
Table A.2A:	<i>Summary of mean snow depths, thaw depths, and water depths from Colleen Site A</i>	29
Table A.2B:	<i>Summary of mean snow depths, thaw depths, and water depths from the Airport site</i>	33
Table A.3A:	<i>Summary of mean snow depth, density, SWE from center and trough plots, Colleen Site A</i>	37
Table A.3B:	<i>Summary of mean snow depth, density, SWE from center and trough plots, Airport site</i>	38
Table A.4A:	<i>Results of borehole drilling at Colleen Site A</i>	40
Table A.4B:	<i>Results of borehole drilling at the Airport site</i>	41
Table A.5A:	<i>Mean annual air temperature along transects by distance from road and iButton height</i>	43
Table A.5B:	<i>Mean annual temperature in centers and troughs by distance from road and soil depth</i>	44
Table A.6:	<i>Temperature logger serial numbers and locations on Colleen Site A, August 2015–July 2016</i>	45

CONTRIBUTORS

DONALD A. WALKER

Alaska Geobotany Center, Institute of Arctic Biology and Department of Biology and Wildlife,
University of Alaska Fairbanks, Fairbanks, Alaska

MARTHA K. RAYNOLDS

Alaska Geobotany Center, Institute of Arctic Biology, University of Alaska Fairbanks, Fairbanks, Alaska

MIKHAIL KANEVSKIY

Institute of Northern Engineering, University of Alaska Fairbanks, Fairbanks, Alaska

YURI L. SHUR

Department of Civil and Environmental Engineering, University of Alaska Fairbanks, Fairbanks, Alaska

MARCEL BUCHHORN

Alaska Geobotany Center, Institute of Arctic Biology, and Hyperspectral Imaging Laboratory, Geophysical Institute,
University of Alaska Fairbanks, Fairbanks, Alaska. Current address: Flemish Institute for Technological Research
(VITO), Mol, Belgium

JANA L. PEIRCE

Alaska Geobotany Center, Institute of Arctic Biology, University of Alaska Fairbanks, Fairbanks, Alaska

KSENIA K. ERMOKHINA

Earth Cryosphere Institute, Siberian Branch of Russian Academy of Sciences, Moscow, Russia

LISA A. DRUCKENMILLER

Alaska Geobotany Center, Institute of Arctic Biology, University of Alaska Fairbanks, Fairbanks, Alaska

1 Introduction

1.1 Overview of the 2016 field season

This is third and final data report of the ArcSEES project, “Cumulative Effects of Arctic Oil Development—Planning and Designing for Sustainability.” It includes data collected during five field trips in 2014–2016 from five research transects established at the Lake Colleen Site A and Airport study sites in the vicinity of Deadhorse, Prudhoe Bay, Alaska.

This report focuses on methods, data and results in the following areas:

- **Summer thaw and water depths** at the Colleen Site A and Airport study sites during field trips in August 2014, 2015, and 2016.



Figure 1.1. Alaska Geobotany Center data reports AGC15-01 and AGC 16-01 can be downloaded from www.geobotany.uaf.edu/arcsees and arcticdata.io.

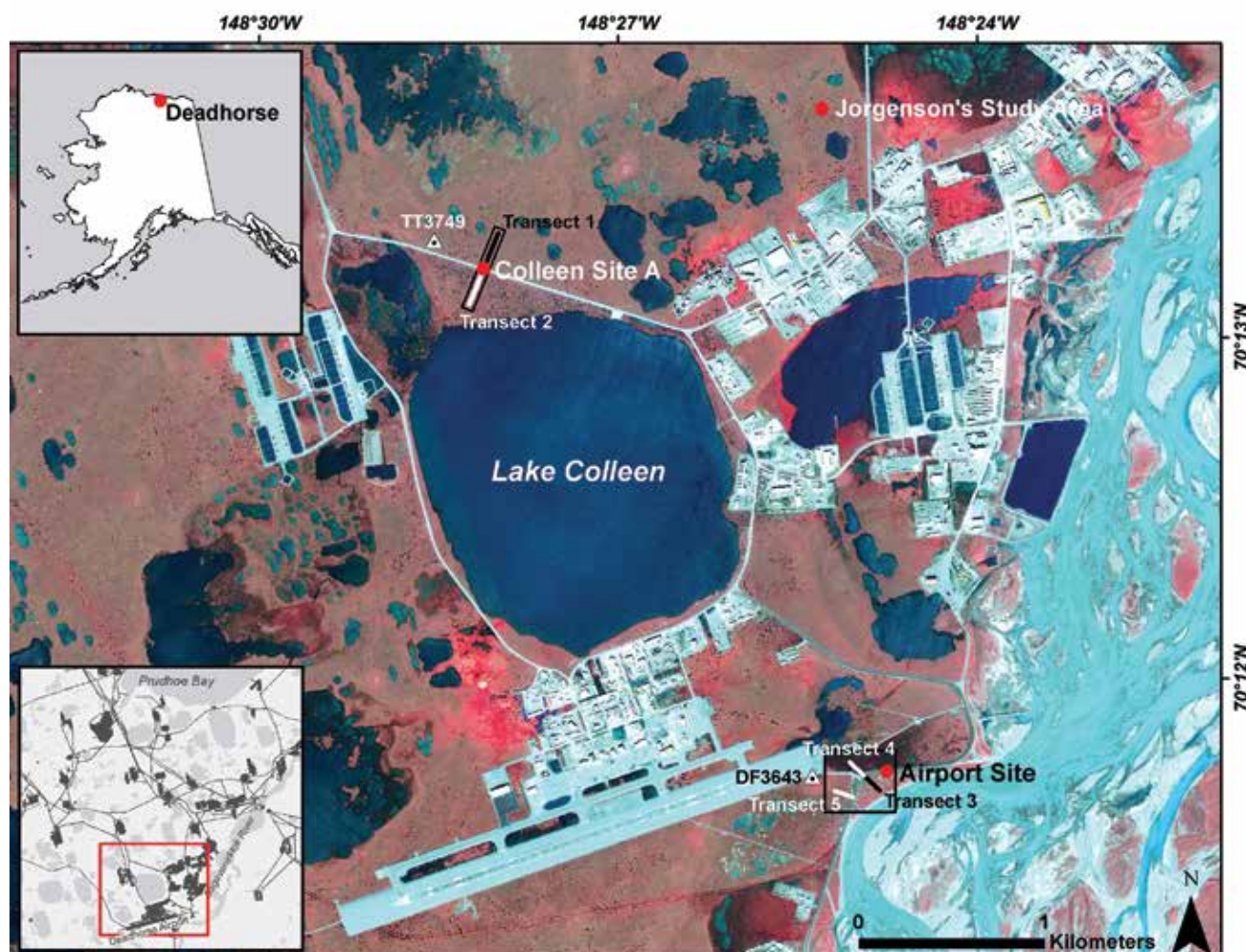
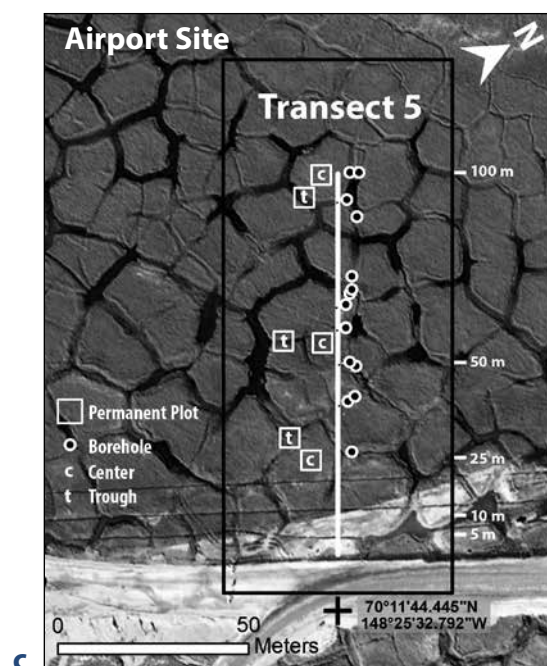
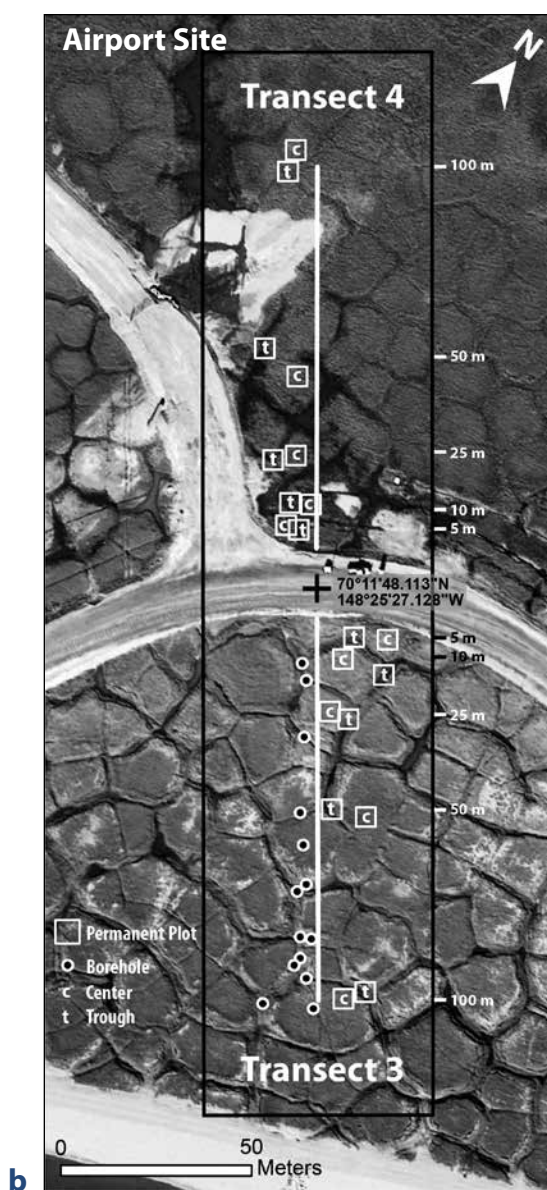
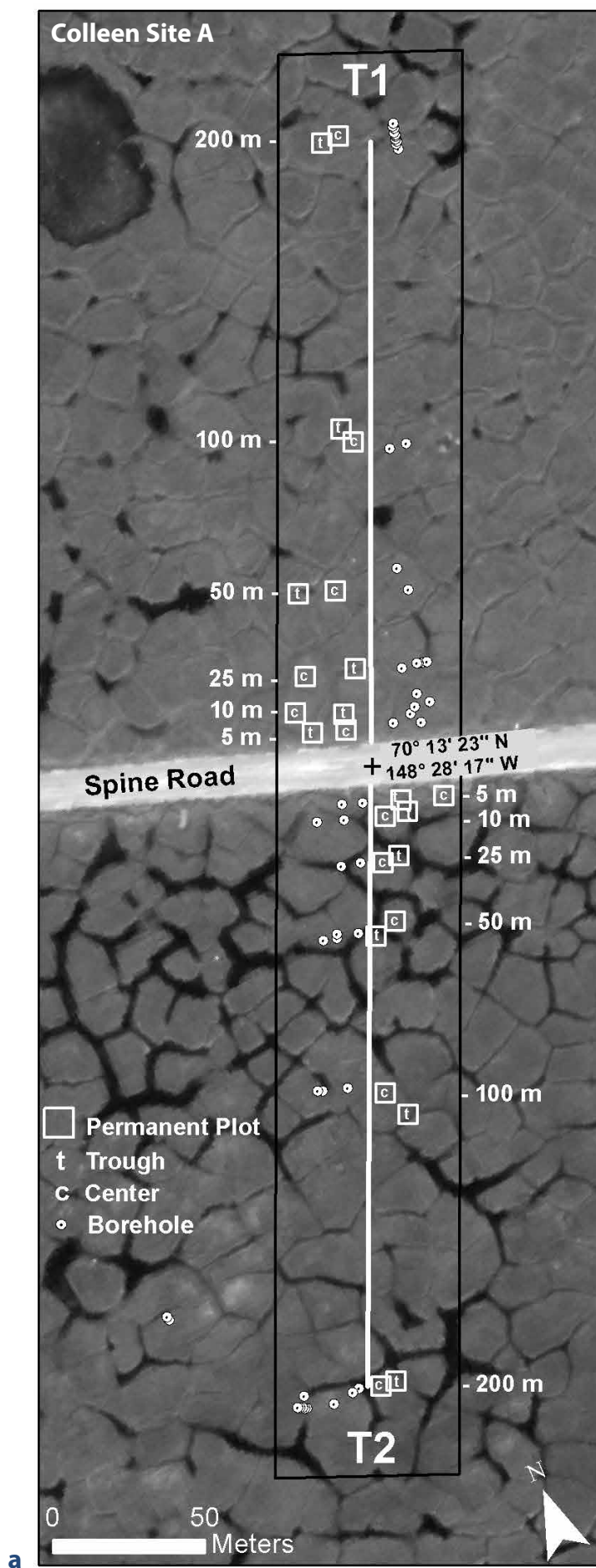


Figure 1.2. Location of the Colleen Site A and Airport site. Prudhoe Bay region, Alaska. Base image: False color-infrared World View (July 9, 2010).



- **Snow depths and snow-pit descriptions** collected during 27–30 March 2016.
- **Thermokarst boreholes:** 28 boreholes at the Airport study site in August 2015, and 3 boreholes in thermokarst pits on Transect 1 (Colleen Site A) and Transect 5 (Airport site) from 27–30 March 2016.
- **Air, snow, and soil temperature** data recorded with iButton® temperature loggers placed along transects and at permanent vegetation plots in 2014–2016.
- **Quintillion fiber optic cable disturbance** photos obtained in August 2016.

Readers should reference earlier data reports (Fig. 1.1) for project background, methods and other data collected from plots, transects, and boreholes established at the Colleen Site A and Airport study sites (Fig. 1.2 & 1.3) in 2014 and 2015 (Walker *et al.*, 2015, 2016a). The data are also archived in digital format on the Alaska Geobotany Center's ArcSEES website (www.geobotany.uaf.edu/arcsees) and the NSF Arctic Data Center (arcticdata.io). See also the BLM record of decision regarding the Quintillion fiber optic cable project (BLM, 2015).

Figure 1.3. Locations of transects (T), permanent plots, and boreholes in ice-wedge-polygon terrain at (a) Colleen Site A (T1, T2) and (b) the Deadhorse Airport site (T3, T4) and (c) T5. Transects are shown as bold white lines. T1 and T2 are each 200 m long. T3, T4, and T5 are 100 m long. Permanent plots (white squares) are 1 x 1-m vegetation plots located in centers (c) and troughs (t) of ice-wedge polygons on the left side of the transect (facing the transect from the road) at 5, 10, 25, 50, 100, and (on T1 and T2) 200 m from the road. Boreholes (white circles with black centers) are located at the same distances from the road in centers and troughs. Base image is black and white World View image (July 9, 2010).

2 Methods

Chapter 2 provides a record of the methods used in data collection. Many methods are described in more detail in Alaska Geobotany Center Data Reports AGC 15-01 and AGC 16-01 (Walker et al., 2015, 2016a). Data tables referenced in this section appear in Appendix A. Data tables are also archived in digital format on the Alaska Geobotany Center's ArcSEES project website (www.geobotany.uaf.edu/arcsees) and at the NSF Arctic Data Center (arcticdata.io).

2.1 Snow, water, and thaw-depth studies

Snow studies were conducted 27–30 March 2016, during a period of cold, relatively calm weather. Snow depth and density were measured along transects and at permanent plots at the Colleen and Airport sites (Fig. 1.3). Transects and plots were marked with PVC posts, so they could be located in winter (Fig. 2.1).

A 7–10-cm layer of fresh snow occurred two days prior to measurement, which persisted during the four days of data collection. On the day following the measurement, strong winds redistributed the new snow and changed the microtopography of the snow surface (Fig. 2.2).

2.1.1 Snow transects

The pin flags that were placed at every meter along the transects in 2014 and 2015 were not visible, so a

meter tape was stretched between the vertical PVC markers, and snow measurements taken along the tape. Snow depths were measured every meter along the first 100 m of the Colleen Site A transects, then every 5 m from 105 to 200 m. Transects 3, 4, and 5 at the Airport site are 100 m long, and snow was measured every meter. Transect 5 is heavily disturbed in the first 25 m, so we measured snow every meter from 25 to 100 m.

2.1.2 Snow depths and snow pits at permanent vegetation plots

Snow data from the permanent plots complement the data from the transects and provide more detailed information on snow properties. In addition to snow depths, the plot data include photographs



Figure 2.1. Measuring snow depths, snow density, and describing snow pits at permanent plots along Transect 4 on 28 March. Vertical PVC posts with red stripes mark the location of the permanent plots at 5, 10, 25, 50, and 100-m intervals along the transect. Photo: DSC 8801.



Figure 2.2. A night of strong winds altered the microtopography of the snow surface. On 31 March, Transect 4 had a rough surface with small dunes 10–20 cm deep. Note the difference from the relatively smooth surface of the undisturbed areas of snow in Figure 2.1. Photo: DSC 8892.

of the snow pits at each plot, snowpack density and snow water equivalent (SWE) plus a description of the snow pit at several key plots. Snow depths were measured at five points at each plot (four corners and center) and averaged. At five roadside plots, 14-1 through 14-5, near Lake Colleen, roadside snowdrifts covered the wooden stakes, so snow depth for these plots was estimated using the depths of snow at comparable (5-m) distances from the road along transects T1 and T2.

Snow pits were also dug at all the permanent vegetation plots and photographed. Snow density was measured using a plastic ESC 30 tube (7.1-cm diameter), except at plot T4-010-C where a SIPRE corer (7.5-cm diameter) was used because of very high-density snow. Snow samples from the coring devices were placed into 1-gallon zip-seal bags, and later weighed to determine the mass of snow and the snow water equivalent. Photos of the snow pits are in Appendix B.

Detailed descriptions of the snow profiles were made at seven of the snow pits, following UNESCO procedures (Colbeck *et al.*, 1992). Profiles were described at 5, 25, and 200 meters from the road to capture the surface-snow conditions and the characteristics of the main layers (hardness, temperature, and snow-grain shapes and sizes) with respect to roadside drift characteristics, effects of road dust, and microtopography.

The seven snow-pit descriptions accompany the photos of the snow pits in Appendix B.

2.1.3 Water and thaw-depth measurements

Thaw and water depths were measured along all transects on 16–17 August using a 1-m steel probe in most situations, or a 1.5-m copper probe in deep water (Fig. 2.3). Thaw and water depths were measured at the pin flags placed along Transects 1, 2, 3, and 4 as described in previous data reports. Five measurements of thaw were taken inside permanent plots as in years past, and the mean for each plot is reported here.

2.2 Thermokarst-pond boreholes

Information regarding the ice and soil stratigraphy beneath deeper thaw ponds was obtained during 28–29 March 2016, when the ponds were frozen, which provided a dry stable platform for drilling. Three cores were obtained using a motorized SIPRE corer. One borehole (T1-74.0 m) was drilled in Pond Marcel at the Colleen Site A (Fig. 2.4), and two boreholes (T5-94.5 m, and 96.8 m) were drilled in a thaw pond along Transect 5 at the Airport site (Fig. 2.5). The cryostratigraphy of the upper permafrost table was described as in other boreholes (Kanevskiy *et al.*, 2017).

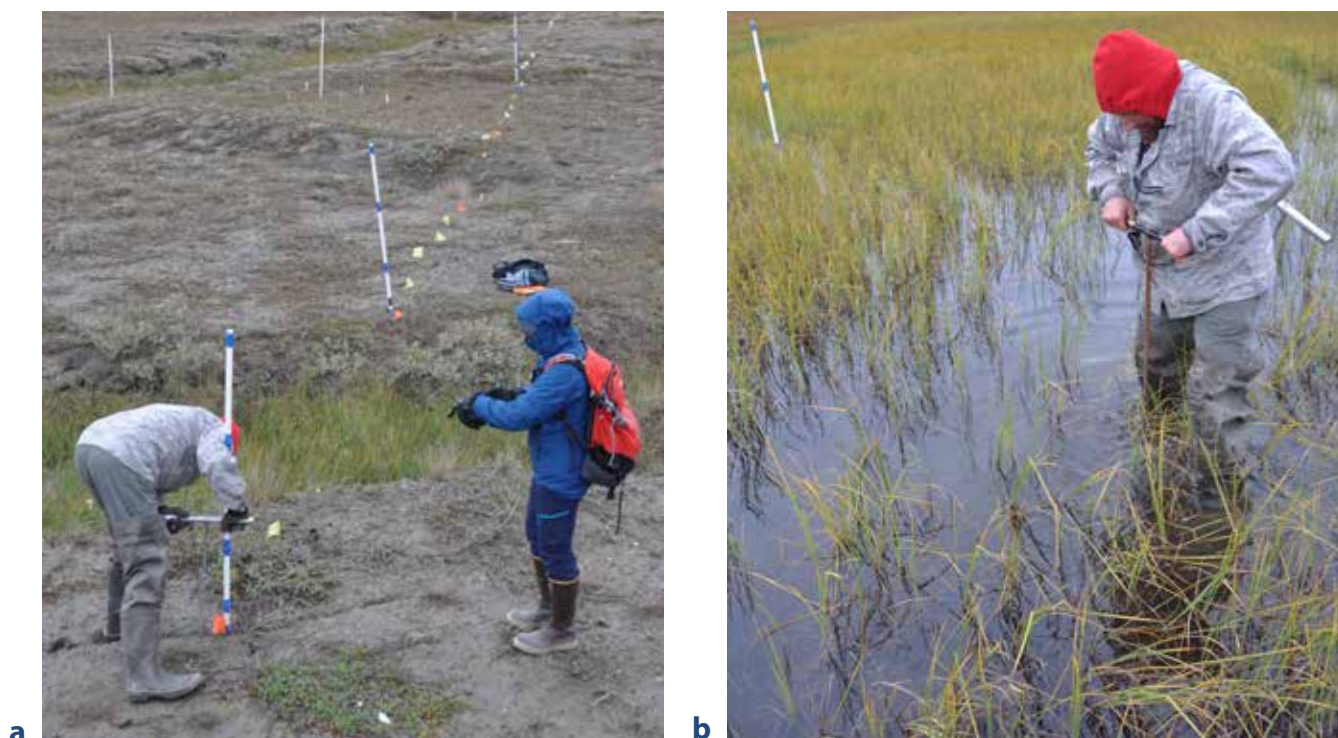


Figure 2.3. (a) Measuring thaw depth along Transect 3 with a 1-m steel probe. Photo: DSC 9329.jpg. (b) Measuring thaw and water depth along Transect 4 with a 1.5-m probe. Photo: DSC 9388.jpg.



Figure 2.4. Core removed from Pond Marcel, 74.0 m from the road on Transect 1, Colleen Site A. Photo: IMG7710.

2.3 Soil, snow, and air temperatures

2.3.1 iButton® temperature logger distribution

The locations and dates of the iButton placement are summarized in Table 2.1. Temperature data were collected over two time periods:

August 2014–July 2015: Maxim iButton® temperature loggers were installed adjacent to permanent vegetation plots on Transects 1 and 2 at Colleen Site A on 16 August 2014. No loggers were placed on the flag transects during this first year of measurements. At all vegetation plots established in polygon centers and troughs on T1, loggers were placed below ground at 0, -20 and -40 cm depths and above ground at 10, 20, 50 and 100 cm heights. At plots at 5, 10, and 25 m from the road, where snow would be deepest, iButtons were also installed at 150 cm above ground. The same distribution of loggers was used below ground for vegetation plots along T2, but no loggers were placed above ground on T2.

For all installations, temperature loggers were placed in small 2 mil zip-seal polyethylene bags before being duct-taped to PVC pipes at marked heights (depths) above and below ground. The PVC pipes were sunk into the ground for soil temperature measurement. For air temperatures, a 50-cm piece of rebar was placed in the soil with about 25 cm above the soil to provide internal support for the PVC (Fig. 2.6).

August 2015–July 2016: iButtons placed in 2014 were retrieved, read and replaced, and additional temperature loggers deployed at the Airport site. Some changes to the methodology were made to



Figure 2.5. Borehole in thermokarst pond, Transect 5, Airport site. Photo: DSC 8706.

improve placement along the transects and better protect dataloggers from water damage. The above ground iButtons were moved from the vegetation plots to the flagged transects, where they were placed at distances 0, 5, 10, 25, 50 and 100 m from the road to better record the formation and melting of the roadside snowdrift. These iButtons were again taped to PVC pipes at 0, 5, 10, 20, 50 and 100 cm in the air. Nearest the road, at least one iButton on each transect was also placed at 150 cm to ensure collection of air temperature above the roadside snow drifts. Below ground iButtons continued to be placed at all permanent vegetation plots at 0, -20 and -40 cm soil

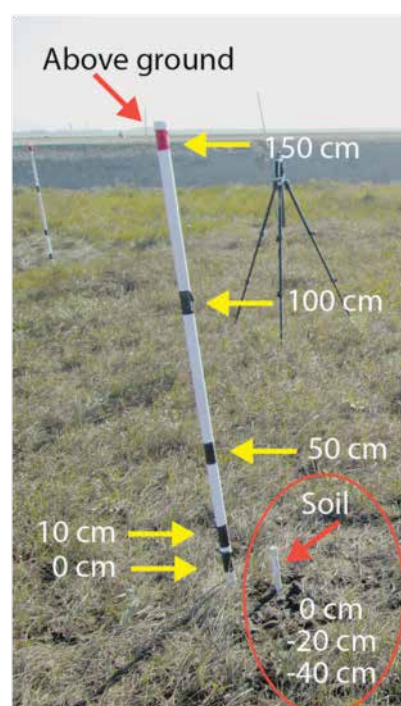


Figure 2.6. Placement of iButtons on PVC poles for monitoring air and soil temperatures along transects and at permanent plots. Photo: IMG 0871.

Table 2.1. Placement of Maxim iButton® temperature loggers, 2014–16.

		2014–15		2015–16			
		Colleen Site A		Colleen Site A		Airport Site	
<i>iButton location</i>		<i>T1</i>	<i>T2</i>	<i>T1</i>	<i>T2</i>	<i>T3</i>	<i>T4</i>
Vegetation plots	Air	X					
	Soil	X	X	X	X	X	X
Flag transects	Air			X	X	X	X
	Soil						

depths in polygon centers and troughs on both sides of the road. Below ground iButtons were not placed along flagged transects. This placement scheme was applied on Airport and Lake Colleen study sites on T1–T4. No iButtons were placed on T5.

Due to the change in placement of above ground iButtons for the second field season, the opportunity to look at two years of air temperature data for the same transect, distance from road, and height above ground is limited to Transect 1. Two years of soil temperature data are available for all vegetation plots on Transects 1 and 2. Analysis of air temperature data shows that there is little to no variation between locations for points that are above the height of snow cover.

2.3.2 iButton data collection settings and interpolation of missing time periods

iButtons were programmed to record the temperature 6 times per day (at 0:00, 4:00, 8:00, 12:00, 16:00, and 20:00), a sampling rate of 240 minutes. The iButtons were set to start recording on August 16, 2014, and recorded their last full day of temperature readings on July 22. When the iButtons were retrieved and reset, the new mission was programmed to start on 15 August 2015, and the last full day of readings were logged on 20 July 2016.

Note: Maxim uses the term sample rate to refer to the time between consecutive measurements. The sample rate is specified in minutes and must be between 0 and 255. The DS1921-series loggers can only store up to 2048 readings once activated, though a delayed start can be programmed. Because of this storage limitation and the fact that the sampling rate cannot exceed 255 minutes (4.25 hours), we could not program the iButtons to capture a full year of temperature data. Taking readings every 4 hours (6 times a day) for 365 days would result in 2190 readings and require 2190 bytes of storage capacity—more than the 2048 byte capacity. DS1922/3 models have a higher sampling capacity.

For the missing dates between 22 July and 15 August 2015, we estimated temperatures through linear interpolation. Where no data were available for a given location (due to the change in iButton placement in the second year), missing data was modeled using the average change in temperature over the period for points at the same depth or height from the soil surface and same microrelief feature (center or trough).

Table 2.2 shows the microrelief at the points along the flag transects where aboveground iButtons were placed for 2015–16. iButtons at 25, 50, and 200 meters from the road on T1 were in troughs, as were the iButtons placed at 50 meters from the road on T2. All other data loggers placed along transect lines were on polygon rims or centers.

Table 2.2. Microrelief at flag transect points where above-ground iButtons were placed on PVC poles at measured distances from the road.

m	T1	T2	T3	T4
0	Road Berm	Road Berm	HC	Road Berm
5	R	HC	HC	FC
10	R	HC	R	FC
25	T	HC	HC	FC
50	T	T	T	T
100	LC	HC	HCr	FC
200	T	R		

Meters from road (m), Flat-centered polygon (FC), low-centered polygon (LC), high-centered polygon (HC), high-center polygon with rim (HCr), low-centered polygon rim (R), and trough (T).

2.3.3 Temperature logger protection methods

Experience over the first field season revealed that iButtons are not sufficiently water resistant to survive a full, annual vegetation cycle in wet locations. Almost 15% of iButtons failed in the first year. Over 84% of those that failed were iButtons that had been placed in water or soil, with the greatest failure rate among those placed deepest in the soil (–40



Figure 2.7. Tube wax, rubber gloves and contact lens cases purchased at the Prudhoe Bay General Store were used to keep temperature loggers drier in the field. Failure rates were lowest when iButtons were coated in the soft wax before being placed in the cut off finger of a Nitrile rubber glove, which was then knotted and placed in a small plastic bag. Photo: IMG 5519.

cm). Over half (58%) of the iButtons that failed in the first year were on T2, the wetter of the two transects at Colleen Site A.

Since the devices do not log data into protected long-term storage, all data is lost if the device fails due to water exposure during the year or if the battery dies before the iButton is retrieved and read. Before placing iButtons back in the field in August 2015, changes were made to the methods used to protect temperature loggers that would be placed in wetter locations. The iButtons were placed in waterproof sleeves made from the fingers of disposable Nitrile rubber gloves, and then inserted into small (1.5" x 2") 2 mil zip-seal bags before being taped to PVC poles. iButtons that were placed in soil were also coated in a microcrystalline petroleum wax (TrueTap® Wax Stick, CRC Industries, Inc.). Appendix A, Table A.1 describes methods

and results of protecting iButton temperature loggers from moisture in 2014 and 2015. Despite being used only in wetter locations, the tube wax lubricant lowered the failure rate of iButtons after a year in the field to 3–4%, compared with 10% for similarly protected iButtons that were unwaxed, and 12–15% for iButtons that were protected only by a 2 mil zip-seal bag and duct tape.

Overall, we installed 129 iButtons at Colleen Site A in the 2014 field season and 260 iButtons in 2015 (137 at Colleen Site A and 123 at the Airport site). The serial numbers and locations of iButtons placed at Colleen Site A in 2014 are included in the AGC 15-01 data report. The same information for iButtons placed at the Airport site in 2015 are included in the AGC 16-01 data report. Appendix A, Table A.6 includes previously unpublished serial number and location information for iButtons replaced at the Colleen Site A in 2015.

2.4 Quintillion fiber-optic cable disturbance observations

The Quintillion fiber optic network is designed to deliver high-speed telecommunication services to remote areas of Alaska, including several northern villages (Falsey, 2017). One component of the system is a terrestrial fiber-optic cable installed along the Dalton Highway to connect Prudhoe Bay with Fairbanks (Baird, 2017). In March 2016, crews completed this portion of the network.

The cable is buried in a trench dug during the summer and winter of 2015–2016 that resulted in severe disturbance to vegetation and permafrost along the highway corridor between Prudhoe Bay and Fairbanks (Fig. 3.20–3.22). The disturbances are especially noticeable in tundra environments north of the Brooks Range. During our August 2016 field trip, we took 100 photographs of some of the damage in the area from approximate Dalton Highway mileposts 300 to 355. Forty selected photos are included in Appendix C.

3 Results & Discussion

Chapter 3 provides preliminary data analysis and discussion of the results. More in-depth analysis and discussion will be included in forthcoming publications.

3.1 Snow, water, and thaw-depths

3.1.1 Snow, water, and thaw along transects

March 2016 snow depths and August 2016 water depths and thaw depths are plotted against distance from the road along the five ArcSEES transects (Fig. 3.1a–e). Transect 4 had the deepest average depth of snow (47 ± 18 cm), water (13 ± 17 cm), and thaw (71 ± 20 cm) (Fig. 3.1f). Transect 3 had the shallowest and most highly variable snow depth (32 ± 22 cm). Most of the variation in snow, water, and thaw is caused by two factors: snowdrifts that form on both sides of the road in response to the elevated road berms, and microtopographic variation due to ice-wedge polygons. Now, water, and thaw data from all transects are provided in Appendix A, Tables A.2a and A.2b. All data collected from the five transects in 2014, 2015, and 2016 are available online at www.geobotany.uaf.edu/arcsees/data.

Figure 3.2 shows trends in snow, water, and thaw depth for each transect grouped by vegetation moisture category (dry & barren, moist, wet, and aquatic). This also groups the points into broad microtopographic categories: The dry sites correspond to the highest microsites (dry high-centered polygons, and roadside margins); moist sites correspond mainly to well-drained polygon centers and low-centered rims; wet sites are mainly polygon troughs and wetter low-centered polygon basins; and aquatic sites correspond to the low microsites in polygon troughs. The plots that are broken out by moisture category primarily show weakly decreasing trends in thaw and snow depth with distance from the road and less point-to-point variation than the plots for the entire transects (Fig. 3.2).

Snow depth. Snowdrifts form on both sides of roads. The depth and length of the drifts are affected by the height of the road above the tundra, the direction of the road with respect to the winter winds, and small slopes at the base of the road berms formed

by accumulated road dust. Prevailing winter winds at Deadhorse are from the ENE (Dolchok & Devine, 2006), resulting in deeper, harder, dustier drifts on the leeward (west) sides of roads. Winter storm winds are usually from the WSW, resulting in somewhat shallower, less dense, and cleaner drifts on the east sides of the roads. All four transects have the deepest snow near the road with a negative exponential regression with distance from the road (Fig. 3.1a–e).

The road surface at Colleen Site A is 1.25 m above the surface to the tundra. A dust slope forms at the base of heavily-traveled road berms due to the accumulation of road dust. At the Colleen site, this slope is approximately 25 cm high and 10 m long. This slope reduces the depth of the drift near the road. Maximum snow depth was 80 cm in the roadside drift along Transect 1 (windward side of the road) and 110 cm along Transect 2 (leeward side). The Airport site is on a curve, and the roadbed is inclined and elevated toward the outside of the curve, resulting in a shallower snowdrift (maximum depth 77 cm) on the inside (windward) of the curve along Transect 3, and a deeper snowdrift (maximum depth 122 cm) on the outside (leeward) of the curve along Transect 4.

The roadside drifts are deepest (over 100 cm) on the downwind side of the road at Transects 2 and 4, and shallowest on the upwind sides at Transects 1 and 3. Drift lengths downwind of the roads, although variable, generally are confined to within 25 m of the road, in agreement with literature stating that snowdrifts that form downwind of barriers such as snow fences are usually 10–15 times the height of the barrier forming the drift (Tabler, 1980).

Downwind of the drifts, snow depths mainly varied in association with ice-wedge-polygon microtopography (Fig. 3.3). For all transects combined, the deepest snow occurs in the sites with ponded water (51 ± 11 cm), and the shallowest snow occurs in

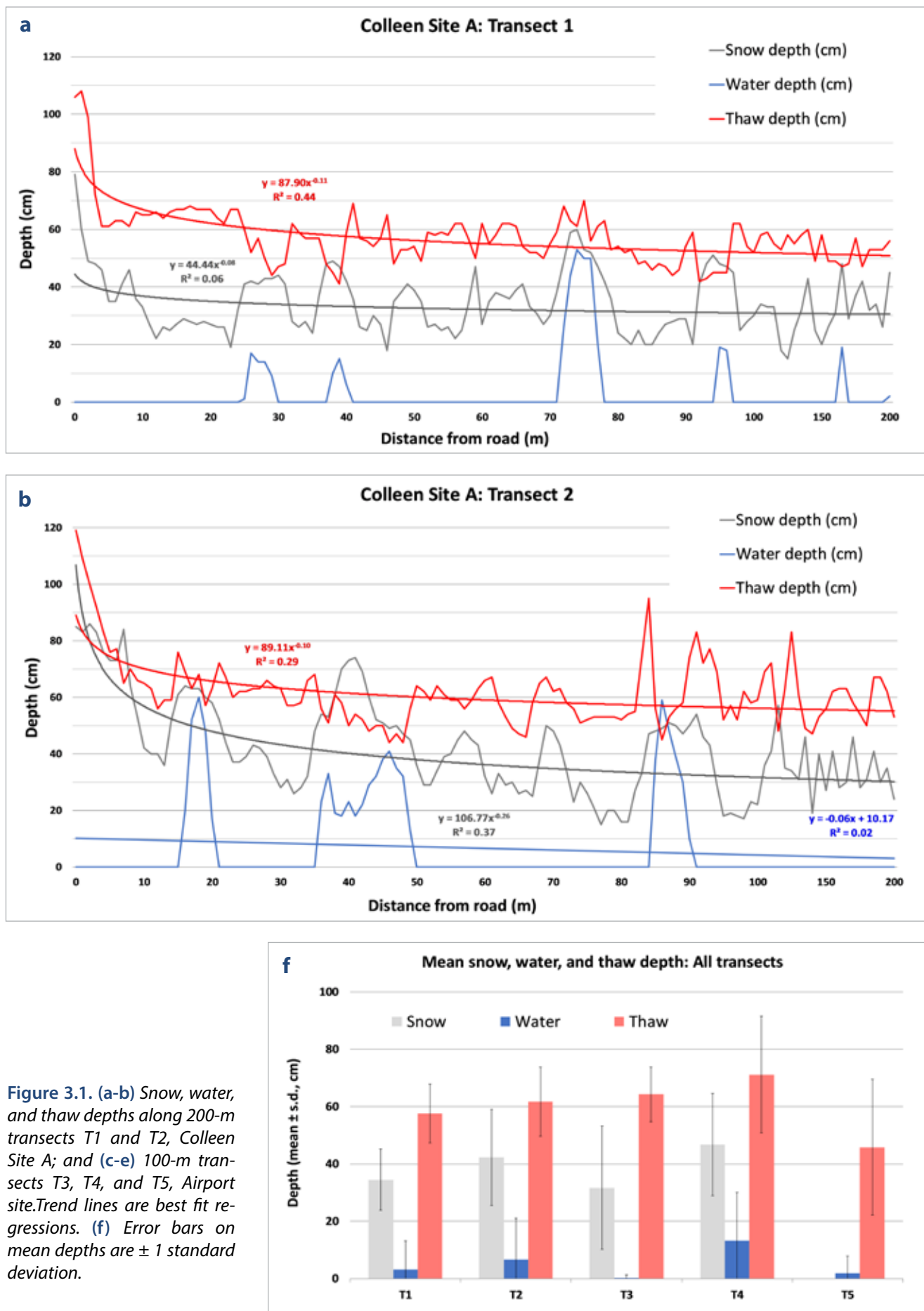


Figure 3.1. (a-b) Snow, water, and thaw depths along 200-m transects T1 and T2, Colleen Site A; and (c-e) 100-m transects T3, T4, and T5, Airport site. Trend lines are best fit regressions. (f) Error bars on mean depths are ± 1 standard deviation.



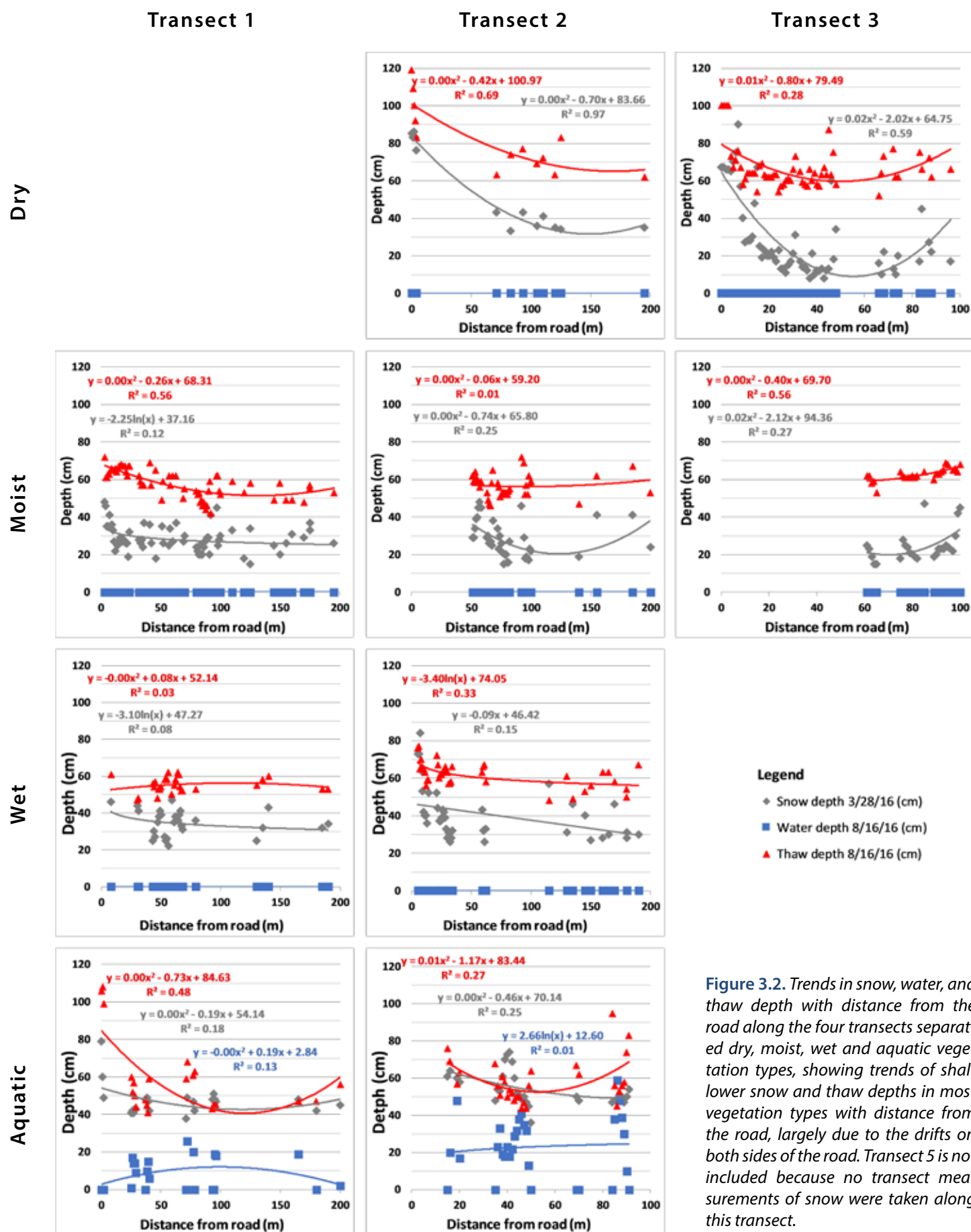


Figure 3.2. Trends in snow, water, and thaw depth with distance from the road along the four transects separated dry, moist, wet and aquatic vegetation types, showing trends of shallower snow and thaw depths in most vegetation types with distance from the road, largely due to the drifts on both sides of the road. Transect 5 is not included because no transect measurements of snow were taken along this transect.

Transect 4

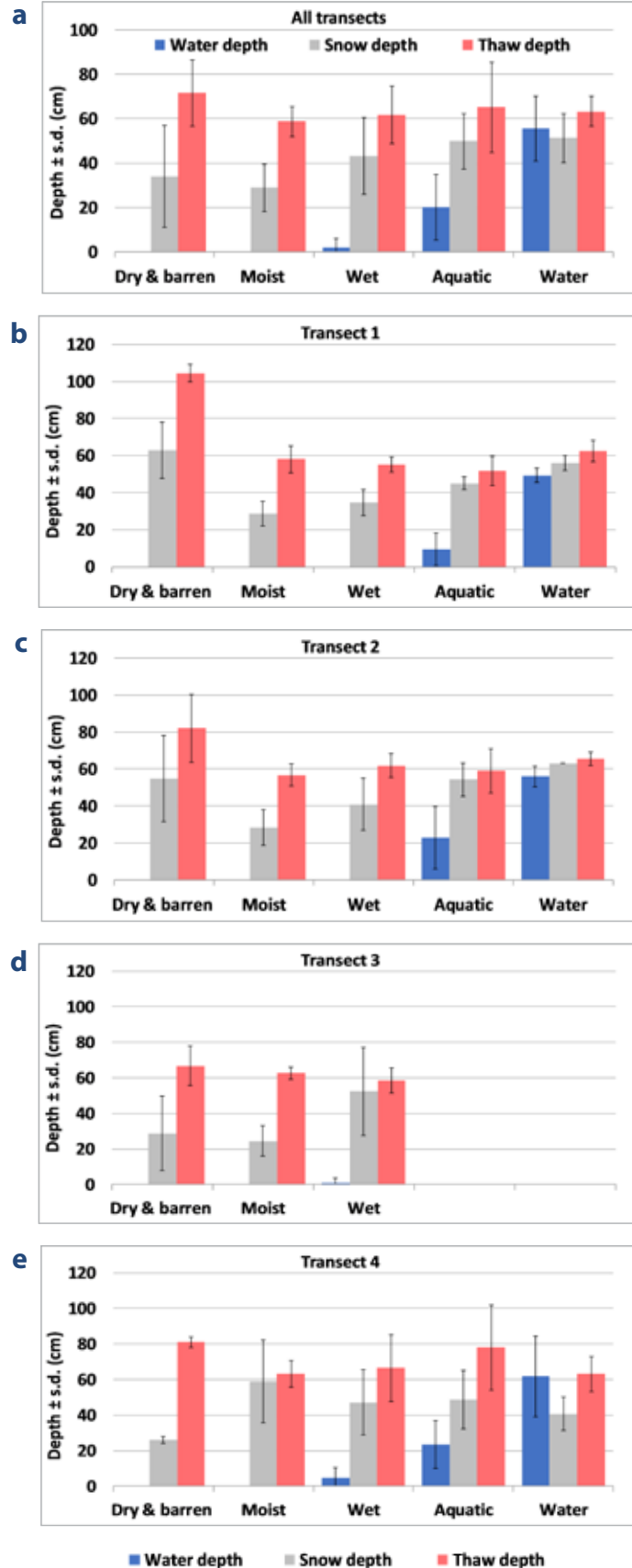
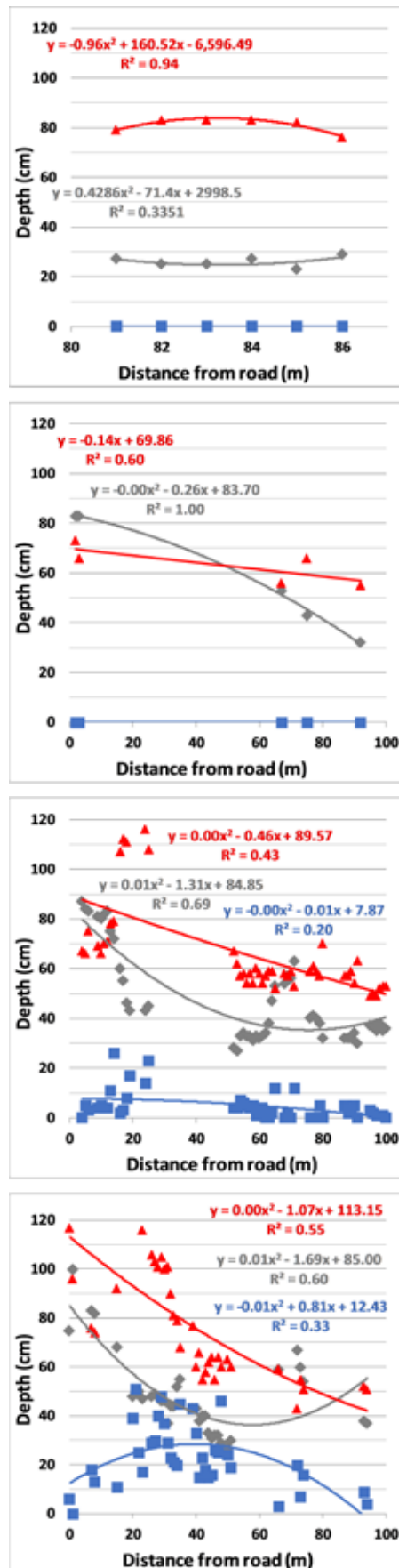


Figure 3.3. Mean snow, water, and thaw depth by vegetation moisture groups (a) across all transects and (b-e) by individual transect, T1–T4. Error bars are ± 1 standard deviation.

moist sites (29 ± 11 cm), mainly associated with moist polygon centers and rims. This varies considerably by transect. Transect 3 has the shallowest snow overall (32 cm), mainly because of the predominance of dry sites, with a mean snow depth of 29 cm, but also a very high standard deviation (± 21 cm) because of the high micro-topographic variation associated with the high-centered polygons.

Thaw depth. Overall, thaw depths show weak curvilinear trend with snow depth, and a very weak linear trend with water depth (Fig. 3.4). As with snow depths, thaw depths along all transects show high point-to-point variations due mainly to variations in microtopographic relief and moisture status of the soils associated with ice-wedge polygon troughs, centers, rims, and thermokarst ponds (Fig. 3.1). When grouped by moisture categories and all transects, thaw depths were greatest in the dry & barren sites and shallowest in the moist sites (Fig. 3.3a). The dry and barren category included sites in deep drifts adjacent to the roads, and dry tundra areas further downwind with shallow snow. Transect 3 consisted of well-developed high-centered polygons with shallow snow (29 ± 21 cm deep) on the dry polygon centers and deep snow (52 ± 25 cm deep) in the troughs (Fig. 3.3d). Transect 4 had the most disturbed vegetation caused by a variety of factors including roadside drifting, flooding, and displaced gravel, which resulted in the overall deepest snow, water, and thaw of the five transects (Fig. 3.3e). Along Transect 4, a large area of gravel displaced by a road washout from a previous flood was classed as barren and had relatively shallow snow (23–30 cm). Transect 4 had patterns of snow and thaw depth that were most variable within moisture categories.

Water depth. Water might be expected to be somewhat deeper near the roads on flooded sides of the road, but the trends for water depth vs. distance from the road for the flooded Transects 2 and 4 are very weak and are controlled mainly by the position of water-filled troughs along the transects (Fig. 3.1b, d). When grouped by moisture categories, as expected, the deepest water occurs in the unvegetated-water microsites (56 ± 15 cm), followed by aquatic vegetation sites (20 ± 15 cm), and wet vegetation (2 ± 4 cm). The entire set of thaw-depth measurements shows a weak positive nonlinear trend with snow depth (Fig. 3.4a) and essentially no trend with water depth (Fig. 3.4b).

3.1.2 Snow, water, and thaw depths at permanent plots

The snow, water, and thaw data from the permanent vegetation plots reflect many of the same trends as the data from the transects, but the trends with distance from the road are clearer because the sites were selected as representative of the conditions in polygon centers and troughs at distances of 5, 10, 25, 50, 100 and 200 m from the road. Mean snow depth, SWE, water depth, and thaw depth at the permanent plots are summarized by distance from the roads (Fig. 3.5) and grouped by all plots (Fig. 3.5a), centers (Fig. 3.5b), and troughs (Fig. 3.5c). Snow depths and SWE on 27–28 March 2016 at 5, 10, and 25 m from the road reflected the drifts which were mainly confined to the area within 25 m of the road. The average snow depth (with SWE in parentheses) across all plots at 5 m was 68 ± 22 (17 ± 6) cm, and 40 ± 17 (8 ± 4) cm at 25 m.

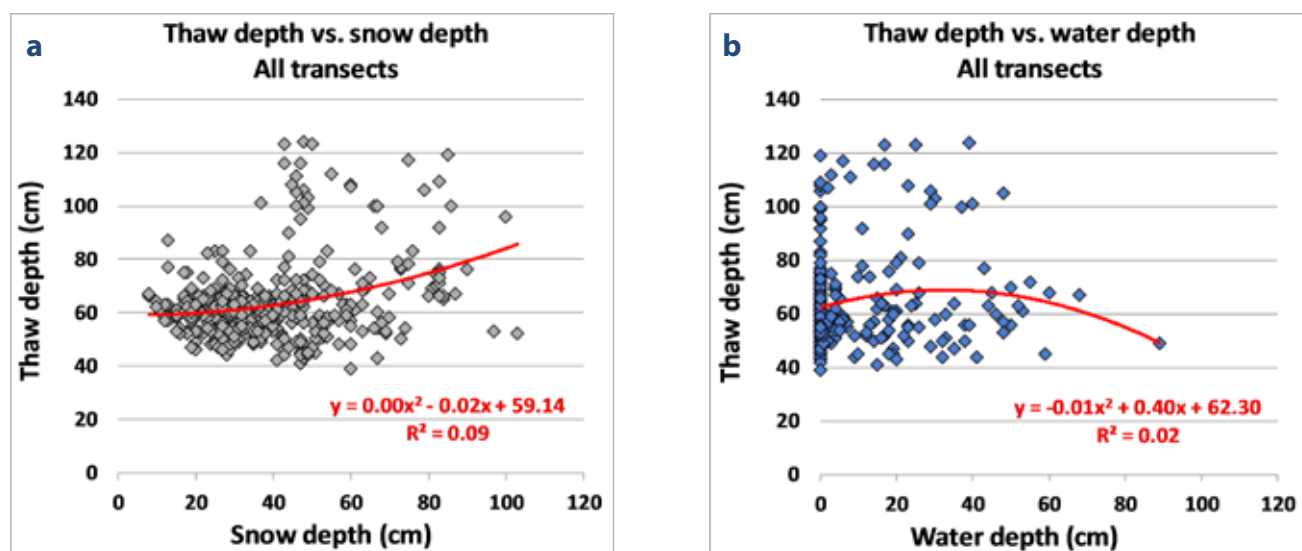


Figure 3.4. Thaw depth vs. (a) snow depth and (b) water depth at all points on Transects 1, 2, 3, and 4.

The snow depth (SWE) of plots in polygon centers averaged 57 ± 2 (14 ± 6) cm at 5 m; 52 ± 20 (14 ± 12) cm at 10 m; 30 ± 11 (6 ± 5) cm at 25 m; and 31 ± 6 (5 ± 2) cm at 100 m. The snow depths of plots in polygon troughs averaged 80 ± 19 (20 ± 6) cm at 5 m; 69 ± 23 (18 ± 8) cm at 10 m; 50 ± 17 (10 ± 3) cm at 25 m; and 53 ± 20 (13 ± 6) cm at 100 m.

Average thaw depths on 16–17 August 2016 across all permanent plots also decreased with distance from the road; but in contrast to snow, thaw was deeper in

ice-wedge-polygon centers than in the troughs because of drier soils and closer proximity to the frozen ice wedges. Thaw depths in polygon centers averaged 72 ± 7 cm at 5 m, 72 ± 23 cm at 25 m, and 58 ± 4 cm at 100. Thaw depths in polygon troughs averaged 62 ± 8 cm of thaw at 5 m, 62 ± 12 cm at 25 m, and 54 ± 4 cm at 100 m.

Water depths were greatest in the polygon troughs, and peaked overall at 10 m from the road, but showed no clear trend with distance from the road (Fig. 3.5c).

Snow, water, and thaw depths at the permanent plots were also strongly affected by which side of the road the transects were on with respect to the dominant wind direction and surface flow of water. Snow was generally deeper and dustier in polygon centers on Transects 2 and 4 on the downwind side of the road (see next section regarding dust in the snow drifts) compared with comparable plots in polygon centers on Transects 1 and 3. However, deeper snow occurred in polygon troughs on the upwind Transect 3 compared to troughs on Transect 4, because of greater trough-center microtopography contrasts on the upwind side of the road. Transects 2 and 4, which were on the flooded side of the roads, also had much more water in the troughs compared with troughs on Transects 1 and 3 respectively (Fig. 3.5c).

Appendix A, Tables A.3A and A.3B contain the snow depth, SWE, water depth, and thaw depth data from the permanent vegetation plots along each transect. (All data collected from plots in the 2014, 2015, and 2016 field seasons are available online at www.geobotany.uaf.edu/arcsees/data.)

3.1.3 Snow pit photos

Photos of the snow pits at each plot reveal some of the major differences in snow of the dusty roadside drifts (Fig. 3.6), compared to the relatively clean snow in mesic tundra sites far downwind of the road (Fig. 3.7). Snow in the roadside drifts is characterized by numerous dirty layers caused by road dust. Winds are predominantly from the ENE at Prudhoe Bay, so the dust is most conspicuous in snow drifts on the west side of the roads (Fig. 3.8). Photos from all snow pits are in Appendix B, along with descriptions of snow pits at plots T1-200-T, T2-005-C, T2-005-T, T2-200-C, T2-200-T, and T5-025-C, and T5-025-T.

3.2 Thermokarst-pond boreholes

One borehole (T1-74.0) (Fig. 3.9a) was drilled in Pond Marcel at 74 m on Transect 1, Colleen Site A. At the Air-

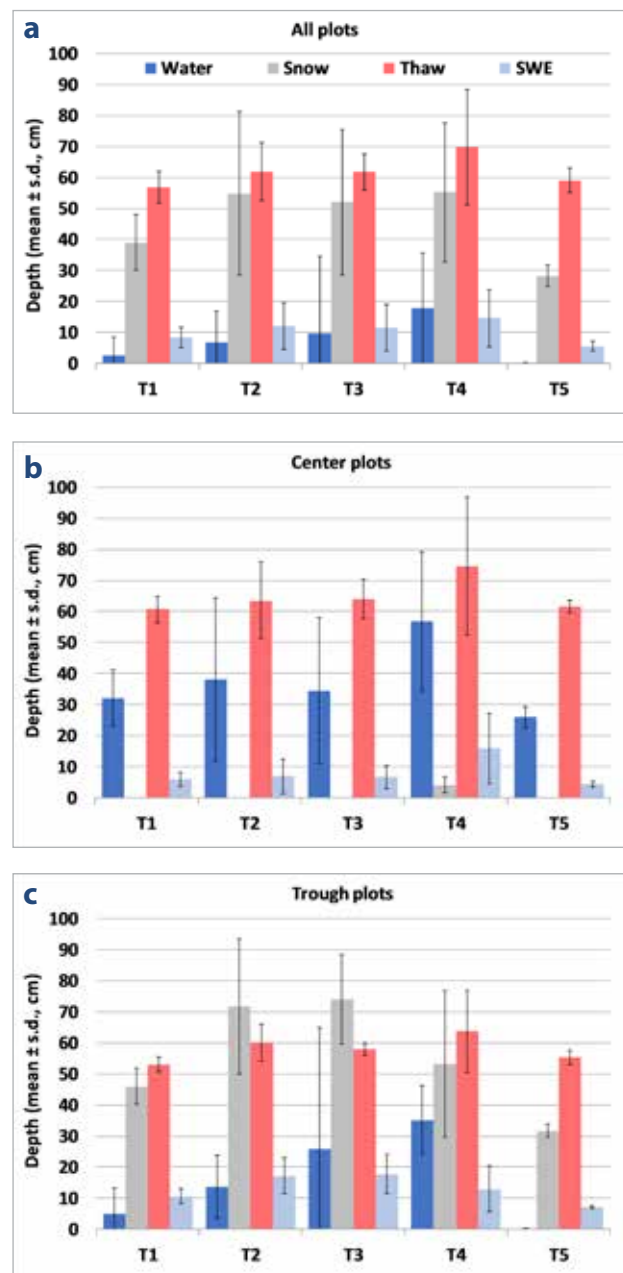


Figure 3.5. Mean snow (27–28 March 2016), water and thaw depth (16–17 August 2016), and snow water equivalent (SWE) for permanent plots grouped by transect, T1–T5, for (a) all plots, (b) plots in polygon centers, and (c) plots in polygon troughs. Error bars are one standard deviation.



Figure 3.6. Snow pit at plot T2-005-T (Colleen Site A, Transect 2, 5 meters from road, polygon trough). Note the overall deep snow (97 cm), brown layers of dirty snow caused by road dust, several layers of high-density wind-packed snow, a thin hard layer at 8–19 cm (probably caused by a rain-on-snow event), and the dirty depth-hoar layer at the base of the snowpack. See profile in Appendix B. Photo: DSC 8811.



Figure 3.7. Snow pit at plot T2-200-C (Colleen Site A, Transect 2, 200 meters from road, polygon center). Note shallow snow depth (28 cm), overall clean snow, and clean depth-hoar layer. The thin hard layer at 10–11 cm corresponds to the layer at 18–19 cm in Fig. 3.6. See snow profile in Appendix B. Photo: DSC 8858.



Figure 3.8. Dust coated snow on downwind side of the road near Toolik Lake. The dust has major consequences to the phenology of the snowpack, timing of emergence of roadside vegetation, and ecology of several species of birds and mammals. Photo: DSC 8997.

port site, highly disturbed gravelly soils and extensive deep flooding prevented drilling with the SIPRE corer. Instead, two boreholes (T5-95.5 and 96.8) (Fig. 3.9a, b) were drilled in a thaw pond along Transect 5.

Data from all boreholes at Colleen Site A and the Airport site are summarized in Appendix A, Tables A.4A and A.4B. Borehole data are organized by the stage of ice degradation and stabilization. They include both site characteristics (water depth, thaw depth) and core details (depth to permafrost, depth to massive ice, thickness of the frozen protective layer, and thickness of the intermediate layer).

Descriptions of the three boreholes drilled in March 2016 appear below.

Borehole T1-74.0 (Fig. 3.9a), 29 March 2016, in the old thermokarst pond (Pond Marcel) ~1.2 m to the east Transect T1.

0–37 cm – Pond ice, clean, colorless, without air bubbles.

37–106 cm – Frozen active layer and (possibly) transient layer: Ice-poor organic-mineral soil (mainly organic silt and sandy silt with inclusions of peat, coarse sand and small gravel), almost no visible ice, at 80–92 cm – friable silty peat (part of the active layer that lost moisture during the winter freezing).

106–123 cm – Frozen intermediate layer: Ice-rich sandy silt with coarse and organic inclusions; reticulate to ataxitic cryostructure, with distinctive horizontal ice layers ('belts') at 106–107 (~1.5 cm thick), 111–113 (2 cm thick), 115 (0.2 cm thick), and 120 (0.5 cm thick).

123–137 cm – Wedge ice, typical, with vertical foliation and thin elongated air bubbles, vertically oriented.

Analysis. The ice wedge at this site was well protected from thawing by the 17-cm-thick intermediate layer. The thickness of the frozen active layer (69 cm) was estimated based on differences in cryostructures and ice content. Probably this value also included the thickness of the transient layer because measurements of thaw depth performed at this site on 16 September 2015 showed that the active-layer thickness under the water in Pond Marcel (located at 71–78 m along Transect 1) varied from 48 to 67 cm, and the thaw depth nearby at 74 m on Transect 1 (~1 m from the drilling location) was 52 cm on both 10 August and 16 September 2015. This means that the probability of maximum thaw depth being greater than 69 cm at the drilling location was rather low, even con-

sidering frost heave caused by freezing of the active layer, which could slightly increase its thickness in the frozen state. Interestingly, the water depth at 74 m on Transect 1 was 50 cm on 10 August and 62 cm on 16 September 2015, while the thickness of pond ice on 29 March 2016 was only 37 cm. Based on high-resolution aerial photographs, Pond Marcel formed prior to 1949 when the first aerial photographs of the area were taken.

Borehole T5-94.5 (Fig. 3.9b), 28 March 2016, ~2.8 m to the north from the transect

0-32 cm – Pond ice, clean, colorless, without air bubbles.

32-55 cm – Open cavity.

55-73 cm – Loose debris at the cavity bottom: sublimated soil, ice crystals.

73-120 cm – Frozen active layer and (unlikely) transient layer: Ice-poor organic-mineral soil (mainly organic-rich silt with sub-vertically oriented inclusions of peat), almost no visible ice, at ~90-97 cm – friable silty peat (part of the active layer that lost moisture during the winter freezing), at 97-115 cm – ice-poor silt with some organics (friable at some parts), from ~115 – with several ice lenses and veins <0.1 cm thick.

120-128 cm – Wedge ice, typical, with vertical foliation and thin elongated air bubbles, vertically oriented.

Analysis. The ice wedge at this site was not protected from thawing by the intermediate layer, or (more likely) by the frozen transient layer. The thickness of the frozen active layer was 47 cm, which is very similar to the thaw depth measured on 21 September 2015 at the adjacent borehole T5-93.0 (45 cm) in the shallow part of the same pond, where the degrading ice wedge was not protected by any layers of frozen soil. The formation of a large cavity beneath the pond ice is a problem that still needs to be resolved. Based on high-resolution aerial photographs, this pond began to form in 1995 as the ice-wedges in the area were actively degrading.

Borehole T5-96.8 (Fig. 3.9c), 28 March 2016, ~3.8 m to the north from the transect

0-33 cm – Pond ice, clean, colorless, without air bubbles.

33-60 cm – Open cavity.

60-66 cm – Loose debris at the cavity bottom: sublimated soil, ice crystals.

66-114 cm – Frozen active layer and (possibly) transient layer: Ice-poor organic-mineral soil (mainly organic-rich silt with layers and inclusions of peat),

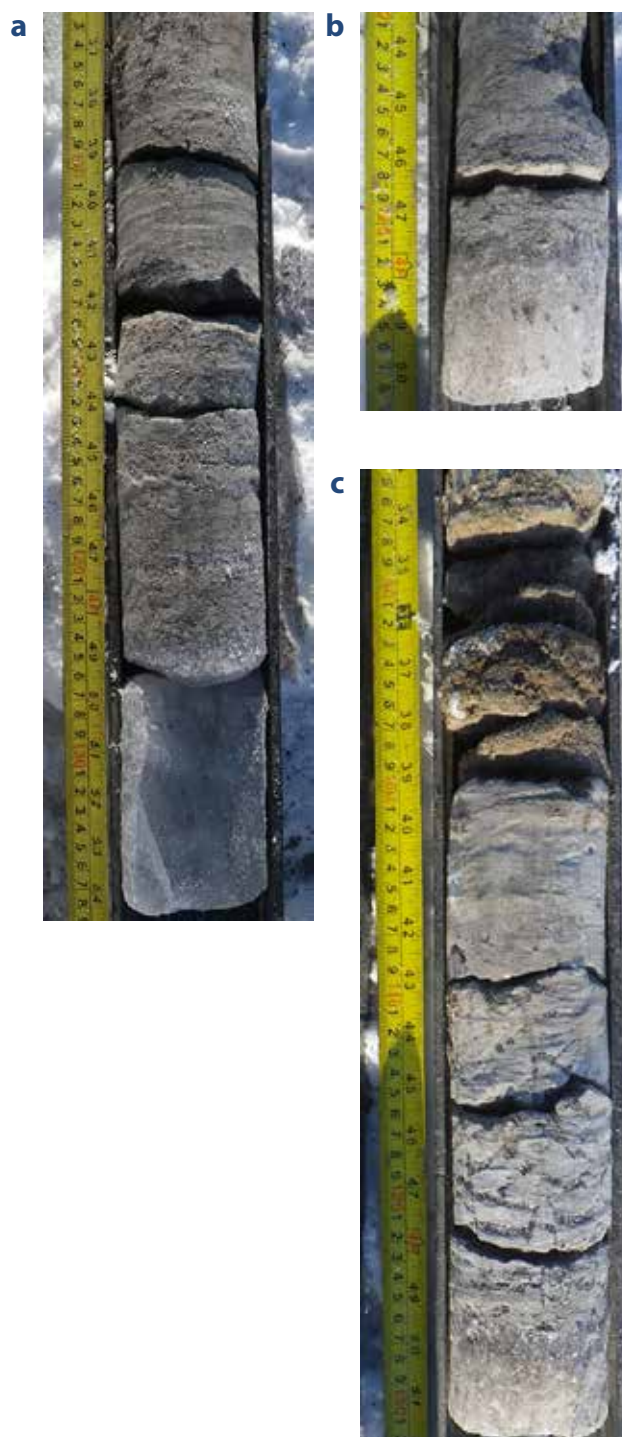


Figure 3.9. (a) Lower part of the frozen core obtained from Borehole T1-74.0 (Pond Marcel on transect T1). Permafrost table was detected at 106 cm based on differences in cryostructures and ice content. Photo: IMG P7694. (b) Lower part of the frozen core obtained from Borehole T5-94.5 on transect T5. Permafrost table was detected at 120 cm (above the ice wedge). Photo: IMG P7674. (c) Lower part of the frozen core obtained from Borehole T5-96.8 on transect T5. Permafrost table was detected at 114 cm based on differences in cryostructures and ice content. Photo: IMG P7687.

almost no visible ice, at ~90-102 cm – friable silt and peat (part of the active layer that lost moisture during the winter freezing), at 102-114 cm – ice-poor silt with some organics, from ~112 – with several ice lenses and veins <0.2 cm thick.

114-125 cm – Frozen intermediate layer: Ice-rich silt with reticulate cryostructure, ~30% visible ice, ice lenses <0.4 cm thick, mineral blocks ~0.5 x 2.0 cm.

125-131 cm – Wedge ice, typical, with vertical foliation and thin elongated air bubbles, vertically oriented.

Analysis. The ice wedge at this site was not protected from thawing by the 11-cm thick intermediate layer, or (more likely) by the transient layer. The

thickness of the frozen active layer was 48 cm, which significantly exceeds the thaw depth measured on 21 September 2015 (36 cm) at the adjacent borehole T5-100.6 in the shallow part of the same pond, where the ice wedge was protected by the 15-cm-thick, ice-poor transient layer and the 3-cm-thick, ice-rich intermediate layer. Thus, there is a possibility that the 48-cm-thick, ice-poor layer detected in the core of borehole T5-96.8 consisted not only of the active layer of 2015, but also included the transient layer of unknown thickness that remained frozen by fall 2015.

With the additional data obtained during the March 2016 drilling, we compiled cryostratigraphic cross-sections across and along ice-wedge troughs

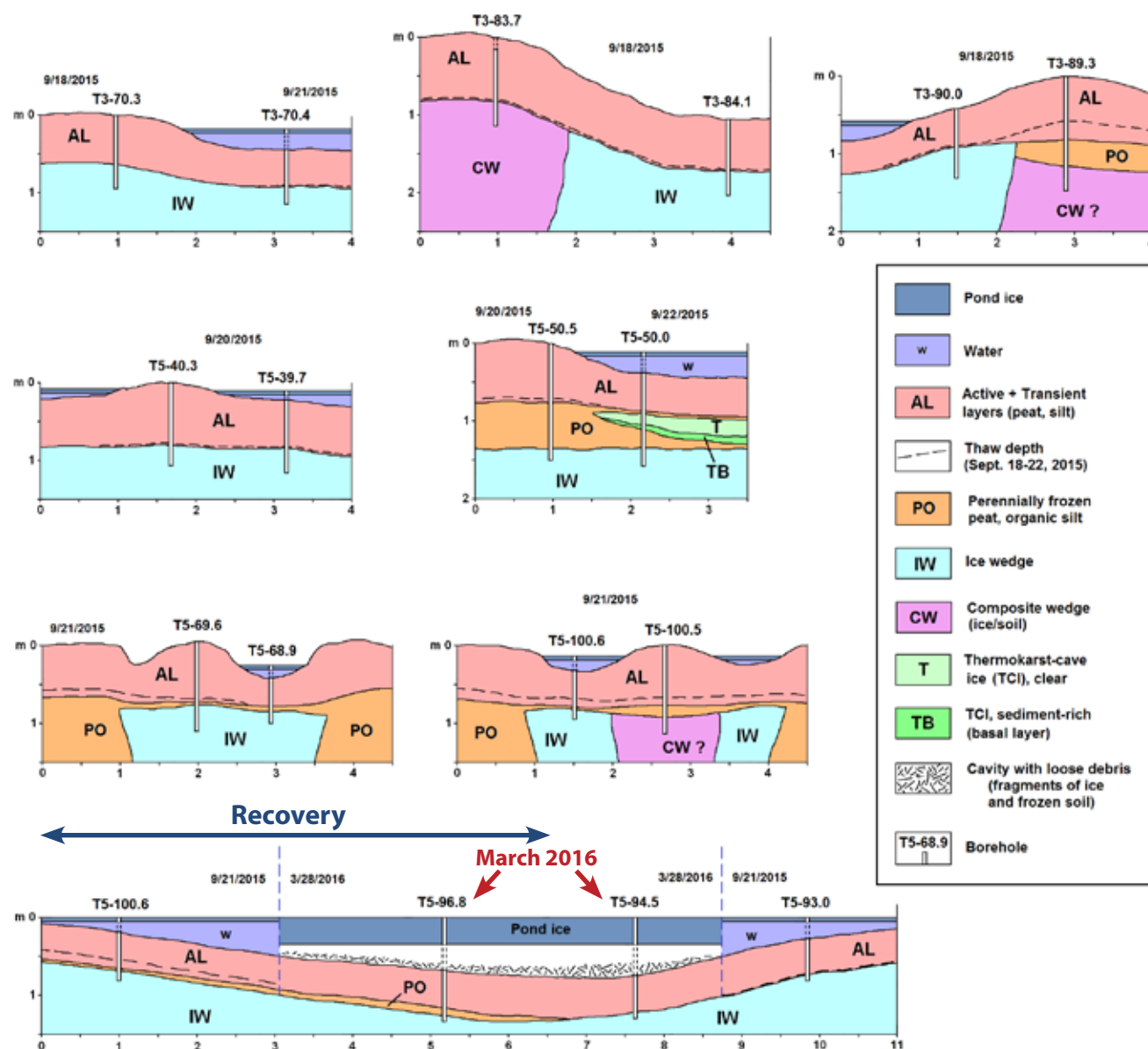


Figure 3.10. Cryostratigraphic cross-sections across and along ice-wedge troughs, Airport site. Boreholes are labeled by transect number (e.g. T3) and its distance in meters from the road. See Fig. 1.2b & c for location of boreholes.

for the Airport site, Transects 3 and 5 (Fig. 3.10), and we finalized identification of the stages of ice-wedge degradation/stabilization for all borehole locations within our study areas (Appendix A, Tables A.4A and A.4B).

3.3 Soil, snow, and air temperatures

Mean annual temperatures (MAT) for July 2015 to July 2016 are summarized in Appendix A by distance from road and height (depth) from soil surface for points along Transects 1 to 4 (Table A.5A) and at permanent vegetation plots (Table A.5B). In order to calculate a mean annual temperature, daily temperatures were interpolated as described in the Methods section (2.3.2) for the seven weeks in summer when temperature loggers were not recording data.

3.3.1 Temperatures in polygon centers and troughs

Mean annual surface temperatures were 1.6°C (± 0.86) colder in polygon centers (Fig. 3.11a) than in polygon troughs (Fig. 3.11b). Warmer mean annual soil-surface temperatures correspond to deeper trough depths (Fig. 3.12), most likely due to deeper winter snow in the deeper troughs. Mean annual surface temperatures were also warmer on wetter transects (T2, T4) than on drier transects (T1, T3) in both polygon centers and troughs (Figs. 3.11a & 3.11b). During the 2015 fall phase change from water to ice, temperatures in wet plots remained nearly constant at 0°C for up to 12 weeks (Fig. 3.13, green line, and Fig. 3.14, blue line), compared with 2–3 weeks in dry polygon centers. In dry troughs, soil surface temperatures remained close to but lower than 0°C during the same period, while in both wet and dry polygon centers, surface temperatures fell sharply after only 2 to 3 weeks near 0°C . Surface temperatures in dry centers were 10 to 20 degrees lower than in troughs in early December before significant snow accumulation (Figs. 3.13 & 3.14).

Fig. 3.13 illustrates how changes in snow depths during the winter differentially affect the soil temperatures in center vs. trough microsites. The continuous temperature records are shown for August 2015–July 2016 in a polygon center (Plot T1-050-C, yellow line) and an adjacent trough (Plot T1-50-T, green line). These plots are located along Transect 1 at Lake Colleen Site A. The flat polygonal terrain along this transect is comparable to the terrain at Vlad Romanovsky's Deadhorse permafrost-borehole, where a continuous record of

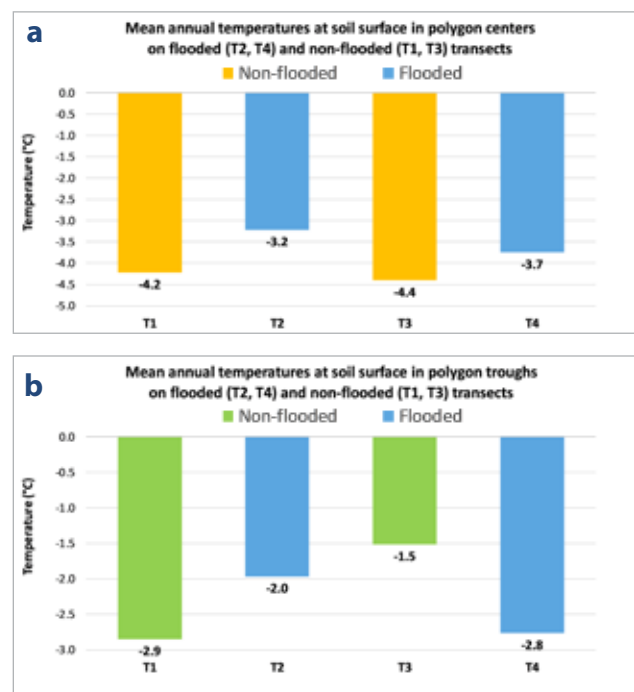


Figure 3.11. Mean annual surface temperatures in (a) polygon centers and (b) troughs on flooded (T2 and T4) vs. non-flooded transects (T1 and T3), July 2015–July 2016.

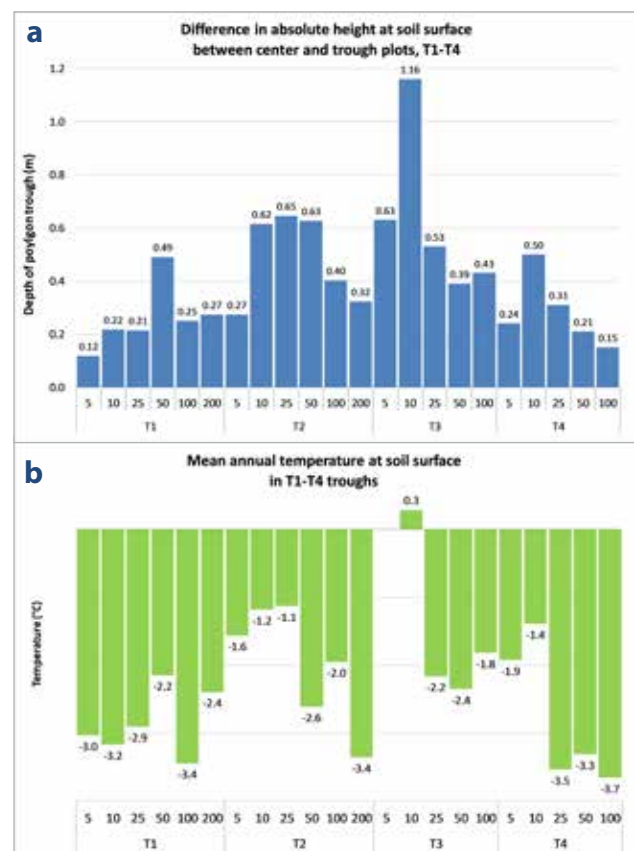


Figure 3.12. (a) Depth of polygon troughs and (b) mean annual surface temperatures in T1–T4 troughs, 2015–2016. Trough depth is measured by the difference in absolute height of vegetation plots established at polygon centers and troughs at the same distance from the road.

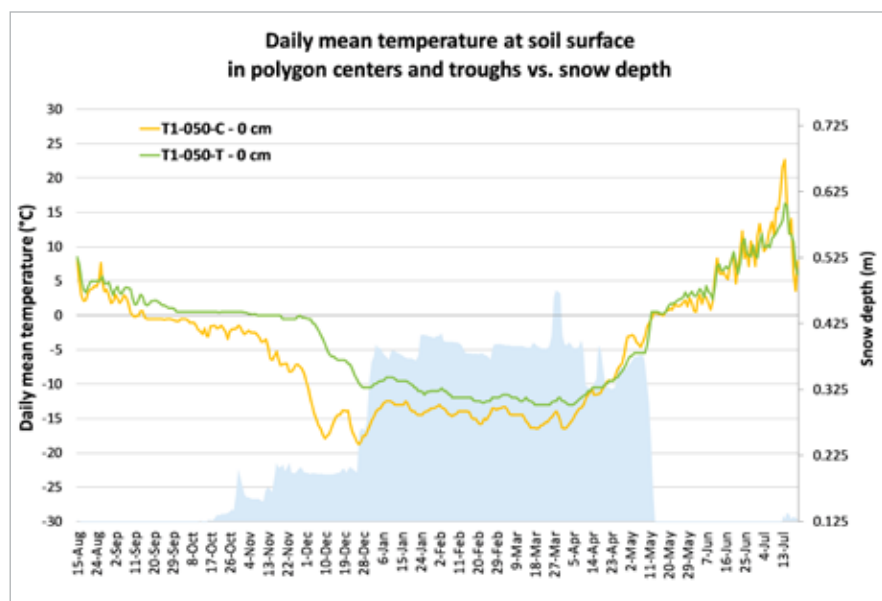


Figure 3.13. Daily mean surface temperature in polygon troughs and centers, compared with snow depth at Vlad Romanovsky's Deadhorse site (August 2015–July 2016). The 0.5 m deep trough 50 m from the road on Transect 1 (T1-50-T) held 50 cm of snow in March 2016 and 20 cm of water in August 2016, compared with 31 cm of snow and 0 cm of water at the nearby plot in the polygon center (T1-50-C). In Mean annual surface temperature in 2015–2016 was -2.2°C in the trough and -4.5°C in the center.

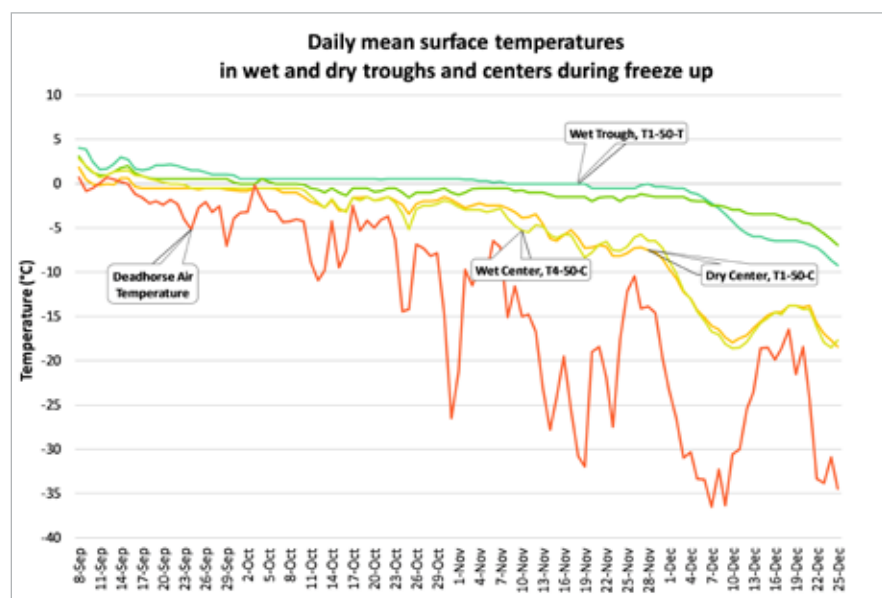


Figure 3.14. Daily mean air and soil-surface temperatures in wet and dry polygons during freeze up, September–December 2015. Following the drop in average daily air temperatures below freezing in Deadhorse on September 15, 2015, temperature at the soil surface stayed near 0°C for 12 weeks in both wet (T1-50-T) and dry (T3-25-T) troughs, compared with 3 weeks in wet (T4-50-C) and dry (T1-50-C) polygon centers. Deadhorse daily air temperature data are from Vladimir Romanovsky.

snow depth was recorded for the same winter using a Campbell Scientific Sonic Distance Sensor (Fig. 3.13, blue shaded area). Shallow snow, less than 20 cm deep, occurred in early winter (14 Oct–25 Dec), when soils temperatures were much colder in the polygon center than in the trough. Most likely the trough had collected deeper snow that insulated the soil from the cold air temperature. The difference in temperatures between the center and trough decreased after deeper snow developed in late December.

Soil temperatures were measured at 20 and 40 cm below the surface on all permanent vegetation plots. Mean annual temperatures decrease with soil depth on both polygon centers and troughs, but the difference between centers and troughs gets smaller with depth. The average difference between centers and

troughs across all transects (T1–T4) was -1.56°C at the soil surface, -1.38°C at -20 cm , and -1.28°C at -40 cm (Fig. 3.15), with centers experiencing colder temperatures than troughs.

The temperature contrasts between polygon centers and troughs is best illustrated along Transect 3, where the warmest winter temperatures (Fig. 3.11 b) were due to deep snow in many of the polygon troughs. The deepest trough along all four transects was T3-10-T, which had a center-trough contrast of 1.16 m, 71 cm water depth in August 2016, 85 cm of snow in March 2016, and a mean annual temperature of $+0.3^{\circ}\text{C}$ at the soil-surface—the only point in the two study areas with a mean annual surface temperature above 0°C in 2015–2016. (Note: Trough depths were not measured directly but are represented by the

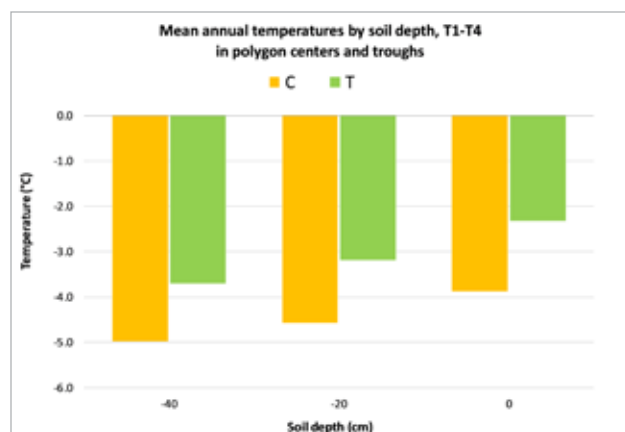


Figure 3.15. Mean annual temperatures decrease with soil depth on both polygon centers and troughs, but the difference between centers and troughs gets smaller with depth. The average difference across all transects (T1-T4) is -1.56°C at the soil surface, -1.38°C at -20 cm , and -1.28°C at -40 cm .

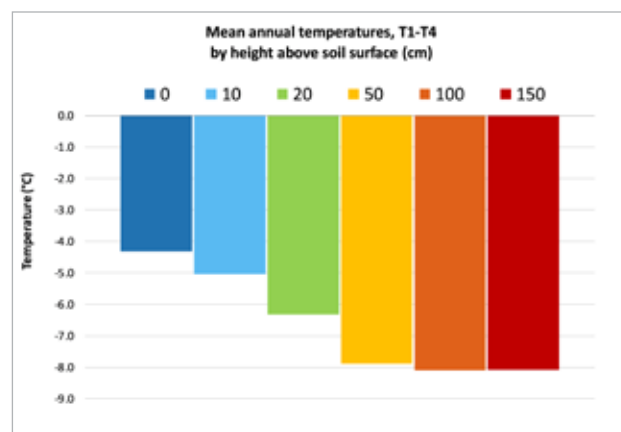


Figure 3.16. Mean annual air temperatures decrease with distance from the ground due primarily to winter snow accumulation. In 2015-2016, the snow pack moderated temperatures up to 50 cm from the ground. The MAT at the surface on T1-T4 was 3.8 degrees warmer than at 100 cm in the air.

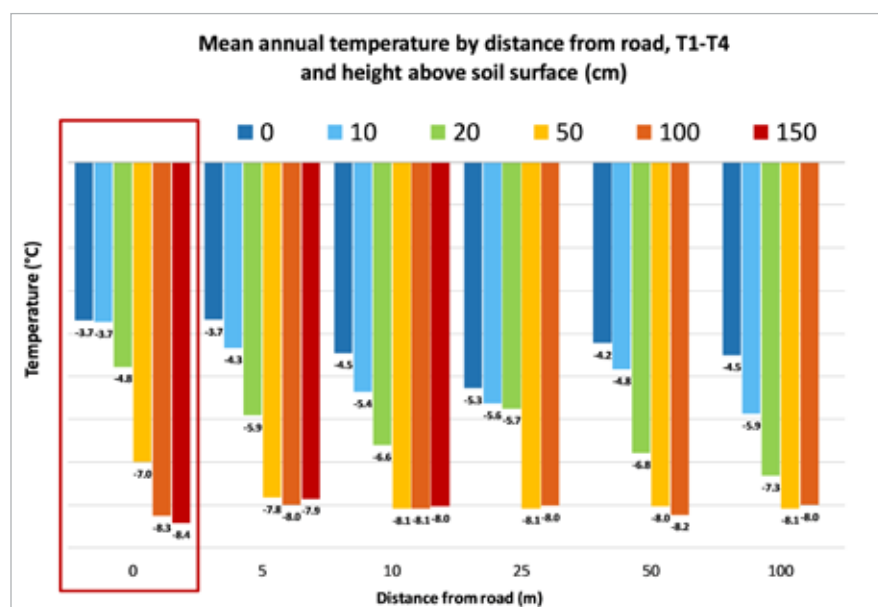


Figure 3.17. The difference in ground and air temperature is greatest at the road berm (where the snow pack is deepest) and decreases with height above surface and distance from the road. In 2015-2016, the mean annual surface temperature within 5 meters from the road was $0.5 - 1.6^{\circ}\text{C}$ higher than surface temperatures further from the road. The deeper snow pack at the road berm (red rectangle) insulated the air temperature up to 50 cm from the ground.

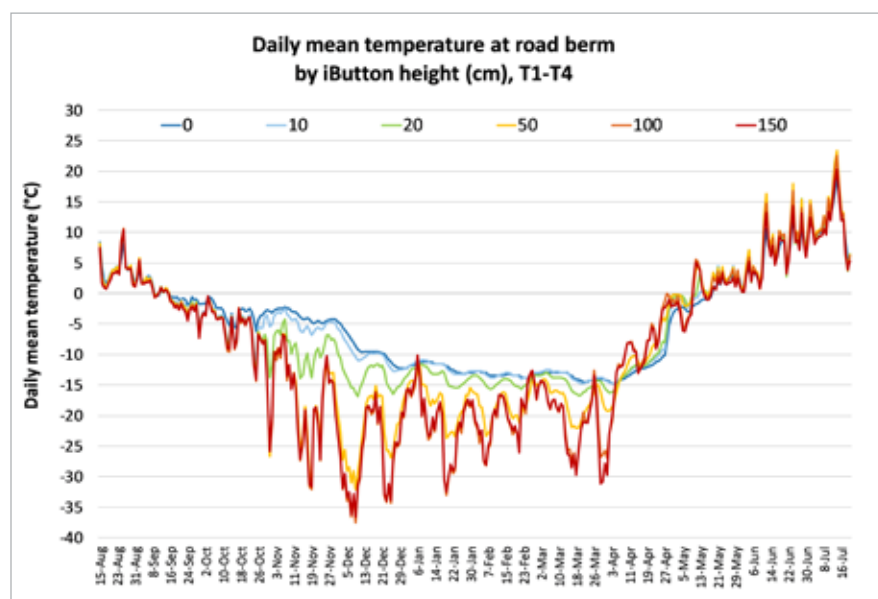


Figure 3.18. Early in winter (2015-16), snow pack at the road berm insulated iButtons near the ground ($0-10\text{ cm}$) from falling temperatures and daily extremes (blue lines). By early November, enough snow had accumulated next to the road to moderate temperatures up to 20 cm above the surface (grey line). At 50 cm (yellow line), snow had a small moderating effect on temperature starting in December. Once the air temperature started rising in April, iButtons above the snow pack ($50-100\text{ cm}$) recorded higher daily temperatures than iButtons nearer the ground until the snow melted in mid-May.

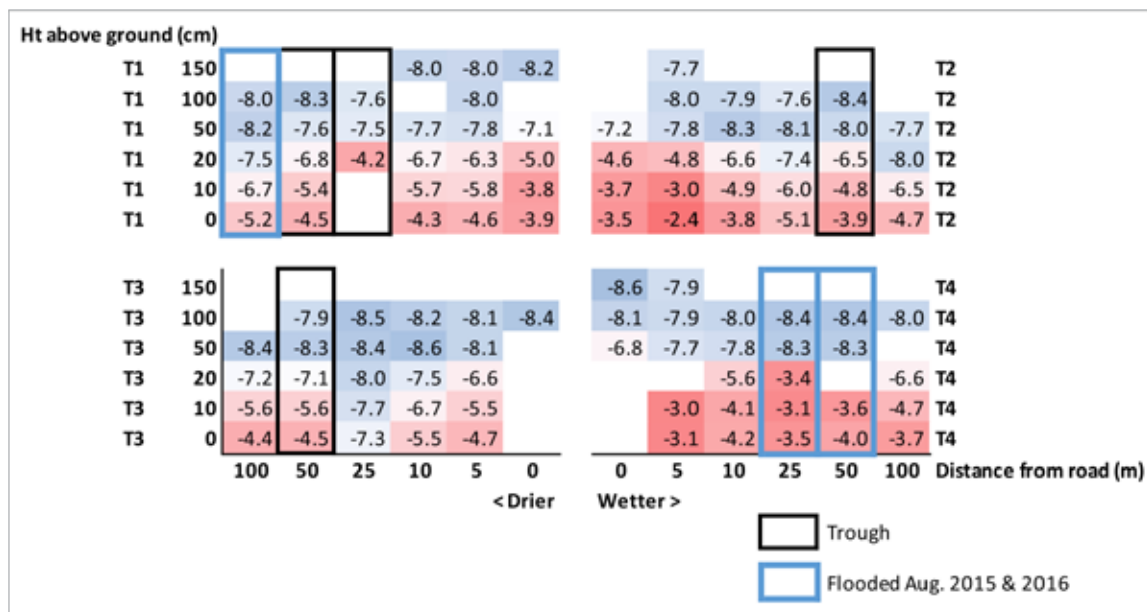


Figure 3.19. Heat map showing mean annual temperatures along four transects (T1-T4) by height above the soil surface and distance from the road, July 2015 to July 2016. The highest temperatures are shaded the deepest red and the lowest are shaded the deepest blue. Black borders indicate where the transect crosses a polygon trough. Blue border are transect points that were flooded when water depth was measured in August 2015 and 2016. The highest mean annual temperatures were recorded on the wetter transects (right side of the figure) at the soil surface. On dry transects the highest temperatures were found near the soil surface and the road bed (center of figure).

difference between the absolute height measured at the center of a vegetation plot in the polygon trough compared with the absolute height of the adjacent plot in the polygon's center.) Aerial photos taken in 1949, show that the area in the vicinity of Transect 3 was originally covered in wet low-centered polygons. Altered drainage patterns caused by construction of the Dalton Highway and westward migration of the Sagavanirktok River led to deep erosion of the ice-wedge polygon troughs and drainage of the originally wet-tundra landscape. Transect 3 now passes through high-centered polygons on well-drained low bluff of the Sagavanirktok River with deeply eroded troughs and generally dry polygon centers.

3.3.2 Air temperature on transects

Air temperature was recorded at 0, 10, 20, 50, and 100 cm above the ground at intervals along four transects (T1-T4). Air temperature was also measured at 150 cm from the ground at transect points nearest the road berm (0, 5, 10 m from the road) where snow accumulation was expected to be deepest. At all points along the transect, mean annual temperatures for July 2015 to July 2016 were highest at the soil surface (-4.3°C) and lowest at 100-150 cm above the surface (-8.1°C) (Fig. 3.16). The largest differences between ground and air temperatures were at the road berm (0 m)

where mean annual surface temperatures were 4.6°C warmer than the air temperature 100 cm above the ground. The deeper snow pack next to the road moderated air temperatures up to 50 cm from the ground (Figs. 3.17 & 3.18). The moderating effect of snow on winter temperatures can be seen at all distances from the road but is greatest within 5 m of the road.

3.4 Quintillion fiber optic cable disturbance observations

Photos of sections of the Quintillion fiber-optic-cable trench document damage to the tundra and permafrost (Appendix C). The damage is especially visible in tundra environments north of the Brooks Range. Severe damage occurred in the scenic Atigun Pass area and north through the Arctic Foothills (Fig. 3.20) and across the Arctic Coastal Plain. Removal of the vegetation mat and ponding of water is causing subsidence of the surface, which is especially severe in hilly areas such as the Sagwon Upland, where the trench has exposed massive ground ice to thermal erosion (Fig. 3.21).

At the northern end of the Dalton Highway, the cable also played a role in the damage caused by the 2015 Sagavanirktok Flood. The cable trench formed the break point where the tundra developed massive erosion of ice wedges (Fig. 3.22).



Figure 3.20. Severe tundra disturbance caused by placement of the Quintillion fiber optic cable in summer, near Milepost 305 of the Dalton Highway, 16 August 2016. The width of the damaged tundra in sections constructed in summer is approximately 8.5 m. Photo: DSC 9199.



Figure 3.21. Thermokarst in the trench of the Quintillion fiber optic cable, Sagwon Upland, near Milepost 355 of the Dalton Highway, 16 August 2016. Photo: DSC 9275.



Figure 3.22 (a) Washed out section of the Dalton Highway near the Deadhorse Airport caused by the 2015 Sagavanirktok River flood. Floodwaters threatened the Deadhorse Airport runway (beyond the upper margin of the photo), and the highway acted as a dam preventing water from flowing away from the airport toward the Sagavanirktok River (lower right). When the road was breached to allow floodwaters to drain away from the airport, massive erosion of ice wedges occurred between the Quintillion fiber optic cable trench and the river. Approximate locations and directions of the photos in (b) and (c) are shown by the white arrows in photograph (a). Orange fiber optic cables are visible in all three frames. Photos courtesy of AK Department of Transportation & Public Facilities.

4 Conclusions

Two previous data reports presented the principal data collected during surveys of the five transects and 48 permanent vegetation plots at Colleen Site A (Walker *et al.*, 2015) and the Airport site (Walker *et al.* 2016a) in August 2014 and 2015. This data report presents information from these same sites collected in 2016: (1) snow, water, and thaw measurements taken along the five transects and at 48 permanent vegetation plots, plus a table summary of all data collected in 2014, 2015 and 2016; (2) winter permafrost boreholes in thermokarst ponds drilled in March 2016; (3) temperature data from transects and plots collected with iButton® data loggers in 2014-2016; and, (4) photographs of impacts related to the Quintillion fiber optic cable taken in August 2016.

The following brief statements summarize the major conclusions from each of these efforts. These are followed by broader conclusions regarding cumulative effects of roads and related impacts.

4.1. Summary of major findings

4.1.1 Snow, water, and thaw along transects and at permanent plots

- Snowdrifts that form on both sides of the road are mainly limited to within 25 m from the road. Snow is deeper, denser, and dirtier near the roads. The depth and length of the drifts were affected by the height of the road above the tundra and the direction of the road with respect to winter winds. The snowdrifts strongly affect patterns of snow, water, thaw depths and soil temperatures.
- Outside of the area of the roadside drifts, snow depths, water depths, and thaw depths were deepest in ice-wedge polygon troughs with wet or aquatic tundra vegetation and were shallowest in the centers of polygons with dry or moist tundra vegetation. The variance in snow depths generally conforms to the variation in the underlying micro-topography associated with the ice-wedge polygons.
- Snow pits at permanent plots within 25 m of the roads had large amounts of dust that were most

noticeable in the drifts on the west sides of the roads and within hard dusty horizons of the snow profiles. The amount of dust was not measured in this study, but other studies have quantified the amount of road dust at varying distances from roads in the Prudhoe Bay area and at other sites along the Dalton Highway using a variety of dust trap designs (Everett 1980, Klinger *et al.*, 1983).

- Snow and thaw also interact in complex ways with road dust and the distribution of water to affect vegetation, soil temperatures, ice in ice-wedges, and local ecosystems near the roads.

4.1.2 Thermokarst-pond boreholes

- Study of the frozen cores obtained from ice-wedge troughs confirmed the idea that stabilization and recovery of degrading ice wedges in the areas of cold continuous permafrost commonly start beneath thermokarst ponds as a result of accumulation of organic matter and mineral soils (Jorgenson *et al.*, 2006, 2015; Kanevskiy *et al.*, 2016, 2017).
- Results of coring at Pond Marcel were particularly interesting because this pond has been relatively stable since at least 1949, when it was visible in an aerial photo. Occurrence of the ice-rich, 17-cm-thick intermediate layer above the ice wedge explains this long-term stability.
- Compared to the ice-wedges sampled at Colleen Site A, those at the Airport site are more susceptible to degradation. At Colleen Site A, thawing ice wedges were encountered in only two of 35 boreholes, both of them at T1 (~9% of boreholes of this transect). At the Airport site, thawing at the time of drilling (August 2014), an ice-rich intermediate layer (PL3) up to 61 cm thick was encountered in 12 boreholes (two at T3 and 10 at T5); the average thickness of the intermediate layer was 4.8 cm (Tables 4.4B). At the highly disturbed Airport site Transect 3, half of the sampled ice wedges were degrading by the end of summer, 2015, while in the relatively undisturbed and better-vegetated tundra along Transect 5, 10% of the ice wedges were degrading.

4.1.3 Air, snow, and soil temperatures

- Daily and mean annual soil temperatures are strongly influenced by the presence of water and snow, which in turn are influenced by the microtopography created through thermokarst and construction of elevated road beds.
- Mean annual surface temperatures are highest in polygon troughs, which accumulated more water and snow than the surrounding tundra. The temperature differences between centers and troughs diminishes with both height above and depth beneath the soil surface.
- Annual temperatures in both polygon centers and troughs are higher in wet plots than dry plots. During the phase change from water to ice in fall 2015, temperatures in wet plots remained constant at 0° C for up to 12 weeks, while in dry plots temperatures started to fall sharply with the air temperature after 2 to 3 weeks near 0° C.
- The largest differences between ground and air temperatures along transects were at the road berm (0 m) where the snow pack moderated air temperatures up to 50 cm from the ground. The moderating effect of snow on winter temperatures can be seen at all distances from the road but is greatest within 5 m of the road.

4.1.4 Quintillion Fiber Optic Cable

- The construction of the cable trench resulted in extensive damage to the tundra and permafrost along much of the length of the cable and is particularly noticeable north of the Brooks Range.
- The trenching was apparently permitted without an environmental assessment. The only record we could find regarding the decision to permit this activity was a BLM memorandum of the decision record, dated 27 October 2015.
- Major questions that should be addressed include: Why such extensive summer off-road activity was permitted that would clearly lead to major damage to tundra vegetation? Why greater precautions were not taken in areas with known massive ground ice deposits? Why areas

with very high scenic value such as Atigun Pass and large areas of the North Slope were not treated with special consideration?

- The contribution of the cable trench to damages caused by the 2015 Sagavanirktok River flood also need to be considered in future planning for possible consequences of these trenches.

4.2 Future directions

To date, published papers and conference presentations from this study have focused on the history of infrastructure expansion on the North Slope, increased thermokarst and wetness of the region (Walker *et al.*, 2014; Reynolds *et al.*, 2014a; Reynolds & Walker, 2016; Walker *et al.*, 2017), studies and evaluation of the risks of degradation of ice wedges (Kanevskiy *et al.*, 2016; 2017), permafrost-related causes and consequences of the Sagavanirktok River flood (Shur *et al.*, 2016), vegetation changes related to the Spine Road (Reynolds *et al.*, 2014b), and development of an international consortium to examine Rapid Arctic Transitions due to Infrastructure and Climate (RATIC) (Walker *et al.*, 2016).

Taken together, the major findings of these investigations are that flooding, road dust, and snowdrifts all contribute to warmer soil temperatures, deeper active layers, and development of thermokarst near roads. These factors also alter the plant canopy, which in turn further alters the surface albedo and ground temperatures, creating a positive feedback to thermokarst processes. A negative feedback discovered by this project is caused by increased plant production in wet thermokarst areas that helps protect ice-wedges from degradation.

A major focus for the near future will be closer examination of changes to the vegetation. We will combine the Colleen and Airport datasets and compare them with vegetation data collected in the 1970s to assess changes to the structure and species composition. Information in this and two previous data reports will provide the basis for a multidisciplinary analysis at the long-term effects of roads in this economically and ecologically important region of Alaska.

5

References

- Baird, K., 2017. Crews install fiber optic cable from Prudhoe Bay to Fairbanks. Fairbanks Daily News-Miner.
- BLM. 2015. Quintillion Fiber Optic Line, Decision Record–Memorandum. NEPA ePlanning, U.S. Bureau of Land Management.
- Colbeck, S., E. Akitaya, R. Armstrong *et al.* 1992. The international classification for seasonal snow on the ground. The International Commission on Snow and Ice of the International Association of Scientific Hydrology, co-issued by International Glaciological Society.
- Dolchok, C., and M. Devine. 2006. Wind resource assessment for Deadhorse, Alaska. Alaska Energy Authority.
- Everett, K. R. 1980. Distribution and properties of road dust along the northern portion of the Haul Road. Environmental engineering and ecological baseline investigations along the Yukon River–Prudhoe Bay Haul Road. Pages 101–128 *in* CRREL Report 80-10. U.S. Army Cold Regions Research and Engineering Laboratory, Hanover, New Hampshire, USA.
- Falsey, J. L. 2017. Fiber-optic broadband set to go live in northern Alaska by year's end. Anchorage Daily News. URL <https://www.adn.com/business-economy/2017/05/08/quintillion-ceo-fiber-based-broadband-set-to-go-live-in-alaska-by-end-of-the-year/> [accessed 31 July 2018].
- Jorgenson, M. T., M. Kanevskiy, Y. Shur, N. Moskalenko, D. R. N. Brown, K. Wickland, *et al.* (2015) Role of ground ice dynamics and ecological feedbacks in recent ice wedge degradation and stabilization. *Journal of Geophysical Research: Earth Surface* 120:2280–2297.
- Jorgenson, M. T., Y. L. Shur, and E. R. Pullman. 2006. Abrupt increase in permafrost degradation in Arctic Alaska. *Geophysical Research Letters* 25: L02503.
- Kanevskiy, M., Y. Shur, T. Jorgenson, *et al.* 2017. Degradation and stabilization of ice wedges: Implications for assessing risk of thermokarst in northern Alaska. *Geomorphology* 297:20–42.
- Kanevskiy, M., Y. Shur, D. A. Walker, *et al.* 2016. Evaluation of risk of ice-wedge degradation, Prudhoe Bay Oilfield, Alaska. Pages 999–1001 *in* F. Günther, and A. Morgenstern, editors. XI. International Conference On Permafrost – Book of Abstracts, 20–24 June 2016, Potsdam, Germany. Bibliothek Wissenschaftspark Albert Einstein [doi: 10.2312/GFZ.LIS.2016.001].
- Klinger, L. F., D. A. Walker, M. D. Walker, and P. J. Webber. 1983. Chapter 6: The effects of a gravel road on adjacent tundra vegetation. Pages 6/i–6/162 *in* Prudhoe Bay Waterflood Project Environmental Monitoring Program 1982. U.S. Army Corps of Engineers, Anchorage, Alaska, USA.
- Raynolds, M. K., D. A. Walker. 2016. Increased wetness confounds Landsat-derived NDVI trends in the central Alaska North Slope region, 1985–2011. *Environmental Research Letters* 11:085004.
- Raynolds, M. K., D. A. Walker, K. J. Ambrosius, *et al.* 2014a. Cumulative geocological effects of 62 years of infrastructure and climate change in ice-rich permafrost landscapes, Prudhoe Bay Oilfield, Alaska. *Global Change Biology* 20:1211–1224.
- Raynolds, M. K., D. A. Walker, M. Buchhorn, and L. M. Wirth. 2014b. Vegetation changes related to 45 years of heavy road traffic along the Spine Road at Prudhoe Bay, Alaska. *Arctic Change* 2014, 8–12 December 2014, Ottawa, Ontario, Canada.
- Shur, Y., M. Kanevskiy, D. A. Walker, M. T. Jorgenson, M. Buchhorn, M. K. Raynolds. 2016. Permafrost-related causes and consequences of the Sagavanirktok River delta flooding in Spring 2015. Pages 1014–1016 *in* F. Günther, and A. Morgenstern, editors. XI. International Conference On Permafrost – Book of Abstracts, 20–24 June 2016, Potsdam, Germany. Bibliothek Wissenschaftspark Albert Einstein [doi: 10.2312/GFZ.LIS.2016.001].
- Tabler, R. D. 1980. Geometry and density of drifts formed by snow fences. *Journal of Glaciology* 26:405–419.
- Walker, D. A. 1985. Vegetation and Environmental Gradients of the Prudhoe Bay Region, Alaska. CRREL Report 85-14. U.S. Army Cold Regions Research and Engineering Laboratory, Hanover, New Hampshire, USA. Retrieved from <http://acwc.sdp.sirsi.net/client/search/asset/1006803>

- [accessed 29 July 2018].
- Walker, D. A., M. K. Raynolds, M. Buchhorn, and J. L. Peirce, editors. 2014. Landscape and permafrost change in the Prudhoe Bay Oilfield, Alaska. Alaska Geobotany Center Publication AGC 14-01. Institute of Arctic Biology, University of Alaska Fairbanks, Fairbanks, Alaska, USA.
- Walker, D. A., M. Buchhorn, M. Kanevskiy, *et al.* 2015. Infrastructure-Thermokarst-Soil-Vegetation Interactions at Lake Colleen Site A, Prudhoe Bay, Alaska. Alaska Geobotany Center Data Report AGC 15-01. Institute of Arctic Biology, University of Alaska Fairbanks, Fairbanks, Alaska, USA.
- Walker, D. A., M. Kanevskiy, Y. L. Shur, M. K. Raynolds, M. Buchhorn, and L. M. Wirth. 2016a. Road Effects at Airport Study Site, Prudhoe Bay, Alaska, Summer 2015. Alaska Geobotany Center Data Report AGC 16-01. Institute of Arctic Biology, University of Alaska Fairbanks, Fairbanks, Alaska, USA.
- Walker, D. A., J. L. Peirce, T. Kumpula, *et al.* 2016b. Rapid Arctic Transitions due to Infrastructure and Climate (RATIC): An ICARP III initiative focusing on the cumulative effects of Arctic infrastructure and climate change. Pages 1234–1236 in F. Günther, and A. Morgenstern, editors. XI. International Conference On Permafrost – Book of Abstracts, 20–24 June 2016, Potsdam, Germany. Bibliothek Wissenschaftspark Albert Einstein [doi: 10.2312/GFZ.LIS.2016.001].
- Walker, D. A., M. Kanevskiy, Y. Shur, M. K. Raynolds, M. Buchhorn, and G. Matyshak. 2017. Rapid transitions caused by infrastructure and climate, Prudhoe Bay Oilfield, Alaska. Arctic Science Summit Week, 31 March–7 April, Prague, Czech Republic.

APPENDIX A Data Tables

Appendix A includes key data tables from the study. Data tables are also archived in digital format on the ArcSEES project website (www.geobotany.uaf.edu/arcsees/data) and at the Arctic Data Center (arcticdata.io). A master table available online includes all data from 2014–2016 field surveys at Colleen Site A and the Airport site presented in relation to key site variables: distance from road, and polygon center vs. trough. Transect data include vegetation type, microrelief, NDVI, LAI, elevation, water depth, thaw depth, snow depth, and SWE. Plot data also include plant-growth-form cover, species cover, soil data, and other site environmental characteristics published in earlier reports (Walker et al. 2015, 2016).

Table A.1. Methods and results of protecting iButtons from water damage.

Protection method	All iButtons			iButtons retrieved			
	Location	Number deployed	Number retrieved	Condition on retrieval	2nd year of use	Percent readable	Percent dead
2014-2015							
2 mil zip-seal plastic bag	0 to -40 cm in soil; 0 to 150 cm in air	129	129	NA. Distribution of dead iButtons: 32% at -40 cm, 21% at -20 cm, 26% at 0 cm, 5% in pond, 11% at 10 cm, 5% at 100 cm	0.0%	85.3%	14.7%
2015-2016							
<i>Analysis based on protection method</i>							
2 mil zip-seal plastic bag	20-150 cm in air	36	33	Dry 93.9% Wet 6.1%	3.0%	87.9%	12.1% (incl. 1 on downed PVC pipe)
Nitrile glove finger (knotted) + 2 mil zip-seal plastic bag	20-150 cm in air	41	40	Dry 97.5% Wet 2.5%	37.5%	90.0%	10.0%
Tube wax lubricant + knotted rubber glove finger + 2 mil zip-seal plastic bag	0 to -40 cm in soil; 0 to 20 cm in air	159	152	Dry 75.7% Damp 11.2% Wet 11.8% Unknown 1.3%	48.7%	96.7%	3.3%
Tube wax lubricant + contact lens case	0 to -40 cm in soil	24	24	Dry 91.7% Damp 8.3%	70.8%	95.8%	4.2%
Total		260	249	Dry 83.1% Damp 7.6% Wet 8.4% Unknown 0.8%	43.0%	94.4%	5.6%
<i>Analysis based on condition on retrieval</i>							
			207	Dry	44.0%	95.2%	4.8%
			19	Damp	42.1%	100%	0.0%
			21	Wet	33.3%	81.0%	19.0%
<i>Analysis based on iButton age</i>							
New iButtons	All	150	142	Dry 81.7% Damp 7.7% Wet 9.9% Unknown 0.9%		92.3%	7.7%
2nd year of use	All	110	107	Dry 85.0% Damp 7.5% Wet 6.5% Unknown 0.9%		97.2%	2.8%

Table A.2A. Summary of mean snow depths, water depths, thaw depths, vegetation types, and microrelief types at 1-m intervals along transects T1 and T2 at Lake Coleen Site A. Five snow-, water-, and thaw-depth measurements were taken at each plot and averaged. **Vegetation type:** Based on Walker (1985, Table 3); suffix 'd' indicates disturbed vegetation types. **Microrelief type:** Frost boil (F), flat-centered polygon (FC), high-centered polygon (HC, some have flat tops), low-centered polygon (LC), thermokarst pit (P), low-centered polygon rim (R), roadside berm (RB), and trough (T). Other environmental variables were published in an earlier data report (Walker et al. 2015) and are included in the master table available online. Shaded rows indicate transect distances where plots and iButtons were installed.

Distance from road (m)	Transect 1					Transect 2				
	Snow depth 3/28/16 (cm)	Water depth 8/16/16 (cm)	Thaw depth 8/16/16 (cm)	Vegetation type	Microrelief type	Snow depth 3/28/16 (cm)	Water depth 8/16/16 (cm)	Thaw depth 8/16/16 (cm)	Vegetation type	Microrelief type
0	79	0	106	B	RB	85	0	119	B	RB
1	60	0	108	Caaq,Salova	RB	83	0	109	B	RB
2	49	0	99	Caaq,Salova	RB	86	0	100	B	RB
3	48	0	72	U4d	RB	83	0	92	B	RB
4	46	0	61	U4d	FC	76	0	83	B	HC
5	35	0	61	U4d	R	73	0	76	M2d	HC
6	35	0	63	U4d	LC	73	0	77	M2d	HC
7	41	0	63	U4d	R	84	0	65	M2d	T
8	46	0	61	M2d	T	64	0	70	M2d	HC
9	36	0	66	U4d	R	53	0	66	M2d	HC
10	33	0	65	U4d	R	42	0	65	M2d	HC
11	27	0	65	U4d	R	40	0	63	M2d	HC
12	22	0	66	U4d	LC	40	0	56	M2d	HC
13	26	0	64	U4d	LC	36	0	59	M2d	HC
14	25	0	66	U4d	LC	52	0	59	M2d	HC
15	27	0	67	U4d	LC	61	0	76	E1d	T
16	29	0	67	U4d	LC	64	20	69	E1d	T
17	28	0	68	U4d	LC	63	52	63	W	T
18	27	0	67	U4d	LC	63	60	68	W	T
19	28	0	67	U4d	LC	60	48	57	E1d	T
20	27	0	67	U4d	LC	58	17	63	E1d	HC
21	26	0	64	U4d	LC	52	0	72	M2d	HC
22	26	0	62	U4d	LC	44	0	67	M2d	HC
23	19	0	67	U4d	R	37	0	60	M2d	HC
24	32	0	67	U4d	R	37	0	62	M2d	HC
25	41	1	60	E1d	T	39	0	62	M2d	HC
26	42	17	52	E1d	T	43	0	63	M2d	HC

Table A.2A (cont.). Summary of mean snow depths, water depths, thaw depths, vegetation types, and microrelief types at 1-m intervals along transects T1 and T2 at Lake Coleen Site A.

Distance from road (m)	Transect 1					Transect 2				
	Snow depth 3/28/16 (cm)	Water depth 8/16/16 (cm)	Thaw depth 8/16/16 (cm)	Vegetation type	Microrelief type	Snow depth 3/28/16 (cm)	Water depth 8/16/16 (cm)	Thaw depth 8/16/16 (cm)	Vegetation type	Microrelief type
27	41	14	57	E1d	T	42	0	63	M2d	HC
28	43	14	50	E1d	T	39	0	66	M2d	HC
29	43	9	44	E1d	T	33	0	64	M2d	HC
30	44	0	47	M2d	T	28	0	63	M2d	HC
31	41	0	48	M2d	R	31	0	57	M2d	HC
32	28	0	62	U4d	R	26	0	57	M2d	HC
33	26	0	59	U4d	R	28	0	58	M2d	HC
34	28	0	57	U4d	R	32	0	66	M2d	HC
35	24	0	57	U4d	R	48	0	68	E1d	T
36	37	0	57	U4d	R	54	23	56	E1d	T
37	48	0	48	E1d	T	53	33	51	E1d	T
38	49	10	45	E1d	T	61	19	61	E1d	T
39	47	15	41	E1d	T	70	18	58	E1d	T
40	42	6	59	E1d	T	73	23	50	E1d	T
41	36	0	69	U3d	R	74	18	54	E1d	T
42	26	0	57	U3d	R	69	22	52	E1d	T
43	25	0	56	M2d	LC	60	29	48	E1d	T
44	30	0	54	M2d	LC	52	32	50	E3d	T
45	27	0	57	M2d	R	51	38	50	E3d	T
46	18	0	65	U3d	R	49	41	44	E3d	T
47	35	0	48	M2d	T	50	35	47	E3d	T
48	38	0	53	M2d	T	47	32	44	E1d	T
49	41	0	53	M2d	T	45	13	56	E1d	T
50	39	0	54	M2d	T	36	0	64	E1d	T
51	35	0	49	U4d	R	29	0	62	U4d	R
52	26	0	59	U4d	R	29	0	59	U4d	R
53	27	0	58	M2d	LC	34	0	64	U4d	R
54	25	0	59	M2d	LC	39	0	61	U4d	R
55	26	0	58	M2d	LC	40	0	59	U4d	R
56	22	0	62	M2d	LC	45	0	59	U4d	R
57	25	0	62	U4d	R	48	0	56	U4d	R

Table A.2A (cont.). Summary of mean snow depths, water depths, thaw depths, vegetation types, and microrelief types at 1-m intervals along transects T1 and T2 at Lake Coleen Site A.

Distance from road (m)	Transect 1				Transect 2				Microrelief type
	Snow depth 3/28/16 (cm)	Water depth 8/16/16 (cm)	Thaw depth 8/16/16 (cm)	Vegetation type	Snow depth 3/28/16 (cm)	Water depth 8/16/16 (cm)	Thaw depth 8/16/16 (cm)	Vegetation type	
58	34	0	57	U4d	R	45	0	59	U4d
59	47	0	50	M2d	T	43	0	63	M2d
60	27	0	62	U4d	R	32	0	66	M2d
61	35	0	55	M2d	LC	26	0	67	M2d
62	38	0	58	M2d	LC	33	0	58	M2d
63	37	0	62	U4d	LC	29	0	53	U4d
64	36	0	62	M2d	LC	30	0	49	U4d
65	39	0	61	M2d	LC	26	0	47	U4d
66	41	0	54	M2d	LC	27	0	46	U4d
67	33	0	52	M2d	LC	25	0	58	U4d
68	31	0	52	M2d	LC	38	0	65	U4d
69	27	0	50	U4d	LC	50	0	67	E1d
70	30	0	55	U4d	R	48	0	62	E1d
71	38	0	59	E1d	P	43	0	63	B
72	49	26	68	E1d	P	34	0	58	U4d
73	59	44	63	W1	P	23	0	56	U4d
74	60	53	61	W1	P	30	0	51	U4d
75	53	50	70	W1	P	26	0	52	U4d
76	52	50	56	W1	P	21	0	53	U4d
77	47	20	61	E1d	P	15	0	53	U4d
78	42	0	63	E1d	P	20	0	53	U4d
79	36	0	53	M2d	R	20	0	53	U4d
80	24	0	54	U4d	FC	16	0	52	U4d
81	22	0	52	U4d	FC	16	0	54	U4d
82	20	0	53	U4d	FC	27	0	55	U4d
83	25	0	48	U4d	FC	33	0	74	B
84	20	0	49	U4d	FC	47	0	95	E1d
85	20	0	46	U4d	FC	48	38	56	E1d
86	24	0	48	U3d	FC	49	59	45	E3d
87	27	0	47	U3d	FC	51	48	53	E3d
88	28	0	44	U3d	FC	50	39	56	E3d

Table A.2A (cont.). Summary of mean snow depths, water depths, thaw depths, vegetation types, and microrelief types at 1-m intervals along transects T1 and T2 at Lake Coleen Site A.

Distance from road (m)	Transect 1					Transect 2				
	Snow depth 3/28/16 (cm)	Water depth 8/16/16 (cm)	Thaw depth 8/16/16 (cm)	Vegetation type	Microrelief type	Snow depth 3/28/16 (cm)	Water depth 8/16/16 (cm)	Thaw depth 8/16/16 (cm)	Vegetation type	Microrelief type
89	29	0	46	U3d	FC	47	30	58	E1d	P
90	29	0	54	U3d	R	50	10	74	E1d	P
91	20	0	59	U3d	R	54	0	83	E1d	P
92	41	0	42	U3d	R	46	0	72	U4d	HC
93	48	0	43	E1d	T	43	0	77	B	T
94	51	0	45	E1d	T	29	0	69	U4d	HC
95	48	19	45	E1d	T	18	0	52	U4d	HC
96	47	18	45	E1d	T	19	0	57	U4d	HC
97	45	0	62	U4d	R	18	0	52	U4d	HC
98	25	0	62	U4d	R	17	0	62	U4d	HC
99	28	0	54	U4d	LC	23	0	58	U4d	HC
100	30	0	52	U4d	LC	22	0	59	U4d	HC
105	34	0	58	U3	R	36	0	69	B	F
110	33	0	59	U4	R	41	0	72	B	F
115	33	0	55	U4	R	57	0	48	M4d	T
120	18	0	53	U3	R	35	0	63	B	F
125	15	0	58	U3	R	34	0	83	B	F
130	25	0	55	M2	LC	31	0	61	M2d	HC
135	32	0	58	M2	LC	46	0	49	M4d	T
140	43	0	60	M2	T	19	0	47	U4d	R
145	25	0	49	U4	R	40	0	53	M2d	HC
150	20	0	58	U4	R	27	0	56	M2d	HC
155	26	0	49	U3	R	41	0	62	U4d	HC
160	31	0	49	U3	R	28	0	63	M2d	LC
165	48	19	47	E1	T	30	0	63	M2d	LC
170	29	0	48	U4	LC	46	0	58	M4d	T
175	37	0	57	U4	LC	28	0	54	M2d	LC
180	42	0	47	E1	P	31	0	50	M2d	LC
185	32	0	53	M2	LC	41	0	67	U4d	R
190	34	0	53	M2	LC	30	0	67	M2d	LC
195	26	0	53	U4	R	35	0	62	B	T

Table A.2A (cont.). Summary of mean snow depths, water depths, vegetation types, and microrelief types at 1-m intervals along transects T1 and T2 at Lake Coleen Site A.

Distance from road (m)	Transect 1				Transect 2			
	Snow depth 3/28/16 (cm)	Water depth 8/16/16 (cm)	Thaw depth 8/16/16 (cm)	Vegetation type	Microrelief type	Snow depth 3/28/16 (cm)	Water depth 8/16/16 (cm)	Thaw depth 8/16/16 (cm)
200	45	2	56	E1	T	24	0	53
Sample (n)	120	120	120			120	120	120
Mean (cm)	34.5	3.2	57.6			42.3	6.6	61.8
St. Dev.	± 10.7	± 9.9	± 10.3			± 16.8	± 14.4	± 12.1

Table A.2B. Summary of mean snow depths, water depths, vegetation types, and microrelief types at 1-m intervals along transects T3, T4, and T5 at the Airport site. Five snow-, water-, and thaw-depth measurements were taken at each plot and averaged. **Vegetation type:** Based on Walker (1980, Table 6); suffix 'd' indicates disturbed vegetation types. See footnotes at end of table. **Microrelief type:** Frost boil (F), flat-centered polygon (FC), high-centered polygon (HC), some flat on top, high-centered polygon with rim (HCr), low-centered polygon (LC), thermokarst pit (P), low-centered polygon rim (R), roadside berm (RB), and trough (T). Other environmental variables were published in an earlier data report (Walker et al. 2016) and are included in the master table available online. Shaded rows indicate transect distances where plots and iButtons were installed.

Distance from road (m)	Transect 3				Transect 4				Transect 5	
	Snow depth 3/27/16 (cm)	Water depth 8/17/16 (cm)	Thaw depth 8/17/16 (cm)	Vegetation type	Microrelief type	Snow depth 3/27/16 (cm)	Water depth 8/17/16 (cm)	Thaw depth 8/17/16 (cm)	Vegetation type	Microrelief type
0	67	0	100	B16 ¹	HC	75	6	117	E1d	RB
1	67	0	100	B16	HC	100	0	96	E1d	RB
2	66	0	100	B16	HC	83	0	73	U4d*	R
3	66	0	100	B16	HC	83	0	66	U4d	R
4	65	0	73	B16	HC	87	0	67	M2d**	FC
5	70	0	67	B16	HC	84	5	66	M2d	FC
6	75	0	71	B16	R	83	3	75	M2d	FC
7	90	0	76	B16	R	83	18	76	E1	T
8	103	12	52	M10d ²	T	82	13	74	E1	T
9	97	1	53	M10d	T	81	4	69	M2d	FC
10	57	0	67	B16	R	80	5	66	M2d	FC
11	40	0	58	B16	HC	82	4	70	M2d	FC
12	27	0	61	B16	HC	83	4	71	M2d	FC
13	28	0	64	B16	HC	75	11	78	M2d	FC
14	28	0	64	B16	HC	72	26	79	M2d	FC
15	30	0	64	B16	HC	68	11	92	E1	T
16	48	0	64	B16	T	60	2	107	M2d	FC

Table A.2B (cont.). Summary of mean snow depths, water depths, vegetation types, and microrelief types at 1-m intervals along transects T3, T4, and T5 at the Airport site.

Distance from road (m)	Transect 3					Transect 4				Transect 5		
	Snow depth 3/27/16 (cm)	Water depth 8/17/16 (cm)	Thaw depth 8/17/16 (cm)	Vegetation type	Microrelief type	Snow depth 3/27/16 (cm)	Water depth 8/17/16 (cm)	Thaw depth 8/17/16 (cm)	Vegetation type	Microrelief type	Water depth (cm)	Thaw depth (cm)
17	67	0	54	B16	T	55	3	112	M2d	FC		
18	25	0	68	B17 ³	R	46	8	111	M2d	FC		
19	19	0	69	B17	R	43	17	123	M2d	FC		
20	23	0	63	B17	HC	48	39	124	E1	T	0	74
21	20	0	62	B17	HC	50	51	N/A	E1	T	2	63
22	20	0	62	B17	HC	50	25	123	E1	T	18	46
23	22	0	62	B17	HC	47	17	116	E1	T	15	49
24	19	0	63	B17	HC	43	14	116	M2d	FC	17	46
25	17	0	63	B17	HC	45	23	108	M2d	FC	8	50
26	23	0	54	B17	R	48	29	106	E1	T	0	66
27	13	0	57	B17	HC	49	30	103	E1	T	0	64
28	13	0	58	B17	HC	48	40	101	E1	T	8	41
29	11	0	60	B17	HC	46	48	105	E1	T	0	72
30	15	0	61	B17	HC	46	37	100	E1	T	0	69
31	17	0	60	B17	HC	37	29	101	E1	T	0	69
32	21	0	66	B17	HC	44	23	90	E1	T	0	70
33	31	0	73	B17	HC	44	21	81	E1	T	0	62
34	60	0	39	?	T	52	20	79	E1	T	0	66
35	17	0	65	B16	HC	55	45	68	E1	T	0	53
36	14	0	59	B16	HC	43	55	72	W	T	0	62
37	14	0	58	B16	HC	46	68	67	W	T	0	65
38	12	0	57	B16	HC	47	89	49	W	T	0	55
39	8	0	66	B16	HC	43	43	77	E1	FC	0	61
40	21	0	60	B16	HC	43	33	60	E1	FC	0	57
41	10	0	64	B17	HC	38	15	66	E1	FC	0	64
42	12	0	58	B17	HC	40	23	55	E1	FC	0	56
43	12	0	57	B17	HC	40	18	58	E1	FC	0	64
44	13	0	63	B17	HC	33	15	62	E1	FC	0	63
45	8	0	67	B17	HC	31	16	64	E1	FC	0	64
46	12	0	63	B17	HC	32	26	55	E1	FC	0	64
47	13	0	87	B17	R	32	25	64	E1	FC	0	65

Table A.2B (cont.). Summary of mean snow depths, water depths, thaw depths, vegetation types, and microrelief types at 1-m intervals along transects T3, T4, and T5 at he Airport site.

Distance from road (m)	Transect 3					Transect 4					Transect 5	
	Snow depth 3/27/16 (cm)	Water depth 8/17/16 (cm)	Thaw depth 8/17/16 (cm)	Vegetation type	Microrelief type	Snow depth 3/27/16 (cm)	Water depth 8/17/16 (cm)	Thaw depth 8/17/16 (cm)	Vegetation type	Microrelief type	Water depth (cm)	Thaw depth (cm)
48	60	0	63	B17	R	29	46	60	E1	FC	0	62
49	59	0	61	M10d	T	27	35	64	W	T	0	62
50	63	0	71	M10d	T	27	24	63	E1	T	0	58
51	18	0	75	B17	R	30	19	60	E1	FC	0	53
52	34	0	58	B17	R	28	4	67	M2d	FC	0	47
53	35	0	63	M2d ^s	HC	27	4	62	M2d	FC	0	49
54	33	0	59	M2d	HC	33	7	57	M2d	FC	0	54
55	31	0	62	M2d	HC	34	6	58	M2d	FC	0	55
56	28	0	63	M2d	HC	33	5	54	M2d	FC	0	54
57	27	0	62	M2d	HC	33	4	58	M2d	FC	0	56
58	31	0	62	M2d	HC	31	5	54	M2d	FC	0	50
59	32	0	62	M2d	HC	33	1	60	M2d	FC	0	57
60	23	0	64	M2d	HCr	32	2	58	M2d	FC	0	59
61	25	0	62	U17 ⁶	R	33	4	54	M2d	FC	0	59
62	23	0	62	U17	R	34	0	57	M2d	FC	0	61
63	19	0	58	U17	R	38	0	59	M2d	FC	0	63
64	15	0	59	U17	R	47	2	59	M2d	R	0	62
65	15	0	53	U17	R	53	12	52	M2d	R	0	62
66	16	0	52	B17	R	59	3	59	E1	T	0	64
67	10	0	64	B17	R	53	0	56	U4d	R	0	59
68	22	0	73	B17	R	54	0	58	M2d	FC	0	60
69	68	0	56	M10d	T	57	2	57	M2d	FC	0	61
70	66	0	54	M10d	T	56	0	59	M2d	R	24	50
71	69	0	53	M10d	T	63	12	53	M2d	FC	32	52
72	13	0	77	B17	R	67	20	43	E1	FC	23	49
73	10	0	62	B17	R	60	7	55	E1	FC	0	59
74	20	0	62	B17	R	54	16	51	E1	FC	0	49
75	18	0	64	U17	HCr	43	0	66	U4d	R	0	53
76	28	0	62	U17	HCr	40	0	59	M2d	FC	0	56
77	25	0	61	U17	HCr	41	0	61	M2d	FC	0	54
78	24	0	61	U17	HCr	40	0	59	M2d	FC	0	53

Table A.2B (cont.). Summary of mean snow depths, water depths, thaw depths, vegetation types, and microrelief types at 1-m intervals along transects T3, T4, and T5 at the Airport site.

Distance from road (m)	Transect 3					Transect 4				Transect 5		
	Snow depth 3/27/16 (cm)	Water depth 8/17/16 (cm)	Thaw depth 8/17/16 (cm)	Vegetation type	Microrelief type	Snow depth 3/27/16 (cm)	Water depth 8/17/16 (cm)	Thaw depth 8/17/16 (cm)	Vegetation type	Microrelief type	Water depth (cm)	Thaw depth (cm)
79	21	0	61	U17	HCr	38	5	57	M2d	FC	0	54
80	20	0	62	U17	HCr	32	0	70	M2d	FC	0	53
81	19	0	61	U17	HCr	27	0	79	gravel*	FC	0	54
82	18	0	62	U17	HCr	25	0	83	gravel	FC	0	52
83	17	0	75	B17	R	25	0	83	gravel	FC	0	55
84	45	0	66	B17	R	27	0	83	gravel	FC	18	44
85	47	0	64	U17	T	23	0	82	gravel	FC	22	47
86	67	0	60	M10d	T	29	0	76	gravel	FC	0	64
87	27	0	72	B17	HCr	32	5	57	M2d	FC	0	52
88	22	0	62	B17	HCr	32	2	57	M2d	FC	0	53
89	19	0	60	U17	HCr	32	3	59	M2d	FC	0	52
90	20	0	63	U17	HCr	34	5	54	M2d	FC	0	56
91	23	0	63	U17	HCr	30	0	63	M2d	FC	0	53
92	23	0	64	U17	HCr	32	0	55	U4d	R	0	56
93	23	0	65	U17	HCr	38	9	52	E1	T	0	54
94	25	0	69	U17	HCr	37	4	51	E1	T	0	57
95	24	0	68	U17	T	37	3	49	M2d	FC	0	54
96	17	0	66	B17	R	37	2	50	M2d	FC	0	57
97	22	0	65	U17	R	35	1	49	M2d	FC	0	57
98	30	0	66	U17	R	38	1	52	M2d	FC	0	54
99	42	0	64	U17	R	35	1	53	M2d	FC	0	55
100	45	0	68	U17	HCr	36	0	53	M2d	FC	0	55
Sample (n)	100	100	100			100	100	100			80	80
Mean (cm)	31.7	0.1	62.9			46.8	13.2	71.2			1.9	57.2
s.d.	± 21.5	± 1.2	± 6.3			± 17.9	± 16.8	± 20.3			± 6.0	± 6.6

Notes: **Vegetation type:** ¹B16 – Dry *Puccinellia angustata*, *Puccinellia andersonii*, *Salix ovalifolia*, *S. lanata* barren; ²M10d – Disturbed versions of type M10 (wet *Carex aquatilis*, *Dupontia fisheri*, *Eriophorum angustifolium*, saline graminoid tundra); ³B17 – Dry *Dryas integrifolia*, *Saxifraga oppositifolia*, *Chrysanthemum integrifolium*, *Carex capillaris*, *Thamnia* spp. prostrate-dwarf shrub, sedge, forb tundra; ⁴No code – Dry *Salix lanata*, *S. ovalifolia*, dwarf-shrub tundra; ⁵M2d – Disturbed versions of M2 (wet *Carex aquatilis*, *Bryaerythrophyllosum recurvirostrum* tundra); ⁶U17 – Moist version of B17.

Table A.3A. Summary of mean snow depth, density, snow water equivalent from center (C) and trough (T) 1-m vegetation plots at Colleen Site A, T1 & T2. Five snow- and thaw-depth measurements were taken at each plot and averaged.

Relevé No.	Mean snow depth (cm) (n = 5)	Snow core weight (g)	Snow core depth (cm)	Snow core volume (cm ³)	Snow density (g/cm ³)	Snow water equivalent (cm)	Mean water depth (cm)	Mean thaw depth (cm) (n = 5)	Vegetation type
Date	3/28/2016	3/28/2016	3/28/2016	3/28/2016	3/28/2016	3/28/2016	8/16/2016	8/16/2016	
Transect 1									
T1-005-C	40.4	345	42	1663	0.2	8.5	0.0	67.6	U4d
T1-005-T	53.2	465	50	1980	0.2	11.5	0.0	53.8	M2d
T1-010-C	33.0	200	24	950	0.2	4.8	0.0	61.0	U4d
T1-010-T	42.4	350	43	1702	0.2	8.6	0.0	55.4	M2d
T1-025-C	28.6	310	31	1227	0.2	7.6	0.0	59.2	U4d
T1-025-T	39.0	315	38	1504	0.2	7.7	0.4	50.6	M2d
T1-050-C	31.2	245	29	1148	0.2	5.9	0.0	59.6	U4d
T1-050-T	50.4	535	51	2019	0.3	13.3	19.6	50.4	E4d
T1-100-C	27.2	130	26	1029	0.1	3.0	0.0	56.2	M2d
T1-100-T	44.4	485	42	1663	0.3	12.0	4.2	54.8	M4
T1-200-C	27.8	155	27	1069	0.1	3.7	0.0	60.0	U4
T1-200-T	46.2	360	47	1861	0.2	8.8	9.4	45.8	M4
Mean of all plots	38.7	325	37.5	1485	0.2	7.9	2.8	56.2	
s.d. all plots	± 9.0	± 128	± 9.7	± 385	± 0.0	± 3.2	± 6.0	± 5.8	
Mean of center plots	31.4	231	29.8	1181	0.2	5.6	0.0	60.6	
s.d. center plots	± 4.9	± 85.3	± 6.4	± 255	± 0.0	± 2.2	± 0.0	± 3.8	
Mean of trough plots	45.9	418	45.2	1788	0.2	10.3	5.6	51.8	
s.d. trough plots	± 4.3	± 80.1	± 4.8	± 189	± 0.0	± 2.0	± 1.1	± 2.0	
Transect 2									
T2-005-C	64.4	525	58	2296	0.2	13.0	0.0	82.2	barren
T2-005-T	99	840	92	3642	0.2	21.0	0.0	70.0	E1d
T2-010-C	53.2	505	52	2059	0.2	12.5	0.0	67.6	M2d
T2-010-T	91	1010	86	3405	0.3	25.3	19.0	56.6	E1d
T2-025-C	22.8	95	18	713	0.1	2.1	0.0	62.4	M2d
T2-025-T	58.8	610	54	2138	0.3	15.2	25.2	60.2	E1d
T2-050-C	21.2	75	16	633	0.1	1.6	0.0	50.6	U4d
T2-050-T	50.6	460	49	1940	0.2	11.4	17.8	54.4	E1d
T2-100-C	29	215	27	1069	0.2	5.2	0.0	54.8	M2d
T2-100-T	58.6	525	55	2178	0.2	13.0	6.8	59.0	E1d
T2-200-C	20.4	85	19	752	0.1	1.9	0.0	45.2	U4d
T2-200-T	48.2	365	48	1900	0.2	9.0	0.0	43.8	M2
Mean all plots	51.4	443	47.8	1894	0.2	10.9	5.7	58.9	
s.d. all plots	± 25.8	± 297	± 24.8	± 983	± 0.1	± 7.5	± 9.4	± 10.8	
Mean of center plots	35.2	250	31.7	1254	0.2	6.1	0.0	60.5	
s.d. center plots	± 18.9	± 212	± 18.6	± 735	± 0.1	± 5.3	± 0.0	± 13.3	
Mean of trough plots	67.7	635	64.0	2534	0.2	15.8	11.5	57.3	
s.d. trough plots	± 15.3	± 192	± 16.0	± 631	± 0.1	± 4.8	± 2.3	± 8.1	

Table A.3B. Summary of mean snow depth, density, snow water equivalent from center (C) and trough (T) 1-m vegetation plots at Airport site, T3, T4 & T5. Five snow- and thaw-depth measurements were taken at each plot and averaged.

Relevé No.	Mean snow depth (cm) (n = 5)	Snow core weight (g)	Snow core depth (cm)	Snow core volume (cm ³)	Snow density (g/cm ³)	Snow water equivalent (cm)	Mean water depth (cm)	Mean thaw depth (cm) (n = 5)	Vegetation type
Date	3/28/2016	3/28/2016	3/28/2016	3/28/2016	3/28/2016	3/28/2016	8/16/2016	8/16/2016	
Transect 3									
T3-005-C	39.4	490	52	2059	0.2	12.1	0	70.6	B16
T3-005-T	82.6	935	78	3088	0.3	23.4	ND	ND	M10d
T3-010-C	41.4	275	32	1267	0.2	6.7	0	69.0	B16
T3-010-T	85.0	915	80	3167	0.3	22.9	71	60.0	W1
T3-025-C	21.4	98	12	475	0.2	2.2	0	61.6	B17
T3-025-T	75.2	440	50	1980	0.2	10.9	0	58.0	M10d
T3-050-C	29.8	185	32	1267	0.1	4.4	0	54.8	M2d
T3-050-T	53.4	550	56	2217	0.2	13.6	6.4	56.0	M10d
T3-100-C	40.4	320	38	1504	0.2	7.8	0	64.2	U17
T3-100-T	84.2	970	88	3484	0.3	24.2	0.8	52.2	M10d
Mean of all plots	55.3	518	51.8	2051	0.2	12.8	8.7	60.7	
s.d. all plots	± 24.3	± 321	± 24.4	± 967	± 0.0	± 8.1	± 23.5	± 6.3	
Mean of center plots	43.2	404	43.2	1710	0.2	9.9	0.2	61.6	
s.d. center plots	± 8.7	± 148	± 14.4	± 570	± 0.0	± 3.7	± 0.0	± 6.3	
Mean of trough plots	76.1	762	70.4	2787	0.3	19.0	19.6	56.6	
s.d. trough plots	± 13.3	± 248	± 16.5	± 652	± 0.0	± 6.3	± 34.4	± 3.3	
Transect 4									
T4-005-C	85.4	940	79	3128	0.3	23.5	2.2	67.6	M2d
T4-005-T	83.2	905	82	3247	0.3	22.6	30.4	61.2	E1
T4-010-C	79	1375	76	3358	0.4	30.9	4.6	66.4	M2d
T4-010-T	58.4	575	54	2138	0.3	14.3	51.6	61.2	E1
T4-025-C	49.6	550	53	2098	0.3	13.6	6.4	113.0	M2d
T4-025-T	44	400	44	1742	0.2	9.9	31	82.0	E1
T4-050-C	34.2	305	37	1465	0.2	7.5	6.6	70.2	M2d
T4-050-T	27.4	219	28	1109	0.2	5.3	27.6	50.4	E1
T4-100-C	35.4	160	36	1425	0.1	3.8	1	55.8	M2d
T4-100-T	35.8	305	39	1544	0.2	7.5	12.6	52.0	E1
Mean of all plots	53.2	573	52.8	2125	0.2	13.9	17.4	68.0	
s.d. all plots	± 22.0	± 388	± 19.7	± 832	± 0.1	± 9.0	± 16.8	± 18.4	
Mean of center plots	56.8	695	56.8	2319	0.3	16.6	6.5	73.8	
s.d. center plots	± 24.1	± 494	± 20.6	± 909	± 0.1	± 11.2	± 2.5	± 22.2	
Mean of trough plots	49.8	481	49.4	1956	0.2	11.9	30.6	61.4	
s.d. trough plots	± 21.9	± 271	± 20.5	± 811	± 0.0	± 6.9	± 13.9	± 12.6	

Table A.3B (cont.). Summary of mean snow depth, density, snow water equivalent from center (C) and trough (T) 1-m vegetation plots at Airport site, T3, T4 & T5.

Relevé No.	Mean snow depth (cm) (n = 5)	Snow core weight (g)	Snow core depth (cm)	Snow core volume (cm ³)	Snow density (g/cm ³)	Snow water equivalent (cm)	Mean water depth (cm)	Mean thaw depth (cm) (n = 5)	Vegetation type
Date	3/28/2016	3/28/2016	3/28/2016	3/28/2016	3/28/2016	3/28/2016	8/16/2016	8/16/2016	
Transect 5									
T5-025-C	26.6	215	30	1188	0.2	5.2	0	62.8	U4d
T5-025-T	33.2	302	33	1307	0.2	7.4	0	56.8	M2d
T5-050-C	26	147	27	1069	0.1	3.5	0	62.6	U4d
T5-050-T	30.2	276	32	1267	0.2	6.7	0.4	53.6	M2d
T5-100-C	25	196	27	1069	0.2	4.7	0	59.4	U4d
T5-100-T	40.2	410	46	1821	0.2	10.1	11.8	50.2	U4d
Mean of all plots	30.2	258	32.5	1287	0.2	6.3	2.0	57.6	
s.d. all plots	± 5.8	± 93.1	± 7.1	± 280	± 0.0	± 2.4	± 4.8	± 5.0	
Mean of center plots	30.9	257	34.3	1359	0.2	6.2	3.9	58.5	
s.d. center plots	± 0.8	± 35.1	± 1.7	± 68.6	± 0.0	± 0.9	± 0.0	± 1.9	
Mean of trough plots	34.5	329	37.0	1465	0.2	8.1	4.1	53.5	
s.d. trough plots	± 5.1	± 71.1	± 7.8	± 309	± 0.0	± 1.8	± 6.7	± 3.3	

Table A.4A. Results of borehole drilling at Colleen Site A, T1 & T2: Stages of ice-wedge degradation / stabilization and thicknesses of protective layers (frozen soil layers on top of massive-ice bodies). Data from 2016 borehole are shaded. **Depth to massive ice:** wedge ice (WI), thermokarst cave ice (TCI). **Permafrost table:** Top of the intermediate layer (based on the analysis of cryo-structures) or massive-ice body (at locations with degrading ice wedges). **Frozen protective layer:** Thickness of frozen soil layer on top of massive ice bodies on the day of drilling (includes the frozen part of the active layer, transient layer, and intermediate layer), for boreholes drilled in August 2014 only.

Borehole	Date	Borehole depth (cm)	Water depth (cm)	Thaw depth (cm)	Permafrost table (cm)	Depth to massive ice (cm)	Frozen protective layer (PL1) (cm)	Inter-mediate layer (PL3) (cm)
Undisturbed wedges (UD)								
T1-10T-2	8/7/14	95		56	56	61 (WI)	5	5
T1-10T-3	8/7/14	151		–	–	No wedge	–	–
T1-50T-1	8/7/14	118		55	65	73 (WI)	18	8
Mean (n=2)				55.5	60.5	67	11.5	6.5
Degradation initial (D1)								
T1-5T-1	8/7/14	98		51	60	60 (WI)	9	0
T1-10T-1	8/7/14	90	1	58	58	58 (WI)	0	0
T1-25T-2	8/13/14	97		40	43	43 (WI)	3	0
T1-25T-3	8/13/14	102		–	–	No wedge	–	–
T1-25T-4	8/13/14	120		48	49	49 (WI)	1	0
T1-100T-1	8/7/14	75		44	45	45 (WI)	1	0
Mean (n=5)				48.2	51	51	2.8	0
Degradation advanced (D2)								
T1-25T-1	8/6/14	75	15	45	47	47 (WI)	2	0
T1-50T-7	8/14/14	81	30	43	43	43 (WI)	0	0
T1-50T-8	8/14/14	51	49	41	44	44 (WI)	3	0
T1-50T-9	8/14/14	88	31	51	56	56 (WI)	5	0
Mean (n=4)			31.3	45	47.5	47.5	2.5	0
Stabilization initial (SI1)								
T1-50T-2	8/13/14	86		28	36	36 (WI)	8	0
T1-50T-3	8/13/14	95		–	–	No wedge	–	–
T1-50T-4	8/13/14	108		43	55	55 (CW)	12	0
T1-50T-5	8/13/14	81		35	46	46 (WI)	11	0
T1-50T-6	8/14/14	98		–	–	No wedge	–	–
T1-200T-1	8/8/14	298		35	42	42 (WI+TCI)	7	0
T1-200T-2	8/9/14	158		27	34	34 (WI+TCI)	7	0
T1-200T-3	8/9/14	155		30	37	37 (TCI+WI)	7	0
T2-50T-1	8/11/14	77		48	58	59 (WI)	11	1
T2-50T-2	8/11/14	178		–	–	No wedge	–	–
T2-200T-3	8/12/14	98		68	68	73 (WI)	5	5
T2-200T-4	8/12/14	92		55	55	60 (WI)	5	5
T2-200T-5	8/12/14	179		59	67	67 (WI)	8	0
T2-200T-6	8/12/14	124		57	60	65 (WI)	8	5
T2-200T-7	8/12/14	82		–	–	No wedge	–	–
Mean (n=11)				44.1	50.7	52.2	8.1	1.5
Stabilization initial (SI2)								
T1-74.0	3/29/16	100	37	–	69	86 (WI)	–	17
T1-200T-4	8/9/14	205	0	33	44	44 (TCI)	11	0
T1-200T-5	8/9/14	150	0	33	46	46 (TCI)	13	0
T1-200T-6	8/9/14	150	0	–	–	No wedge	–	–
T1-200T-7	8/9/14	160	0	31	43	43 (TCI+WI)	12	0
T1-200T-8	8/9/14	204	0	33	49	49 (TCI)	16	0

Table A.4A (cont.). Results of borehole drilling at Colleen Site A, T1 & T2: Stages of ice-wedge degradation / stabilization and thicknesses of protective layers (frozen soil layers on top of massive-ice bodies).

Borehole	Date	Borehole depth (cm)	Water depth (cm)	Thaw depth (cm)	Permafrost table (cm)	Depth to massive ice (cm)	Frozen protective layer (PL1) (cm)	Inter-mediate layer (PL3) (cm)
T1-200T-9	8/9/14	135	0	40	54	67 (TCI)	27	13
T2-5T-1	8/10/14	90	12	43	58	70 (WI)	27	12
T2-25T-1	8/10/14	102	35	45	45	64 (WI)	19	19
T2-50T-3	8/11/14	68	35	46	54	56 (WI)	10	2
T2-100T-1	8/11/14	65	8	43	51	57 (WI)	14	6
T2-100T-2	8/11/14	107	0 (WI)	50	58	61 (WI)	11	3
T2-200T-1	8/12/14	49	70	28	36	36 (WI)	8	0
T2-200T-2	8/12/14	100	0	–	–	No wedge	–	–
T2-200T-8	8/13/14	75	27	44	49	49 (WI)	5	0
Mean (n=13)			16	39.1 (n=12)	50.5	56	14.4 (n=12)	5.5
Stabilization advanced (SA1)								
T2-10T-1	8/10/14	89	0 (WI)	53	59	66 (WI)	13	6
Mean (n=1)				53	59	66	13	6
All boreholes								
Mean (n=36)				44 (n=35)	51.1	54.1	9.2 (n=35)	3

Table A.4B. Results of borehole drilling at Airport site, T3 & T5: Stages of ice-wedge degradation/stabilization and thicknesses of protective layers (frozen soil layers on top of massive-ice bodies). Data from 2016 borehole are shaded. **Depth to massive ice:** wedge ice (WI). **Permafrost table:** Top of the intermediate layer (based on the analysis of cryostructures) or massive-ice body (at locations with degrading ice wedges). **Frozen protective layer:** Thickness of frozen soil layer on top of massive ice bodies on the day of drilling (includes the transient layer and intermediate layer), for boreholes drilled in September 2015 only.

Borehole	Date	Borehole depth (cm)	Water depth (cm)	Thaw depth (cm)	Permafrost table (cm)	Depth to massive ice (cm)	Frozen protective layer (PL2) (cm)	Inter-mediate layer (PL3) (cm)
Degradation initial (D1)								
T3-16.5	9/18/15	92		60	60	60 (WI)	0	0
T3-32.2	9/18/15	79		51	51.5	51.5 (WI)	0.5	0
T3-50.5	9/18/15	75		43	43	43 (WI)	0	0
T3-70.3	9/18/15	92		62	62	62 (WI)	0	0
T3-90.0	9/18/15	88		48	48.5	48.5 (WI)	0.5	0
T3-94.2	9/19/15	79		48	48	48 (WI)	0	0
T3-101.1	9/19/15	90		55	55	55 (WI)	0	0
Mean (n=7)				52.4	52.6	52.6	0.1	0
Degradation advanced (D2)								
T3-70.4	9/22/15	69	27	47	47.5	47.5 (WI)	0.5	0
T5-93.0	9/21/15	50	27	45	45	45 (WI)	0	0
T5-94.5	3/28/16	55	73	–	47	47 (WI)	–	0
Mean (n=3)			42.3	46 (n=2)	46.5	46.5	0.3 (n=2)	0
Stabilization initial (SI1)								
T3-84.1	9/18/15	92		62	63	63 (WI)	1	0
T3-83.7	9/18/15	109		65	66	66 (WI+TCI)	1	0
Mean (n=2)				63.5	64.5	64.5	1	0

Table A.4B (cont.). Results of borehole drilling at Airport site, T3 & T5: Stages of ice-wedge degradation/stabilization and thicknesses of protective layers (frozen soil layers on top of massive-ice bodies).

Borehole	Date	Borehole depth (cm)	Water depth (cm)	Thaw depth (cm)	Permafrost table (cm)	Depth to massive ice (cm)	Frozen protective layer (PL2) (cm)	Inter-mediate layer (PL3) (cm)
Stabilization initial (SI2)								
T3-11.7	9/22/15	81	23	53	53	67 (WI+TCI)	14	14
T5-26.7	9/20/15	63	10	53	53	55 (WI)	2	2
T5-40.3	9/20/15	104	0	77	78	78 (WI)	1	0
T5-39.7	9/20/15	92	8	61	61.5	61.5 (WI)	0.5	0
T5-59.5	9/20/15	61	11	48	48	50 (WI)	2	2
T5-68.9	9/21/15	57	15	36	36	42 (WI+TCI)	6	6
T5-88.3	9/21/15	66	10	46	46	51 (WI)	5	5
T5-100.6	9/21/15	62	17	36	48	51 (WI)	15	3
T5-50.0	9/22/15	118	27	48	48	51 (TCI,WI)	3	3
T5-96.8	3/28/16	65	66	–	48	59 (WI)	–	11
Mean (n=10)			18.7	50.9 (n=9)	52	56.6	5.4 (n=9)	0
Stabilization advanced (SA2)								
T3-89.3	9/18/15	143		–	–	113 (CW?)	–	–
T3-100.7	9/19/15	135		62	62	72 (TCI,WI)	10	10
T5-50.5	9/20/15	150		69	73	134 (WI)	65	61
T5-72.9	9/20/15	93		51	51	57 (TCI,WI)	6	6
T5-69.6	9/21/15	110		71	75	77 (WI)	6	2
T5-100.5	9/21/15	113		–	–	90 (CW?)	–	–
Mean (n=4)				63.3	65.3	85	21.8	19.8
All boreholes								
Mean (n=26)				54.0 (n=24)	54.5	59.3	5.8 (n=24)	4.8

Table A.5A. Mean annual air temperatures (°C), July 2015 to July 2016, at Colleen Site A (T1 & T2) and Airport site (T3 & T4) by distance from road (m) and height of iButton above soil surface (cm). Shaded columns indicate flooded transects. Missing data (blank cells) due to lost or water-damaged iButtons.

Height: 0 cm (soil surface)				
Distance from road (m)	T1	T2	T3	T4
0	-3.9	-3.5		
5	-4.6	-2.4	-4.7	-3.1
10	-4.3	-3.8	-5.5	-4.2
25		-5.1	-7.3	-3.5
50	-4.5	-3.9	-4.5	-4.0
100	-5.2	-4.7	-4.4	-3.7
Height: 10 cm				
Distance from road (m)	T1	T2	T3	T4
0	-3.8	-3.7		
5	-5.8	-3.0	-5.5	-3.0
10	-5.7	-4.9	-6.7	-4.1
25		-6.0	-7.7	-3.1
50	-5.4	-4.8	-5.6	-3.6
100	-6.7	-6.5	-5.6	-4.7
Height: 20 cm				
Distance from road (m)	T1	T2	T3	T4
0	-5.0	-4.6		
5	-6.3	-4.8	-6.6	
10	-6.7	-6.6	-7.5	-5.6
25	-4.2	-7.4	-8.0	-3.4
50	-6.8	-6.5	-7.1	
100	-7.5	-8.0	-7.2	-6.6
Height: 50 cm				
Distance from road (m)	T1	T2	T3	T4
0	-7.1	-7.2		-6.8
5	-7.8	-7.8	-8.1	-7.7
10	-7.7	-8.3	-8.6	-7.8
25	-7.5	-8.1	-8.4	-8.3
50	-7.6	-8.0	-8.3	-8.3
100	-8.2	-7.7	-8.4	
Height: 100 cm				
Distance from road (m)	T1	T2	T3	T4
0			-8.4	-8.1
5	-8.0	-8.0	-8.1	-7.9
10		-7.9	-8.2	-8.0
25	-7.6	-7.6	-8.5	-8.4
50	-8.3	-8.4	-7.9	-8.4
100	-8.0			-8.0
Height: 150 cm				
Distance from road (m)	T1	T2	T3	T4
0	-8.2			-8.6
5	-8.0	-7.7		-7.9
10	-8.0			

Table A.5B. Mean annual temperatures (°C), July 2015 to July 2016, in polygon centers and troughs at permanent vegetation plots on Colleen Site A (T1 and T2) and Airport site (T3 and T4) by distance from road (m) and soil depth (cm). Shaded columns indicate flooded transects. Missing data (blank cells) due to lost or water-damaged iButtons.

	Polygon Centers				Polygon Troughs			
Depth: 0 cm (soil surface)								
Distance from road (m)	T1	T2	T3	T4	T1	T2	T3	T4
5	-4.1	-1.2	-4.3	-2.6	-3.0	-1.6		-1.9
10	-3.9	-3.2	-3.8	-3.6	-3.2	-1.2	0.3	-1.4
25	-4.4	-4.1	-5.2	-3.9	-2.9	-1.1	-2.2	-3.5
50	-4.5	-3.5	-3.9	-4.7	-2.2	-2.6	-2.4	-3.3
100	-4.3	-3.1	-4.8	-3.9	-3.4	-2.0	-1.8	-3.7
200	-4.2	-4.1			-2.4	-3.4		
Depth: 20 cm								
Distance from road (m)	T1	T2	T3	T4	T1	T2	T3	T4
5	-4.4	-2.0	-4.9	-2.8	-4.0	-1.9		-2.7
10	-4.4	-4.0	-4.7	-3.8	-3.9	-2.0	0.3	-2.6
25	-5.6	-5.0	-5.9		-4.1	-2.1	-3.3	-3.9
50	-5.0	-4.3	-4.7	-5.0	-3.8	-2.9	-3.0	-4.1
100	-5.0	-4.1	-5.0	-4.8	-4.6	-2.9	-2.7	-4.4
200	-5.5	-5.0			-4.2	-4.3		
Depth: 40 cm								
Distance from road (m)	T1	T2	T3	T4	T1	T2	T3	T4
5	-4.5	-3.3	-5.3	-3.2	-4.8	-2.5		-3.3
10	-5.5	-4.4	-5.5	-4.4	-4.5	-2.8	-0.7	-3.5
25	-5.9	-5.0	-6.3	-3.9	-4.2	-3.0	-3.9	-4.1
50	-5.5	-4.7	-5.2	-5.9	-4.1	-3.3		-4.3
100	-5.3	-4.4	-5.6	-5.4	-4.8	-3.4	-3.8	-4.8
200	-5.3	-5.3			-4.9			

Table A.6. Placement information for iButton temperature loggers installed on Colleen Site A, T1 and T2, from August 2015–July 2016. See previous data reports for iButton placement at Colleen Site A from August 2014–July 2015 (Walker et al. 2015) and at the Airport site from August 2015–July 2016. (Walker et al. 2016a).

Transect Location or Vegetation Plot No.	Logger ID	AGC ID	iButton Height or Depth	Elevation at Surface (m)
Transect 1 flag transect				
T1-000	2E0000003A183021	241	0 cm	13.52
T1-000	2600000039E93521	248	10 cm	
T1-000	CE00000039DF7221	142	20 cm	
T1-000	4C00000035F69421	048	50 cm	
T1-000	6000000039F32121	150	100 cm	
T1-000	6800000035F2FF21	055	150 cm	
T1-005	8C0000003A0D5A21	212	0 cm	13.55
T1-005	E70000003A378321	167	10 cm	
T1-005	960000003601BA21	041	20 cm	
T1-005	1400000035F27621	067	50 cm	
T1-005	9F00000039F96021	233	100 cm	
T1-005	9F00000039FF3621	273	150 cm	
T1-010	FA00000035F7AD21	057	0 cm	13.38
T1-010	8200000039ECE321	246	10 cm	
T1-010	AD0000003603E321	090	20 cm	
T1-010	2200000039EA3821	143	50 cm	
T1-010	4900000039E34821	247	100 cm	
T1-010	CF00000035F6A621	016	150 cm	
T1-025	780000003A0F0921	274	0 cm	13.24
T1-025	270000003A20B321	266	10 cm	
T1-025	5900000035FF7E21	002	20 cm	
T1-025	7100000036127721	119	50 cm	
T1-025	5100000039DC9921	153	100 cm	
T1-050	0C0000003A3C6521	185	0 cm	13.33
T1-050	7900000035FD6521	120	10 cm	
T1-050	3E0000003A1CCC21	239	20 cm	
T1-050	9000000036101F21	109	50 cm	
T1-050	8C00000039E54B21	138	100 cm	
T1-100	1B0000003A148E21	141	0 cm	13.47
T1-100	5D0000003A2E9121	235	10 cm	
T1-100	D60000003A149721	218	20 cm	
T1-100	350000003A187221	130	50 cm	
T1-100	AD00000035FF1F21	046	100 cm	
Transect 1 vegetation plots				
T1-005-C	310000003A0CB921	174	0 cm	13.44
T1-005-C	120000003A367E21	181	-20 cm	
T1-005-C	9C0000003601E521	030	-40 cm	
T1-005-T	1D00000039E4EB21	147	0 cm	13.32
T1-005-T	FF00000039F3E121	164	-20 cm	
T1-005-T	6D00000039EFEB21	265	-40 cm	
T1-010-C	E200000035FBD521	034	0 cm	13.39
T1-010-C	D800000039E1C321	220	-20 cm	
T1-010-C	9F00000039FB5221	258	-40 cm	
T1-010-T	DE00000035FF6A21	029	0 cm	13.17
T1-010-T	E500000035F19F21	074	-20 cm	
T1-010-T	DB000000360E8021	107	-40 cm	

Table A.6 (cont.). Placement information for iButton temperature loggers installed on Colleen Site A, T1 and T2, from August 2015–July 2016.

Transect Location or Vegetation Plot No.	Logger ID	AGC ID	iButton Height or Depth	Elevation at Surface (m)
T1-025-C	CE00000035FA8F21	004	0 cm	13.44
T1-025-C	160000003A1F8221	163	-20 cm	
T1-025-C	360000003A0F2221	224	-40 cm	
T1-025-T	3A00000035F22621	039	0 cm	13.23
T1-025-T	8F00000035F38921	087	-20 cm	
T1-025-T	83000000360A6221	104	-40 cm	
T1-050-C	DD00000035F24921	023	0 cm	13.39
T1-050-C	2500000035F41421	071	-20 cm	
T1-050-C	C80000003A574B21	162	-40 cm	
T1-050-T	EA00000035F9AB21	027	0 cm	12.90
T1-050-T	D700000036007421	032	-20 cm	
T1-050-T	590000003606FF21	051	-40 cm	
T1-100-C	F30000003A493721	160	0 cm	13.43
T1-100-C	4E00000039DFD621	199	-20 cm	
T1-100-C	2C0000003A3A1A21	216	-40 cm	
T1-100-T	1400000039D5B921	244	0 cm	13.18
T1-100-T	1E00000039EBFA21	250	-20 cm	
T1-100-T	840000003A45C821	251	-40 cm	
T1-200-C	A400000036046521	043	0 cm	13.48
T1-200-C	930000003A4B7E21	191	-20 cm	
T1-200-C	8E0000003A19A421	275	-40 cm	
T1-200-T	3100000035F5B321	064	0 cm	13.21
T1-200-T	2500000036002021	093	-20 cm	
T1-200-T	550000003A227121	161	-40 cm	
Transect 2 flag transect				
T2-000	060000003A2E8121	207	0 cm	13.70
T2-000	ED0000003A2DAF21	263	10 cm	
T2-000	EA0000003A59EF21	146	20 cm	
T2-000	CA0000003A59C621	144	50 cm	
T2-000	250000003A00AB21	260	100 cm	
T2-000	130000003A17E921	132	150 cm	
T2-005	EE00000036057121	024	0 cm	13.40
T2-005	4600000036069B21	066	10 cm	
T2-005	0D00000039E64121	219	20 cm	
T2-005	080000003A006D21	229	50 cm	
T2-005	FA0000003A1C1C21	190	100 cm	
T2-005	C100000035F6DF21	094	150 cm	
T2-010	2200000035FF4721	095	0 cm	13.40
T2-010	D800000035FB3B21	017	10 cm	
T2-010	270000003A377521	168	20 cm	
T2-010	480000003A254921	152	50 cm	
T2-010	AC0000003A04A221	175	100 cm	
T2-025	4800000036028621	006	0 cm	13.40
T2-025	320000003617CE21	116	10 cm	
T2-025	6500000035FD9721	065	20 cm	
T2-025	8000000035F60821	044	50 cm	
T2-025	2500000035FDC521	049	100 cm	

Table A.6 (cont.). Placement information for iButton temperature loggers installed on Colleen Site A, T1 and T2, from August 2015–July 2016.

Transect Location or Vegetation Plot No.	Logger ID	AGC ID	iButton Height or Depth	Elevation at Surface (m)
T2-050	570000003A5A3E21	209	0 cm	13.20
T2-050	1D000000361BB721	108	10 cm	
T2-050	7E0000003A377621	173	20 cm	
T2-050	8F0000003602C021	099	50 cm	
T2-050	AE0000003A40C321	149	100 cm	
T2-100	5B0000003A5C0221	279	0 cm	13.51
T2-100	1E0000003613E921	122	10 cm	
T2-100	E60000003A199321	200	20 cm	
T2-100	7000000039E33021	154	50 cm	
T2-100	4C0000003A519F21	221	100 cm	
Transect 2 vegetation plots				
T2-005-C	2F00000035FAD521	012	0 cm	13.45
T2-005-C	E70000003603EE21	096	-20 cm	
T2-005-C	A90000003A148821	204	-40 cm	
T2-005-T	C100000035FE1721	068	0 cm	13.18
T2-005-T	2300000036033E21	097	-20 cm	
T2-005-T	D7000000361B1E21	111	-40 cm	
T2-010-C	4700000036004821	019	0 cm	13.45
T2-010-C	F10000003A0D5621	192	-20 cm	
T2-010-C	A70000003A4CA621	272	-40 cm	
T2-010-T	520000003608BB21	112	0 cm	12.84
T2-010-T	F000000035FF3A21	070	-20 cm	
T2-010-T	0B0000003A141621	170	-40 cm	
T2-025-C	C50000003A1F7A21	206	0 cm	13.41
T2-025-C	6E0000003A08EB21	261	-20 cm	
T2-025-C	FA0000003A3A4121	264	-40 cm	
T2-025-T	D500000036182621	117	0 cm	12.76
T2-025-T	F700000035F57021	037	-20 cm	
T2-025-T	E500000035F5FB21	011	-40 cm	
T2-050-C	BA0000003A08A321	140	0 cm	13.48
T2-050-C	8000000039F90421	238	-20 cm	
T2-050-C	CF00000039E6A421	267	-40 cm	
T2-050-T	110000003A2D8221	259	0 cm	12.85
T2-050-T	2D0000003A449521	243	-20 cm	
T2-050-T	910000003A364C21	245	-40 cm	
T2-100-C	910000003613B121	125	0 cm	13.41
T2-100-C	700000003A127921	225	-20 cm	
T2-100-C	510000003A359121	240	-40 cm	
T2-100-T	2B00000036098821	126	0 cm	13.00
T2-100-T	0F000000361C7321	114	-20 cm	
T2-100-T	4000000035F1B121	085	-40 cm	
T2-200-C	F400000035F7D421	054	0 cm	13.50
T2-200-C	190000003A1D4C21	172	-20 cm	
T2-200-C	6C00000039E1F021	277	-40 cm	
T2-200-T	A0000000360BC421	124	0 cm	13.18
T2-200-T	3E00000035FD8721	026	-20 cm	
T2-200-T	F0000000360A1721	123	-40 cm	

APPENDIX B Photos and Description of Snow Pits at Plots

Transect 1 snow pit photos and profiles

5 meters from road



*Polygon center
T1-5-C (DSC 8764.jpg)*

10 meters from road



*Polygon center
T1-10-C (DSC 8769.jpg)*

25 meters from road



*Polygon center
T1-25-C (DSC 8773.jpg)*



*Polygon trough
T1-5-T (DSC 8771.jpg)*



*Polygon trough
T1-10-T (DSC 8767.jpg)*



*Polygon trough
T1-25-T (DSC 8775.jpg)*

Transect 1 snow pit photos and profiles (continued)

50 meters from road



Polygon center
T1-50-C (DSC 8777.jpg)

100 meters from road



Polygon center
T1-100-C (DSC 8781.jpg)

200 meters from road



Polygon center
T1-200-C (DSC 8787.jpg)



Polygon trough
T1-50-T (DSC 8778.jpg)

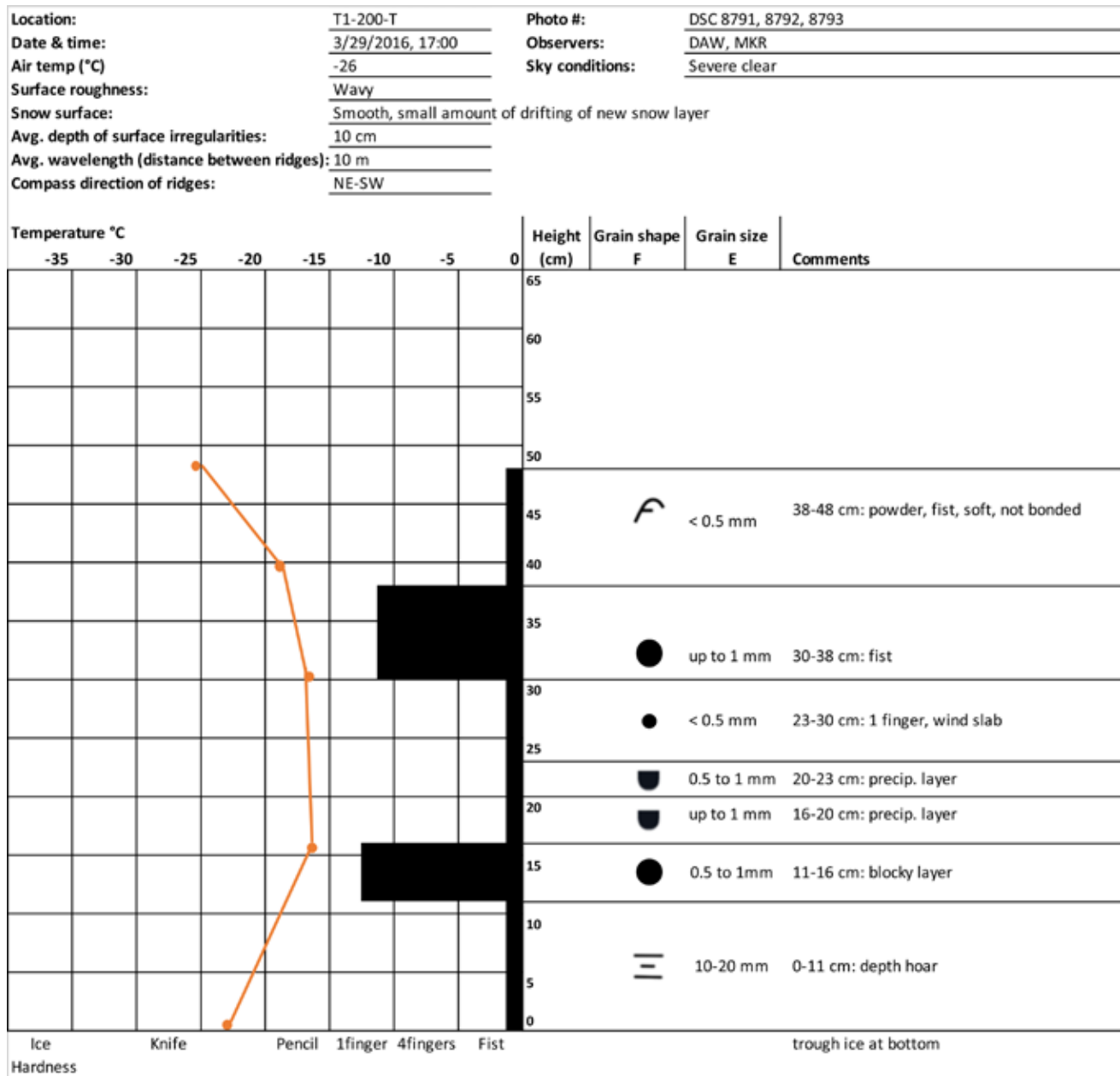


Polygon trough
T1-100-T (DSC 8784.jpg)

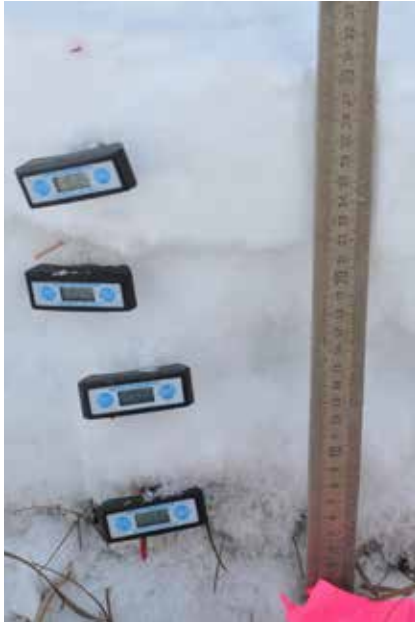


Polygon trough
T1-200-T (DSC 8792.jpg)

Snow pit profile: T1-200-T



See Colbeck et al. (1992) for key to snow profile symbols and terms.

Transect 2 snow pit photos and profiles**5 meters from road****Polygon center**
T2-5-C (DSC 8880.jpg)**10 meters from road****Polygon center**
T2-10-C (DSC 8837.jpg)**25 meters from road****Polygon center**
T2-25-C (DSC 8842.jpg)**Polygon trough**
T2-5-T (DSC 8812.jpg)**Polygon trough**
T2-10-T (DSC 8830.jpg)**Polygon trough**
T2-25-T (DSC 8845.jpg)

Transect 2 snow pit photos and profiles (continued)

50 meters from road



Polygon center
T2-50-C (DSC 8854.jpg)

100 meters from road



Polygon center
T2-100-C (DSC 8858.jpg)

200 meters from road



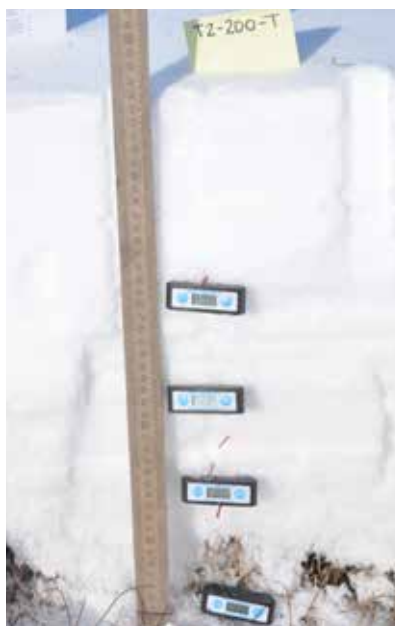
Polygon center
T2-200-C (DSC 8863.jpg)



Polygon trough
T2-50-T (DSC 8851.jpg)

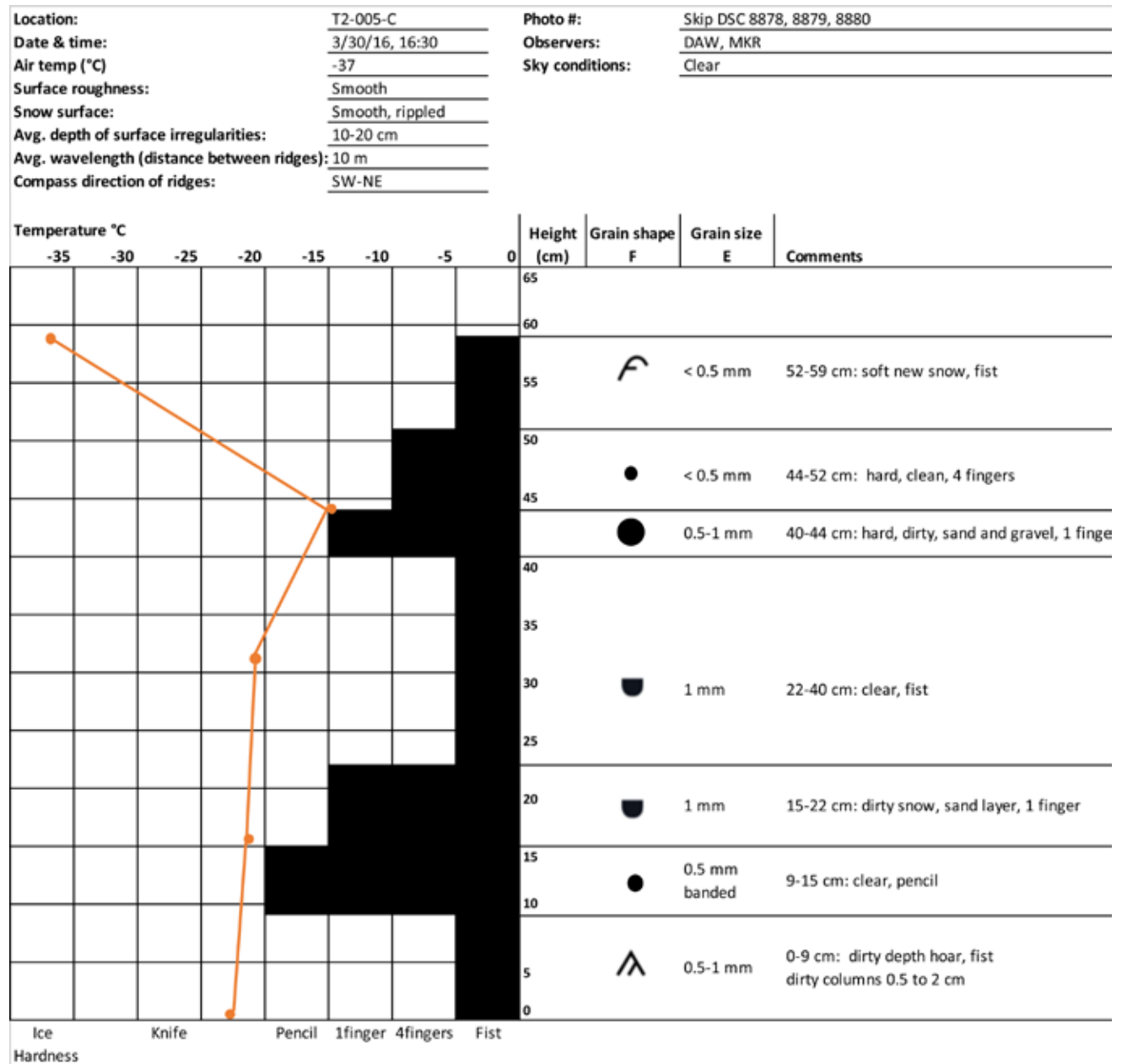


Polygon trough
T2-100-T (DSC 8862.jpg)



Polygon trough
T2-200-T (DSC 8871.jpg)

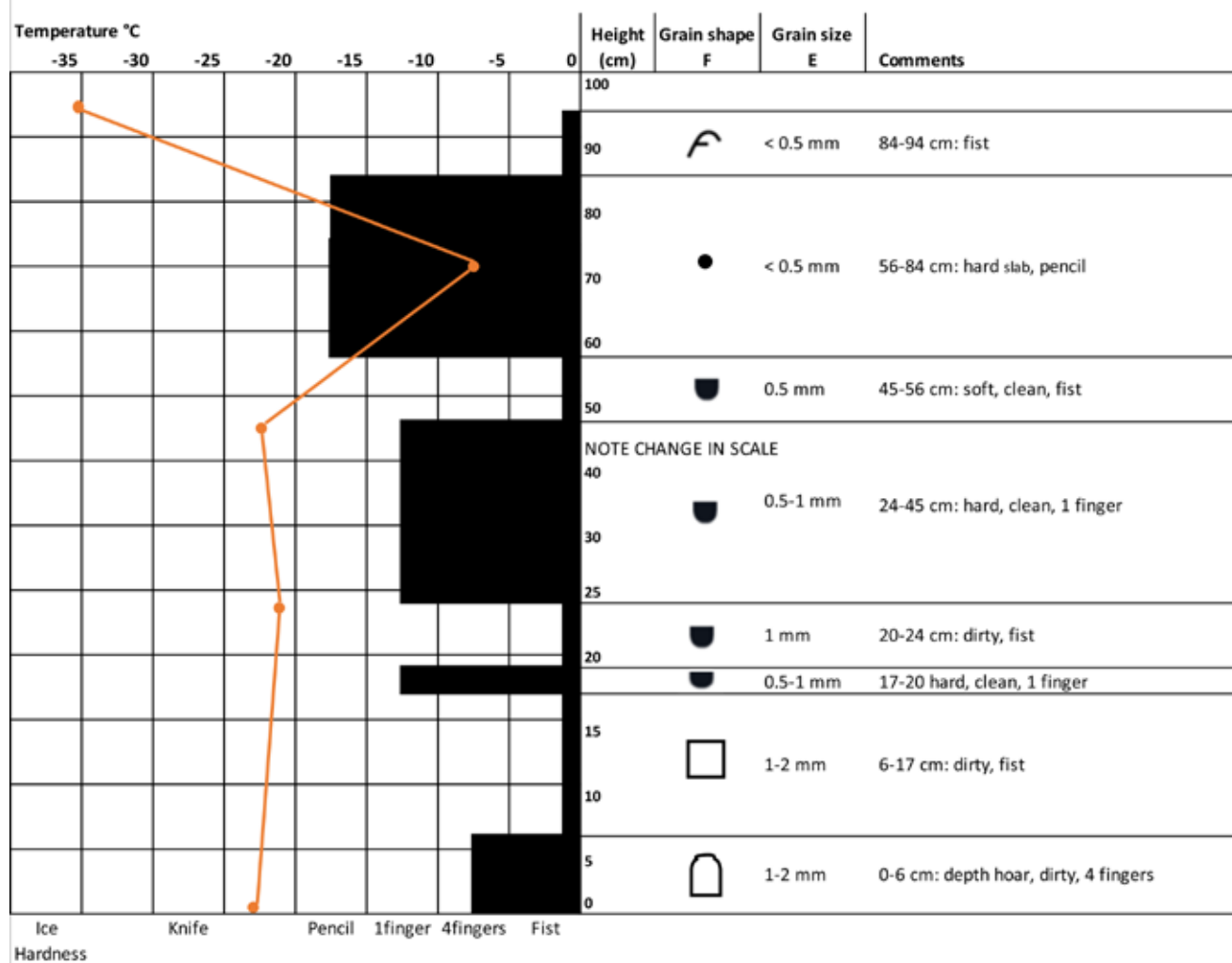
Snow pit profile: T2-5-C



See Colbeck et al. (1992) for key to snow profile symbols and terms.

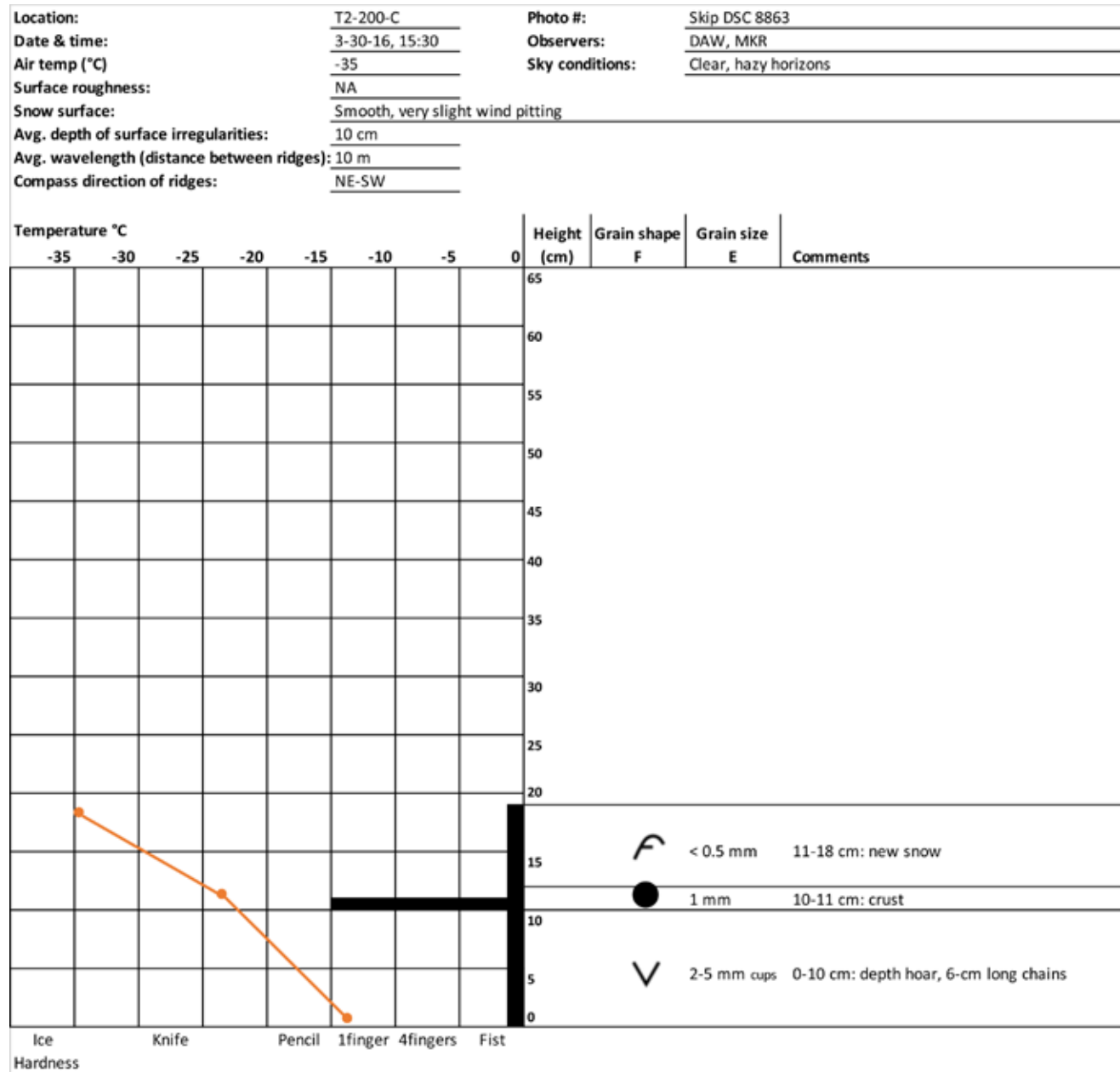
Snow pit profile: T2-5-T

Location:	T2-005-T	Photo #:	Skip DSC8881, 8882, 8883, 8884
Date & time:	3-30-16, 16:00	Observers:	DAW, MKR
Air temp (°C)	-35	Sky conditions:	Mostly clear, haze on SE 1/4
Surface roughness:	Smooth		
Snow surface:	Smooth, some old crust showing through		
Avg. depth of surface irregularities:	none		
Avg. wavelength (distance between ridges):	none		
Compass direction of ridges:	none		



See Colbeck et al. (1992) for key to snow profile symbols and terms.

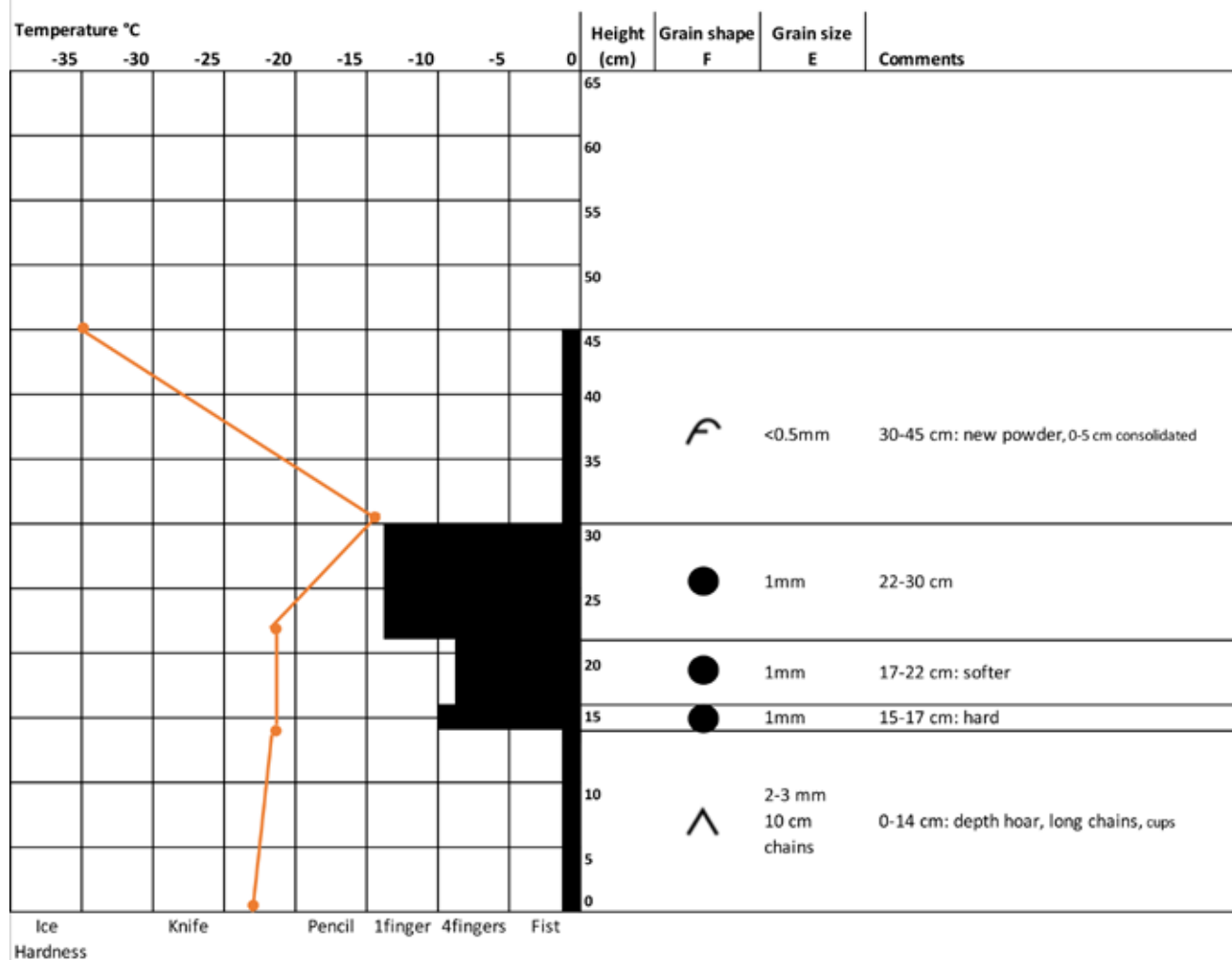
Snow pit profile: T2-200-C



See Colbeck et al. (1992) for key to snow profile symbols and terms.

Snow pit profile: T2-200-T

Location:	T2-200-T	Photo #:	Skip DSC 8870, 8871
Date & time:	3-30-16, 15:00	Observers:	DAW, MKR
Air temp (°C)	-35	Sky conditions:	Clear, hazy horizons, very light breeze changing from E -> W
Surface roughness:	Wavy		
Snow surface:	Smooth, very fine pitting		
Avg. depth of surface irregularities:	5 cm		
Avg. wavelength (distance between ridges):	10 m		
Compass direction of ridges:	NE-SW		



See Colbeck et al. (1992) for key to snow profile symbols and terms.

Transect 3 snow pit photos and profiles

5 meters from road

**Polygon center**
T3-5-C (DSC 8729.jpg)

10 meters from road

**Polygon center**
T3-10-C (DSC 8742.jpg)

25 meters from road

**Polygon center**
T3-25-C (DSC 8745.jpg)**Polygon trough**
T3-5-T (DSC 8726.jpg)**Polygon trough**
T3-10-T (DSC 8739.jpg)**Polygon trough**
T3-25-T (DSC 8746.jpg)

Transect 3 (cont.) & Transect 5 snow pit photos and profiles

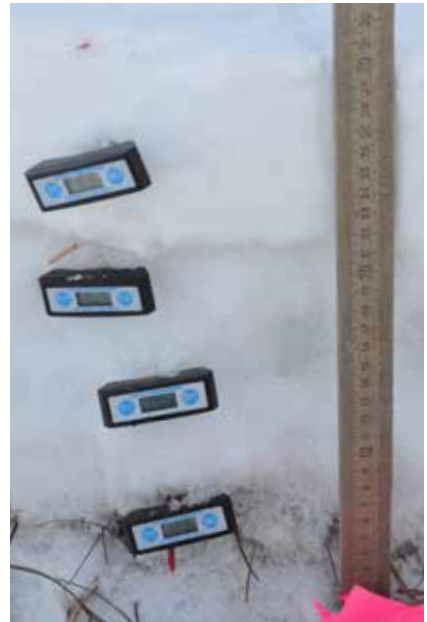
50 meters from road

**Polygon center**
T3-50-C (DSC 8750.jpg)

100 meters from road

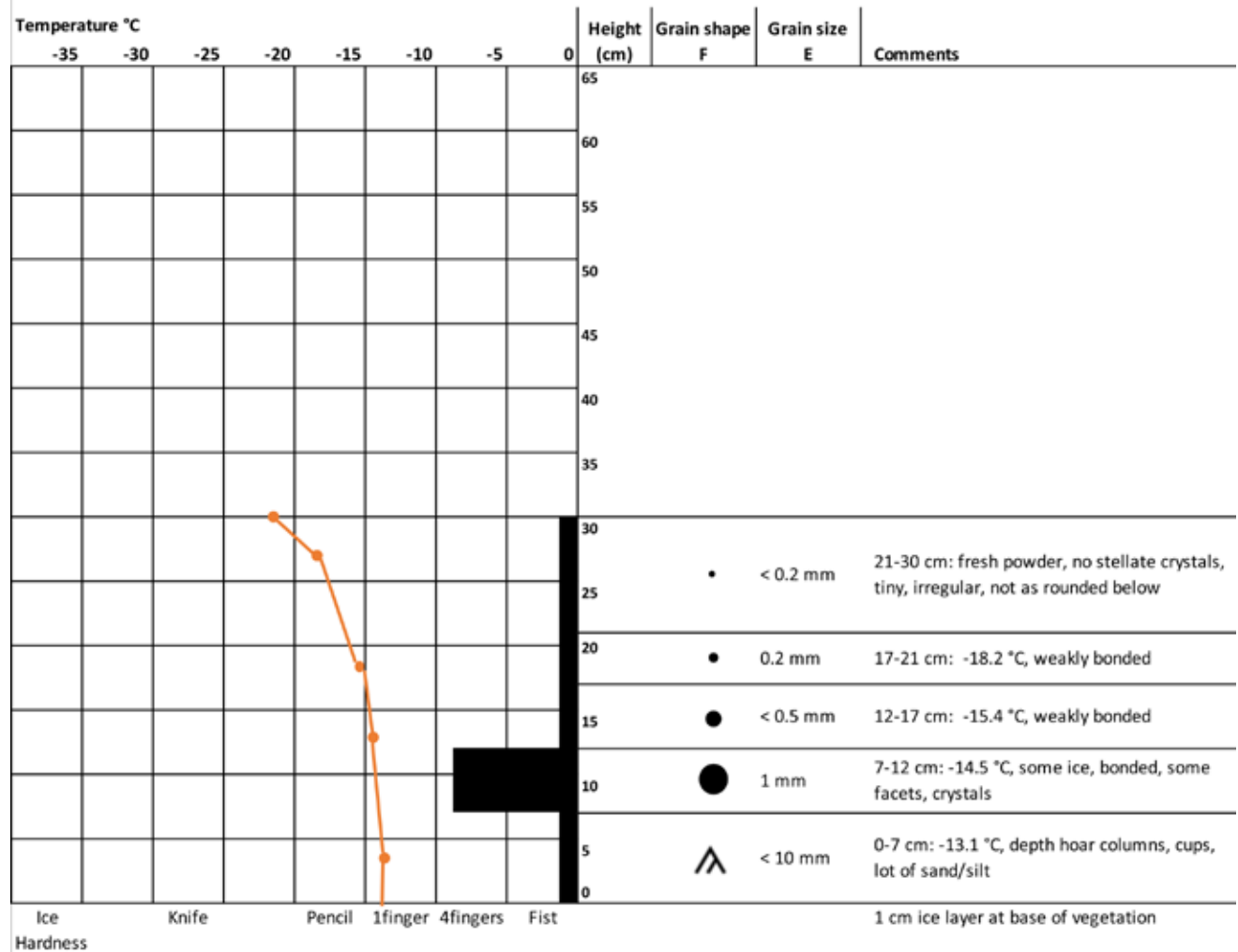
**Polygon center**
T3-100-C (DSC 8753.jpg)

T5 - 25 meters from road

**Polygon center**
T5-25-C (DSC 8694.jpg)**Polygon trough**
T3-50-T (DSC 8749.jpg)**Polygon trough**
T3-100-T (DSC 8754.jpg)**Polygon trough**
T5-25-T (DSC 8704.jpg)

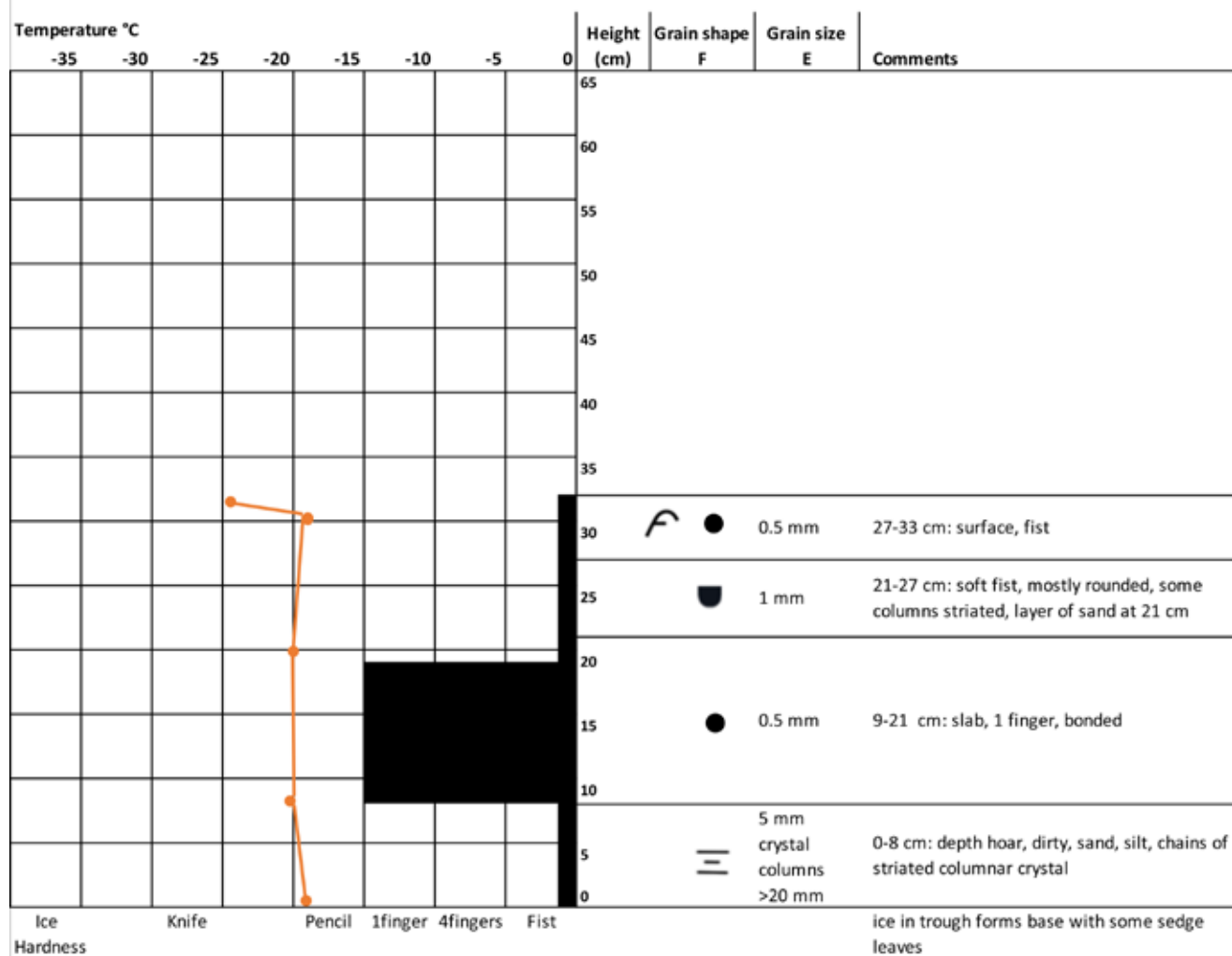
Snow pit profile: T5-25-C

Location:	T5-025-C	Photo #:	Skip DSC 8697 to 8700
Date & time:	3-28-16, 13:30	Observers:	DAW, MKR
Air temp (°C)	-22	Sky conditions:	Sunny above, some low elevation clouds, sun dog only BELO ¹
Surface roughness:	Wavy		
Snow surface:	Smooth, fresh powder, snow starting to move and form drifts		
Avg. depth of surface irregularities:	5 cm		
Avg. wavelength (distance between ridges):	5 m		
Compass direction of ridges:	E-W		



Snow pit profile: T5-25-T

Location:	T5-025-T	Photo #:	Skip DSC 8701 to DSC 8704
Date & time:	3-28-16, 15:00	Observers:	DAW, MKR
Air temp (°C)	-24	Sky conditions:	S 2/3 haze-covered, N 1/3 blue
Surface roughness:	Wavy		
Snow surface:	Smooth, some grainy texture as snow starts to move with wind.		
Avg. depth of surface irregularities:	5 cm		
Avg. wavelength (distance between ridges):	5 m		
Compass direction of ridges:	E-W		



See Colbeck et al. (1992) for key to snow profile symbols and terms.

APPENDIX C Selected Photos of Quintillion Fiber Optic Cable Impacts, July 17, 2016



DSC 9190.jpg



DSC 9191.jpg



DSC 9194.jpg



DSC 9198.jpg



DSC 9200.jpg



DSC 9207.jpg

Selected photos of Quintillion Fiber Optic Cable impacts, July 17, 2016 (continued)



DSC 9209.jpg



DSC 9214.jpg



DSC 9216.jpg



DSC 9218.jpg

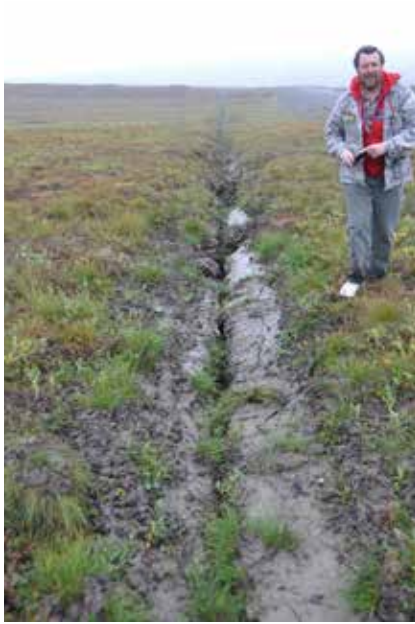


DSC 9194.jpg



DSC 9236.jpg

Selected photos of Quintillion Fiber Optic Cable impacts, July 17, 2016 (continued)



DSC 9244.jpg



DSC 9246.jpg



DSC 9247.jpg



DSC 9248.jpg



DSC 9249.jpg



DSC 9251.jpg

Selected photos of Quintillion Fiber Optic Cable impacts, July 17, 2016 (continued)



DSC 9258.jpg



DSC 9262.jpg



DSC 9263.jpg



DSC 9265.jpg



DSC 9270.jpg



DSC 9272.jpg

Selected photos of Quintillion Fiber Optic Cable impacts, July 17, 2016 (continued)



DSC 9268.jpg



DSC 9269.jpg



DSC 9273.jpg



DSC 9274.jpg



DSC 9275.jpg



DSC 9277.jpg

Selected photos of Quintillion Fiber Optic Cable impacts, July 17, 2016 (continued)



DSC 9279.jpg



DSC 9282.jpg



DSC 9286.jpg



DSC 9288.jpg



DSC 9270.jpg



DSC 9272.jpg

ALASKA GEOBOTANY CENTER

The Alaska Geobotany Center (AGC) is dedicated to understanding northern ecosystems through the use of geographic information systems, remote sensing, field experiments, and cooperative team research projects. We share a commitment to excellence in field research and teaching with the goal of inspiring an appreciation of northern ecosystems and making our research and teaching relevant to societal issues and concerns, particularly issues relevant to the state of Alaska.

Alaska Geobotany Center
Institute of Arctic Biology
University of Alaska Fairbanks

P.O. Box 757000
Fairbanks, AK 99775-7000
Phone 1.907.474.2459

www.geobotany.uaf.edu

